Max-Planck-Institut für Biogeochemie

MPI-BGC Jena

TECHNICAL REPORTS 7

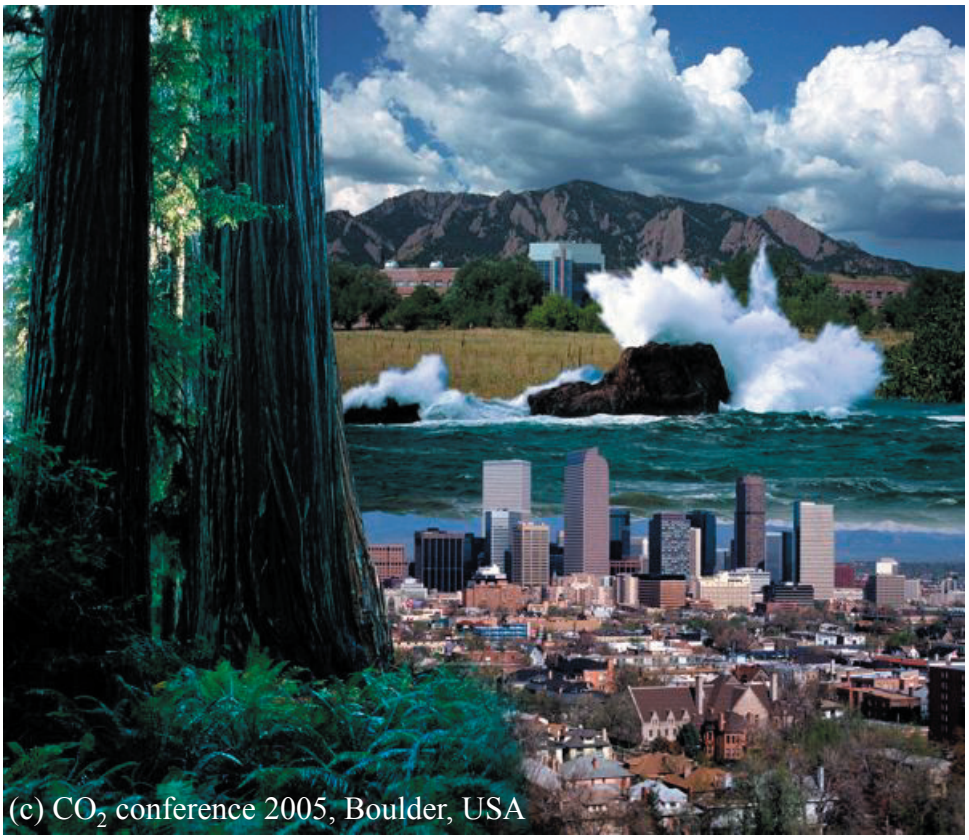

Constraints of Satellite Derived CO_2 on Carbon Sources and Sinks

by

Yogesh Kumar Tiwari

ISSN 1615-7400

MAX-PLANCK-GESELLSCHAFT

Technical Reports - Max-Planck-Institut für Biogeochemie 7, 2006

Max-Planck-Institut für Biogeochemie
P.O.Box 10 01 64
07701 Jena/Germany
phone: +49 3641 576-0
fax: + 49 3641 577300
http://www.bgc-jena.mpg.de

Technical Reports - Max-Planck-Institut für Biogeochemie 7, 2006

Constraints of Satellite Derived CO_2 on Carbon Sources and Sinks

Dissertation zur Erlangung des Doktorgrades der Naturwissenschaften im Fachbereich Geowissenschaften der Universität Hamburg

vorgelegt von

Yogesh Kumar Tiwari
aus Allahabad, Indien

Hamburg 2005

ISSN 1615-7400

Yogesh Kumar Tiwari
Max-Planck-Institute for Biogeochemistry
Hans-Knöll-Str. 10
07745 Jena
Germany

Ph.D. Thesis Supervisors
Dr. Manuel Gloor, *University of Leeds, U.K.*
Prof. Dr. Martin Heimann, *Max-Planck-Institute for Biogeochemistry*
Dr. Christian Rödenbeck, *Max-Planck-Institute for Biogeochemistry*

Ph.D. advisory committee chair
Dr. Sander Houwling, *Space Research Organisation, The Netherlands*

Als Dissertation angenommen
vom Fachbereich Geowissenschafter der Universität Hamburg

auf Grund der Gutachten von
Prof. Dr. Hartmut Graßl
und
Prof. Dr. Martin Heimann

Hamburg, den 7. Februar 2006
Prof. Dr. Helmut Schleicher
Dekan des Fachbereiches Geowissenschaften

Constraints of Satellite Derived CO_2 on Carbon Sources and Sinks

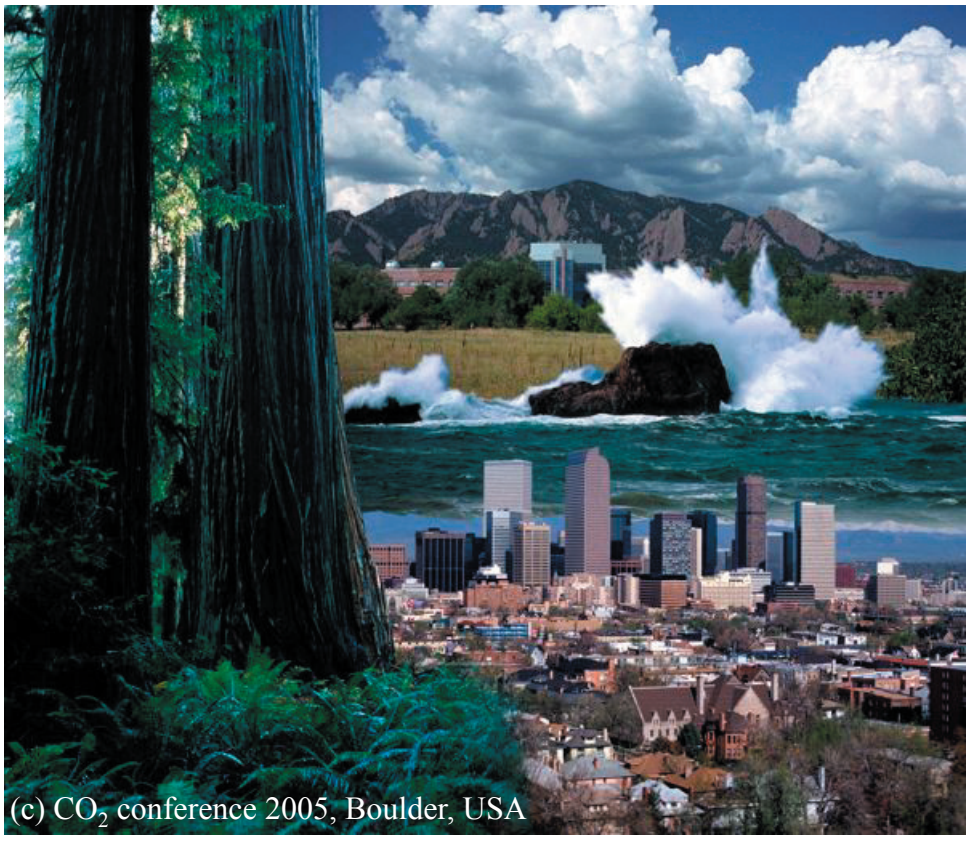

Yogesh Kumar Tiwari

Hamburg 2005

Abstract

This study aims to establish the understanding required to use the satellite derived CO_2 concentration data to constrain surface sources and sinks using inversions of atmospheric transport combined with atmospheric concentration data. CO_2 mixing ratio estimates have recently been derived from space-borne measurements with the TOVS instrument on-board NOAA-11 satellite during 1987-1991 and with the AIRS instrument on the recently launched AQUA satellite during January 2003 to December 2003. Here these satellite retrievals are evaluated through a comparison against modeling results, using two different transport models with surface fluxes optimized to fit surface CO_2 observations.

The TOVS model CO_2 comparison reveals that the RMS (Root Mean Square) difference between retrieval and simulation is around 2 ppm whereas it is only 0.3 ppm between models and is ~0.5 ppm between model and in-situ comparisons when tropics are excluded. In the tropics surface data are very sparse and thus fluxes quite uncertain. Based on a limited set of airborne observations and model simulation, the estimated error (random and bias) in the TOVS monthly product is found to be roughly six times larger than the accuracy needed for improving surface CO_2 flux estimates using an atmospheric approach. The TOVS-model prediction comparison study suggests that confrontation with independent upper air concentration data would be useful to assess more precisely the performance of the models and to exclude unrealistic model transport as reason for model retrieval differences.

The AIRS-model comparison study reveals that simulations of atmospheric CO_2 with both models are much closer to each other than the retrievals. Again there are many features in the retrievals that are difficult to explain from process understanding. This study also raises the question about lower-to-upper troposphere transport pathways and its representation in transport models to rule out biases in model transport as cause of the differences.

As both comparisons suggest to verify model predictions in the upper troposphere with upper air in-situ observations we performed such a study using upper air CO_2 measure-

ments from aircraft campaigns. The comparison shows that model predictions are in good agreement with the long term upper troposphere CO_2 airplane observations. Even short-term transport events as well as longer-term anomalies are well captured. Vertical structures of observed profiles agree also well with simulations but in the tropics absolute magnitudes are often underestimated – the region where surface fluxes used in the model predictions are particularly uncertain.

Overall the study reveals that remotely sensed CO_2 using channels in the thermal infrared exhibit large biases and thus cannot be used to constrain carbon sources and sinks at this stage. However upcoming dedicated missions which focus on the near-infrared region may be more promising. Transport models successfully validated for lower-to-upper troposphere transport are now ready for this purpose.

Acknowledgements

It has been a privilege and motivation to work at the Max Planck Institute for Biogeochemistry (MPI-BGC), Jena, Germany.

I am very much thankful and grateful to my supervisor Prof Martin Heimann (Director, MPI-BGC, Jena), who made a large contribution towards completion of this thesis and gave many good suggestions. He was also personally an enormous help for me. I always found an image of my parents in his personality.

I am very much thankful and grateful to Dr Manuel Gloor (University of Leeds, U.K.) who provided the main scientific guidance for this thesis. Without his guidance and support this work would not have been possible. With his motivating enthusiasm for nature and his profound knowledge of our field he has been an excellent coach. His guidance continuously kept this work on track.

This thesis would not have been possible without the financial support from projects "(COCO) (EVG1-CT-2001-00056), Measuring CO_2 from space exploiting planned missions 2001-2004", and "(EVERGREEN) (EVG1-CT-2002-00079), EnVisat for Environmental Regulation of GREENhouse gases". I am very grateful to project coordinators.

Discussions with Dr Christian Rödenbeck (MPI-BGC, Jena) were invaluable. He always guided my work whenever I needed. I am thankful to him.

I am thankful to my PhD advisory committee (PAC) members and its chair person Dr Sander Houweling (SRON, The Netherlands) for his valuable guidance during all the PAC meetings.

I am thankful to Stefan Körner and Jens Schumacher (MPI-BGC, Jena) for their valuable suggestions and helps.

I am thankful to Karen Schindler (MPI-BGC, Department Secretary) for her supports in non-scientific problems.

I am thankful to the International Max Planck Research School (IMPRS), for Earth System modelling, Hamburg and its coordinator Dr Antje Weitz for her valuable support from time to time.

I am thankful to the computing centers DKRZ, Hamburg and GWDG, Göttingen who provided the computing facilities for this work.

I am thankful to my friends in Hamburg, Abhay, Luca, Manu, Manik, and Semee for their helps and warm reception during my Hamburg trips. A special thanks to Abhay who helped me in thesis printing and binding.

I thank my Grandparents for their great encouragements. I am thankful to my Parents for their life-long moral supports.

I want to convey thanks to those persons who have, directly or indirectly, provided support in my research work and whose names I forgot to mention here.

In the last, but not least, I am thankful and grateful to my wife Dr. Suman Tiwari and my four year old sweet daughter Arushi Tiwari. They are my inspiration, without their help and patient support nothing would have been possible for me.

Contents

List of Tables

List of Figures

Chapter 1

1. Introduction

1.1 Motivation

1.1.1 Carbon dioxide, global carbon cycle and climate

Carbon dioxide is a greenhouse gas. It is a strong absorber in the spectral range of thermal long-wave radiation emitted from the earth surface and thus it increases the opacity of the atmosphere in this spectral range. As incoming solar radiation and outgoing thermal radiation must balance and outgoing long-wave radiation is proportional to the fourth power of the earth's surface temperature (Stefan-Boltzmann law), CO_2 in the atmosphere increases earth's surface temperature compared to a CO_2 free earth atmosphere. To a given greenhouse gas composition of the atmosphere corresponds a stationary state or energy balance with a given earth surface temperature. An increase in atmospheric CO_2 leads to a new stationary state with increased earth surface temperature. Such a change in atmospheric greenhouse composition is currently ongoing due to human activity: fossil fuel burning, cement manufacture and deforestation. Among the greenhouse gases of anthropogenic origin, the increase of atmospheric carbon is of particular concern because carbon is not removed from the atmosphere by chemical reactions in the atmosphere in contrast to other greenhouse gases.

On time-scales relevant to humans carbon is cycled mainly between three reservoirs: the oceans, organic matter on land, and the atmosphere (Figure 1.1). In the atmosphere carbon is predominantly in gaseous form, while in the oceans carbon it is either dissolved (dissolved inorganic carbon DIC), in form of organic matter or of planktonic calcium carbonate shells. Deep ocean DIC is by far the largest reservoir of the three (Figure 1.1).

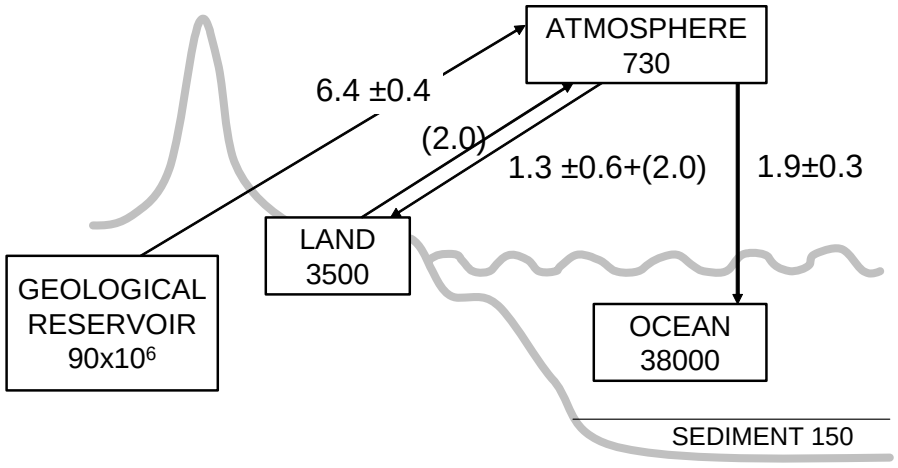

Adapted from IPCC (2001)

Figure 1.1: Carbon reservoirs (PgC) and net exchange fluxes ($PgCyr^{-1}$).

There is a strong link between atmosphere, land biota and soils, and upper ocean carbon reservoirs. The carbon exchange time-scale between upper and deep ocean is set by the replacement time of deep ocean waters which is on the order of hundreds of years [e.g. *Stuiver et al.*, 1983]. This is also the time-scale for eventual ocean uptake of anthropogenic carbon.

In an unperturbed system the oceans take up carbon at high latitudes, and release carbon in the tropics reflecting the temperature dependence of CO_2 solubility in sea water. During photosynthesis carbon is taken up from the atmosphere by land vegetation. During the rest of the year carbon dioxide is respired from dead plants and soils, and reenters the atmospheric reservoirs. Gross fluxes (one way fluxes) of carbon dioxide between the three reservoirs are larger than carbon release to the atmosphere due to human activities but they are almost in balance on an annual basis.

1.1.2 Science history of atmospheric carbon dioxide

Carbon dioxide was first noted in 1754 by the physician Joseph Black [*Jaffe, 1942*]. That atmospheric molecules absorbing thermal radiation emitted from the earth surface lead to an increase of the earth's near surface temperature has been realized nearly 200 years ago [*Fourier*, 1824]. In the second half of the 19th century it was demonstrated by John Tyndall that CO_2 is a strong absorber of thermal radiation emitted from earth's surface [*Tyndall*, 1863]. This lead to the conclusion soon after that CO_2 released by human activity has the potential to lead to a warming of the earth's surface. More recently simulations of atmospheric radiative transfer of various details have indicated that among all anthropogenic greenhouse gases CO_2 contributes the most to greenhouse warming on earth (approximately 50 %) [*Manabe & Strickler*, 1964; *Hansen et al.*, 1988; *IPCC Report*, 2001]. First atmospheric CO_2 measurements are described in the nineteenth century literature [*Callendar*, 1958]. Prior to the late 1950's, atmospheric concentration of CO_2 has been thought to exhibit significant variability until precise and accurate measurements utilizing infrared absorption and monometric technique were initiated by C. D. Keeling at Mauna Loa (Figure 1.2) [e.g. *Vay et al.*, 1999]. C. D. Keeling and subsequently other measurement groups have thereafter extended atmospheric CO_2 measurements to a global network (Figure 1.4). In parallel pre-industrial levels of CO_2 have been reconstructed from CO_2 entrapped in air bubbles in ice cores from Greenland and Antarctica [e.g. *Leuenberger et al.*, 1988].

1.1.3 Atmospheric carbon dioxide measurements

Ice-core and atmospheric carbon dioxide records reveal that CO_2 has been steadily increasing over the last 200 years (Figure 1.2). Values in Figure 1.2 are given in parts per million or ppm = 10^{-6} mol CO_2 / mol dry air. Meanwhile CO_2 has become the largest contributor among all anthropogenic greenhouse gases to warming of the global climate [*IPCC*, 2002]. Besides the fast growth of atmospheric carbon the Mauna Loa atmospheric record of C. D. Keeling reveals also a seasonal cycle caused by the increased uptake of CO_2 by plants in the northern hemisphere during summer and subsequent release by respiration of dead organic matter during the rest of the year. It also reveals interannual variation in the growth rate of atmospheric CO_2.

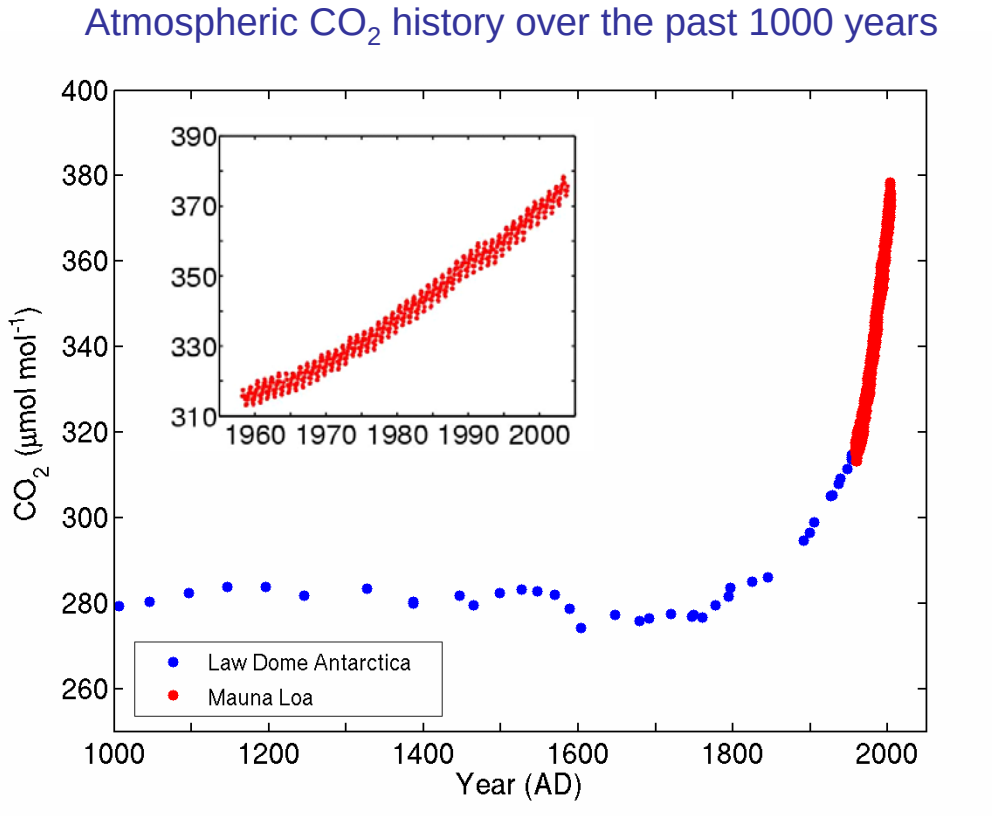

Figure 1.2: Atmospheric CO_2 history over the past 1000 years.

Over the last 50 years approximately 56 % of anthropogenic carbon emitted to the atmosphere, known from national energy statistics, have accumulated in the atmosphere (Figure 1.3). The difference in CO_2 between the anthropogenic perturbation and atmospheric accumulation has entered either the oceans or land pools. According to the carbon cycle summary in Figure 1.1 approximately two-thirds have been taken up by the oceans and one-third by land over the period from 1990-1999. As deforestation fluxes largely from the tropics are on the order of 1-2 PgC yr^{-1} a land sink over this 10 year period on the order of 2-3 PgC yr^{-1} is implied. However neither location nor nature of this land sink is well understood. Similarly consequences for land carbon pools by a warming climate is not well understood and thus prognoses are difficult to make. Different response scenarios are imaginable. Increase in carbon dioxide concentrations could increase plant

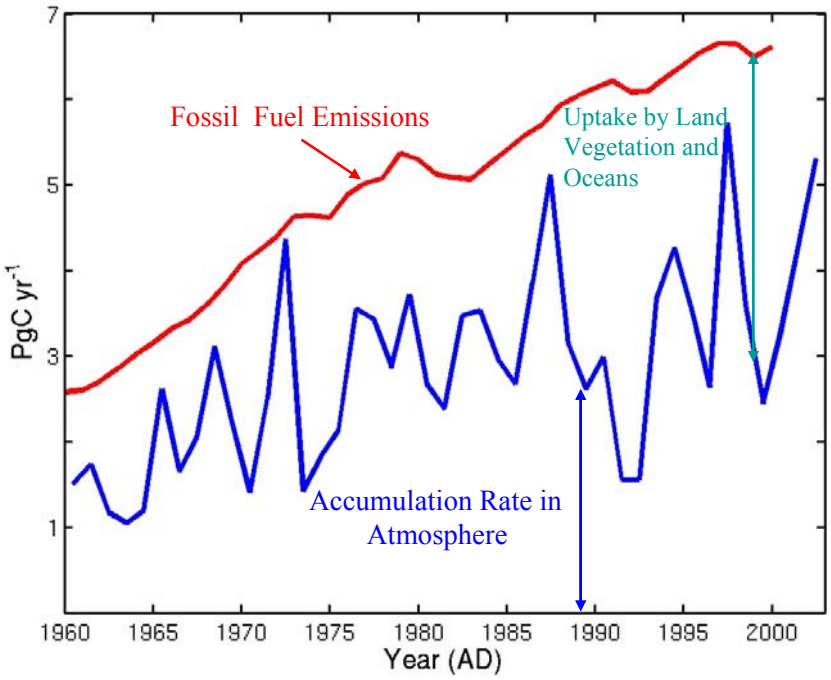

Figure 1.3: Fossil fuel emissions and atmospheric carbon inventory

photosynthesis. On the other hand, increase in temperature could increase soil respiration rates, which would reduce carbon storage in soils. Changes in climate such as decreased rainfall could also reduce plant photosynthesis and thus the ability of vegetation to sequester carbon. Given these uncertainties it is important to be able to observe and understand ongoing carbon pool changes.

To reduce future climate change attempts are being made to reduce anthropogenic CO_2 emissions. On a governmental level, emissions targets are being negotiated. For example, the Kyoto protocol [United Nations Framework Convention on Climate Change] was initiated in 1997 and came into force on 16 February, 2005. This treaty has been signed by 141 countries by 2004. The industrialized countries have committed to cut their emissions by 5.2% by 2012, relative to the reference year 1990, however the verification of the emission targets is a challenge. In summary both from a political and scientific point of view there is a growing need for the capability to locate and estimate CO_2 sources and sinks.

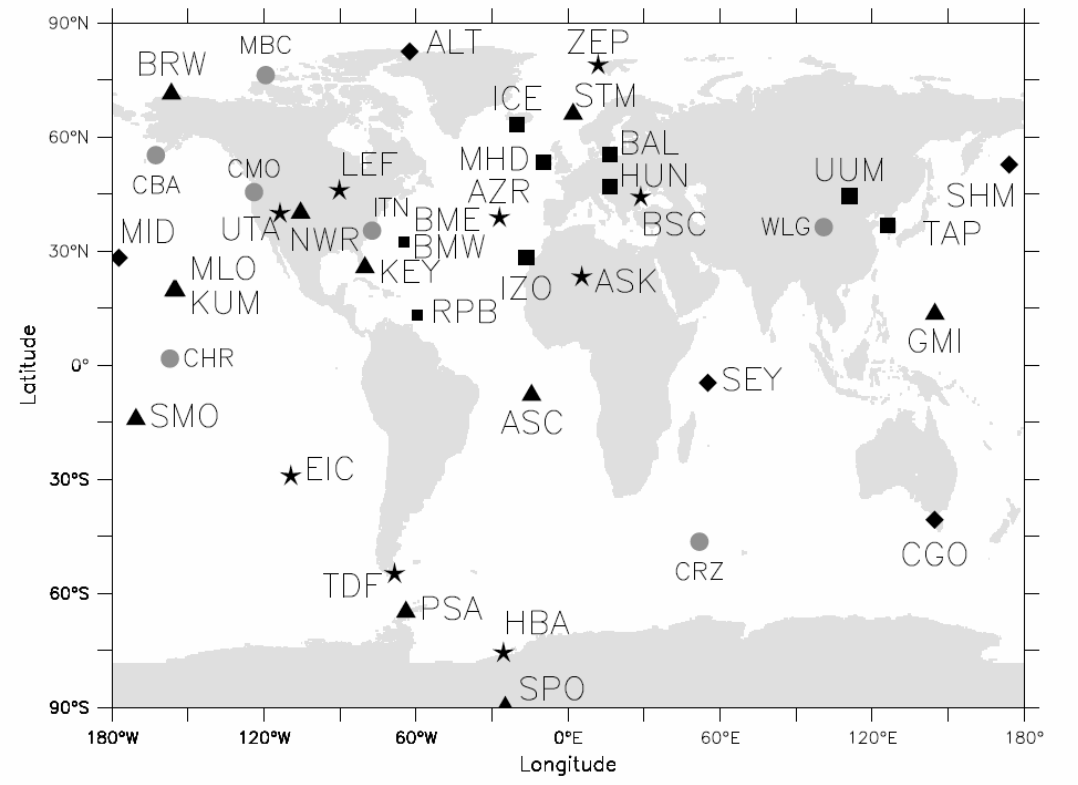

Figure 1.4: Locations of the atmospheric CO_2 measurement sites.
(Courtesy: Rödenbeck et al., 2003)

1.2 Atmospheric approach to constrain carbon sources and sinks

Inverse modeling of atmospheric transport provides, in principle, a means for flux monitoring [*Rayner et al.*, 1999; *Bousquet et al.*, 2000; *Gurney et al.*, 2002; *Rödenbeck et al.*, 2003]. The basic concept of inverse modeling of atmospheric transport to estimate surface sources and sinks can be described conceptually as follows. Atmospheric tracer transport is linear therefore we can write the effect of atmospheric transport on surface fluxes on resulting atmospheric concentrations c as a transport matrix T acting on fluxes

$$c = Tf + C_0 \qquad (1.1)$$

The elements of the vector c are atmospheric concentration observations (in space and time), and the elements of the vector f are sources distributed in space and time. C_0 is

the initial concentration at the beginning of the simulation period. The elements of the matrix T may be interpreted as the sensitivities of the observed concentrations to the surface fluxes. The dimensions of the matrix T equal the number of flux components times the number of observables. The inverse problem consists of inverting the above equation to find a solution for the fluxes f. The inversion of the above equation requires two steps; first, the transport matrix T has to be computed with a transport model and second, the linear equation system has to be solved for the fluxes. Since the source and sink processes are heterogeneous in space and time a possible approach is to solve for a large number of surface fluxes equivalent to high spatial resolution of the fluxes. Since the observables are limited on the global scale T becomes a rectangular matrix with much larger number of columns than rows. In this case the source inference problem is highly underdetermined. Even if the number of source components is restricted to a smaller number than the observations, the equation system is still "ill-conditioned" because of the diffusive nature of atmospheric transport.

An alternative to handle the underdetermined problem without reducing the number of sources (unknowns) is a Bayesian approach, which includes a-priori information in the solution process. Both atmospheric observations and a-priori information are described in terms of Gaussian probability densities. The desired so-called a posteriori flux estimate is then obtained by minimizing the cost function

$$J(f) = (c_{obs} - Tf)^t C_{obs}^{-1} (c_{obs} - Tf) + (f - f_{prior})^t C_f^{-1} (f - f_{prior}) \qquad (1.2)$$

with respect to f. The matrix C_{obs} is the variance-covariance matrix of measurement and modeled uncertainty and matrix C_f is prior flux uncertainty. While a Bayesian approach is a reasonable compromise given the limited set of observations it is not entirely satisfactory as priors are not always based on observations. Therefore results of the approach are currently more of a qualitative than quantitative nature.

So far all inverse modeling studies are based on available observations from a sparse surface network which is biased towards the ocean locations [*Bakwin et al.*, 1995; *Gloor et al.*, 2000] and to the earth's surface. The number of stations with regular measurements was until recently on the order of 50-70 (Figure 1.4).

Table 1.1: Characteristics of different satellite instruments

Satellite Instruments	Characteristics
TOVS	Crosses equator at 1:30 pm local time, scan width 2200 km wide, global coverage every 12 hrs, 20 channels in the 4.3-15μm spectral region, spectral resolution between 50 and 100 cm^{-1}, optical Field of View(FOV) is 1.25^0 which gives a ground Instantaneous Field of View (IFOV) of 17.4 km diameter at the nadir.
SCIAMACHY	Crosses equator at 10:00 am local time, foot print 30x60 km^2, spectral range 240nm-2380nm with 0.22nm-1.48nm spectral resolution, Field of View (FOV) $+/-0.003^0$ - $+/-0.200^0$.
AIRS	Crosses equator at 1:30 am, 1:30 pm covering globe twice a day, spectral region 3.7 μm to 15 μm with spectral resolution of $\lambda/\Delta\lambda$=1200, recording 2378 channels, FOV 1.1^0, nadir foot print 13 km at surface, scan angle -49^0 to $+49^0$.
OCO	Equator crossing at 1:15 pm, spectral region 1.61-2.06 μm with resolving power(spectral resolution) R= $\lambda/\Delta\lambda$~21000, FOV 10 km wide, foot print 10 km^2
GOSAT	Spectral region 1.6-2 μm with spectral resolution 0.1-0.3 cm^{-1}, FOV 5-8km

A primary reason for the sparse network is the high accuracy and precision of the measurements required as large-scale source sink signals are small (on the order of few ppm for annual mean concentrations). These measurements are intensive in labor, infrastructure and expertise.

A new perspective has emerged recently with the advent of satellite remote sensing of CO_2. The value of space based data for the CO_2 transport inverse problem lies primarily in the large increase in temporal and spatial coverage and the ability to sample areas that have been difficult to sample until now, such as the tropical troposphere. It may therefore have the potential to strongly increase the value of the atmospheric inversion flux estimation approach.

The first CO_2 estimate derived from space borne measurements was obtained using the Television Infrared Observation Satellite (TIROS-N) Operational Vertical Sounder (TOVS), NOAA series satellite flown in 1984 [*Chedin et al.*, 2003]. In the series of re-

cent products *Engelen and McNally* [2005], retrieved atmospheric CO_2 from AIRS (Atmospheric Infrared Sounder) radiances during the year 2003. AIRS is flown on NASA, Aqua satellite since May, 2002.

Recently, one more satellite instrument has been examined for retrieving CO_2, the SCIAMACHY instrument (Scanning Imaging Absorption Spectrometer for Atmospheric Chartography) [*Buchwitz et al.,* 2004]. SCIAMACHY is flown on ENVISAT, ESA (European Space Agency) platform launched in March, 2002.

There are also planned missions dedicated to CO_2: OCO (Orbiting Carbon Observatory) from NASA, planned for 2007 [*Crisp et al.*, 2004], and GOSAT (Greenhouse gases Observing Satellite) from Japan, planned for 2008. The characteristics of all above satellite instruments are given in Table 1.1. The concept of CO_2 retrieval process is summarized in chapter 2 of this thesis.

1.3 Aim of this Ph.D. thesis

While the advent of CO_2 retrievals from space is very exciting the recent retrievals should still be viewed as experimental in nature. It is unclear at which spatial and temporal scale spaceborne estimates are reliable and add information to our knowledge about the carbon cycle. It is therefore important to confront and analyze these recent satellite retrievals with our best knowledge and expectations of atmospheric CO_2 before drawing conclusions about carbon sources and sinks based on them. The validation process is of great interest not only to improve our current knowledge of the carbon cycle but also to better design the evaluation of upcoming missions like OCO and GOSAT dedicated to CO_2 and to interpret these data once available.

This thesis is dedicated to the investigation of accuracy and information content of the first spaceborne estimate of atmospheric CO_2 concentration retrieved from TOVS between July 1987 to June 1991, and CO_2 estimates from AIRS retrievals, January 2003 to December 2003. As both AIRS and TOVS are sensitive to CO_2 in the upper troposphere only, an important component of the work has been to quantify and understand the realism of lower-to-upper troposphere transport simulated by atmospheric transport models as well.

1.4 Contents of the Ph.D. thesis

The contents of the thesis are arranged as following:

Chapter 2 deals with the comparison of AIRS retrievals with two different atmospheric transport models using the same surface fluxes. The comparison shows good agreement in some carbon cycle features like seasonal cycles, however agreement is not so good with regards to others. Agreement between the two model predictions is closer than between model predictions and retrievals. This poses the question whether lower-to-upper troposphere model transport is biased in both models or whether the retrievals are biased.

In *Chapter 3* we present comprehensive comparisons between TOVS retrievals and two different model predictions. Some upper troposphere airplane data are used as well, to check the accuracy of the TOVS estimates and model predictions. Again model predictions are closer to one another than to the retrievals. In this case the retrievals are even more different than for the AIRS retrievals.

Both studies above suggest that lower-to-upper troposphere transport simulated by models needs to be investigated to rule out the possibility that the simulation retrieval differences are due to transport biases which is the goal of the study presented in *Chapter 4*.

In *Chapter 5* the results from the three chapters are shortly recapitulated and an outlook is given for the use of satellite retrievals to improve the atmospheric inversion approach to constrain carbon sources and sinks at the Earth surface.

1.5 Publications

Chapter 2 and *Chapter 3* are based on the manuscripts which have been submitted for publication. *Chapter 4* is based on a draft of another article which is in preparation.

Chapter 2: **Tiwari, Y. K.**, M. Gloor, R. J. Engelen, F. Chevallier, C. Rödenbeck, S. Körner, P. Peylin, B. H. Braswell, M. Heimann (2005), "Comparing CO_2 retrieved from AIRS on the AQUA satellite with model predictions: implications for constraining surface fluxes and lower–to-upper troposphere transport", Journal of Geophysical Research (JGR), in press.

Chapter 3: Peylin, P., F. M. Breon, S. Serrar, **Y. K. Tiwari**, A. Chedin, M. Gloor, F. Chevallier, C. Rödenbeck, P. Ciais, M. Heimann (2005), "Evaluation of TOVS space-borne CO2 estimates using simulations and aircraft data", Journal of Geophysical Research (JGR), submitted.

Chapter 4: **Tiwari, Y. K.**, et al. (2005), "Evaluation of model simulated lower-to-upper troposphere transport for the purpose of constraining surface sources and sinks using remotely sensed upper troposphere CO_2", is based on a draft of another article, which will be submitted to a peer-reviewed journal, soon.

Chapter 2

Comparing CO_2 retrieved from AIRS on the AQUA satellite with model predictions: implications for constraining surface fluxes and lower–to-upper troposphere transport

Abstract

Large-scale carbon sources and sinks can be estimated by combining atmospheric CO_2 concentration data with atmospheric transport inverse modeling. This approach has been limited by sparse spatio-temporal tropospheric sampling. CO_2 estimates from space using observations on recently launched satellites (AIRS), or platforms to be launched (IASI, OCO) have the potential to fill some of these gaps. Here we assess the realism of initial AIRS-based mid-to-upper troposphere CO_2 estimates from ECMWF by comparing them with simulations of two transport models (TM3 and LMDZ) forced with one data set of surface fluxes. The simulations agree closer with one another than with the retrievals. Nevertheless, there is good overall agreement between all estimates of the seasonal cycle and North-South gradients within the latitudinal band extending from 30°S to 30°N, but not outside this region. At smaller spatial scales, there is a contrast in the satellite-based retrievals above continents versus above oceans that is absent in the model predictions.

Hovmoeller diagrams indicate that in the models, high Northern hemisphere winter CO_2 concentrations propagate towards the tropical upper troposphere via northern hemisphere high latitudes, while in retrievals elevated winter CO_2 appears instantaneously throughout the northern hemisphere. This raises questions about lower to upper troposphere transport pathways. A prerequisite for the use of retrievals to provide an improved constraint on surface fluxes is therefore a further improvement of retrievals, and better understanding / validation of lower-to-upper troposphere transport and its modeling. This calls for more independent upper troposphere transport tracer data like SF_6, APO ($=O_2+1.1xCO_2$) and CO_2.

2.1 Introduction

Atmospheric CO_2 concentration has risen since pre-industrial times from ~280 ppm to ~380 ppm today, and a halt of the rise is not in sight [*Indermuehle et al.*, 1999; *Conway et al.*, 1994]. The principal reason for this trend is increased emissions associated with human activities, such as combustion of fossil fuel, cement manufacture, and land use change [*Keeling et al.*, 1989]. Carbon dioxide is one of the most important and long-lived anthropogenic greenhouse gases, accounting for more than half of human-induced radiative forcing [*IPCC Report*, 2001]. While much progress in understanding the global carbon cycle has been made, we still lack an adequate understanding of many of the important components of the system. Among them is the nature and spatio-temporal distribution of the land carbon sink implied by atmospheric and oceanic carbon inventories [*Sabine et al.*, 2004] when combined with fossil fuel burning emissions [*Marland et al.*, 1985; *Andres et al.*,1996; *Keeling et al.*, 1989; *Tans et al.*, 1990].

One method to estimate carbon sources and sinks is by inverse modeling of atmospheric transport using CO_2 concentration observations [*Rayner et al.*, 1999; *Bousquet et al.*, 2000; *Gurney et al.*, 2002; *Rödenbeck et al.*, 2003]. The method estimates spatio-temporal fluxes by minimizing the mismatch between modeled and observed atmospheric concentrations (e.g., using least squares). These inverse calculations tend to be unstable, but the inclusion of *a priori* information about fluxes is commonly used to regularize the inversion [*Enting et al.*, 1995]. This Bayesian approach allows simultaneous estimation of an arbitrarily large number of individual fluxes, based on prescribed constraints about

spatial and temporal patterns and their covariance structure. All inverse modeling studies published so far are based on observations from a sparse surface network of atmospheric sampling sites that are furthermore biased towards ocean locations [e.g. *Bakwin et al.*, 1995; *Gloor et al.*, 2000]. The number of surface stations is on the order of 100. In addition, there are continuous records measured on a few tall tower stations, as well as several locations where aircraft are used to measure vertical profiles. Thus, while inversion studies give important insights on the nature of inter-annual flux variability, the magnitude of the estimates remain of a more qualitative rather than quantitative nature [e.g. *Gloor et al.*, 1999], in large part due to the observational sampling issues discussed above and transport model uncertainties.

Satellite remote sensing of CO_2 represents one potential means for extending atmospheric sampling from the surface to the free troposphere, in order to increase the value of the atmospheric inversion flux estimation approach. The value of space based data for the CO_2 transport inverse problem lies primarily in the large increase in both spatial and temporal coverage, and the ability to sample areas that have been difficult to sample until now, such as the tropical troposphere. Indeed, several studies that evaluated potential improvements in the results of atmospheric inversion using such data [*Rayner and O'Brien*, 2001; *Houweling et al.*, 2004] confirmed that carbon flux uncertainties would be reduced substantially, assuming unbiased retrievals with normally distributed errors.

Chedin et al. [2002, 2003] pioneered the retrieval of CO_2 in the upper troposphere from infrared radiances observed on the NOAA Television and Infrared Observation Satellite Next Generation (TIROS-N) Operational Vertical Sounder (TOVS). The retrievals exhibited qualitatively the expected seasonal cycles and spatial gradients, and agreement with aircraft data and with model predictions were quite good [*Chedin et al.*, 2003]. In May 2002, the AQUA satellite, which carries the Atmospheric Infrared Sounder (AIRS) instrument, was launched by NASA. Compared to the HIRS-2 (High Resolution Infrared Sounder - 2) instrument on TOVS, the AIRS instrument samples the infrared spectral region with a much higher spectral resolution. AIRS covers the 3.7μm to 15.4μm region with a spectral resolution of $\lambda/\Delta\lambda$ = 1200 [*Aumann et al.*, 2005], recording 2378 channels. In comparison, HIRS-2 measures 20 channels in the 4.3μm to 15μm spectral regions, with a spectral resolution between 50 and 100. Taking advantage of these new

data, *Crevoisier et al.* [2004] and *Engelen et al.* [2004, 2005] have recently developed methods for atmospheric CO_2 retrieval and have begun to estimate atmospheric CO_2 using data from the AIRS instrument.

These recent retrievals using AIRS data should still be viewed as experimental in nature. It is therefore important to confront and analyze these satellite retrievals with our best knowledge and expectations of atmospheric CO_2, before using them to make conclusions about carbon sources and sinks. While the CO_2 distribution at mid to upper tropospheric levels (the atmospheric region where AIRS is mainly sensitive to CO_2) is heavily undersampled, at least some insight can be gained from simulation results of the expected signal using atmospheric transport models and the most "credible" estimates of surface carbon sources and sinks.

The study we present in this paper is dedicated to a comprehensive comparison of the AIRS retrievals of *Engelen and McNally* [2005], with forward model predictions based on the CO_2 flux estimates of *Rödenbeck et al.* [2003] used as boundary conditions in the TM3 and LMDZ models. We will first give the necessary information on the satellite-based retrievals and CO_2 simulations used here, in order to put the results of the comparisons into perspective. Next, we will discuss in a zonal mean context the upper troposphere CO_2 signal that is expected from a modeling perspective, given our best knowledge of surface processes and atmospheric transport. An analysis of similarities and differences between retrievals and simulation predictions will then be presented, starting from spatially and temporally averaged quantities, and proceeding gradually from coarser to finer-scale spatial features. We will then summarize and discuss the value of the AIRS data to constrain analyses of carbon cycling and tropospheric transport.

2.2 Methods

2.2.1 AIRS CO_2

2.2.1.1 Retrieval approach

AIRS CO_2 retrievals for the year 2003 used in this study were obtained with a column estimation method that was implemented in the ECMWF 4D-Var data assimilation system by *Engelen et al.* [2004, 2005]. The main principle employed is that radiances in the thermal infrared region (3.7µm-15.4 µm) are sensitive to both temperature and, to a lesser

extent, the concentration of CO_2. If temperature profiles can be estimated with high accuracy, then the remaining difference between predicted and observed radiances can be attributed to CO_2 (assuming perfect spectroscopy and radiative transfer modeling) [e.g. *Chedin et al., 2003*; *Crevoisier et al.*, 2003]. More formally, the relation between the radiance observed by the satellite,

$$I_\nu = F_\nu(CO_2, \alpha) + \varepsilon_{meas} \tag{2.1}$$

at a set of frequencies ν, which are selected optimally with respect to signal to noise, is inverted within the framework of the ECMWF 4D-Var data assimilation system. Here, CO_2 stands for the CO_2 profile along the line of sight of the satellite instrument, α represents the remaining parameters that characterize the thermodynamic state and atmospheric condition of the profile, and ε_{meas} is the measurement error. Because inversion of this equation is an ill-posed problem, the following functional

$$J = (I - F_{\mathrm{mod}el})^t S_{meas}^{-1} (I - F_{\mathrm{mod}el}) + (CO_{2,prior} - CO_2)^t S_{prior}^{-1} (CO_{2,prior} - CO_2) \tag{2.2}$$

is minimized instead. Here, $CO_{2,\mathrm{prior}}$ is an *a priori* prescribed CO_2 profile and S_{meas} and S_{prior} are the error covariance matrices of the measurements and of the *a priori* CO_2 profile, respectively. The function *F* is approximated by the solution of the radiative transfer equation for a nonscattering plane-parallel atmosphere in local thermodynamic equilibrium, and is a nonlinear function of the CO_2 profile [see *Engelen and McNally*, 2005]. The other relevant parameters in the radiative transfer equation (temperature, water vapor, and ozone) are initially provided by the model forecast and are adjusted within the assimilation at the same time as CO_2, using various sources of observations. All observations are bias corrected to fulfill the requirement of unbiased Gaussian statistics. The bias correction used by ECMWF is based on one month of radiance model prediction versus observation comparisons. The retrieval results presented here are based on a temporally and spatially uniform prior CO_2 distribution, and with a prior uncertainty of 376 ppm and 30 ppm, respectively. Instrument and observation errors are assumed to be uncorrelated

and to be 0.6 K. Eighteen channels were selected that are sensitive almost exclusively to mid- and upper-tropospheric CO_2. The vertical distribution of the sensitivity of the radiances to CO_2, measured at the 18 frequencies, is given in Figure 2.1 (reproduced from *Engelen and McNally* [2005]).

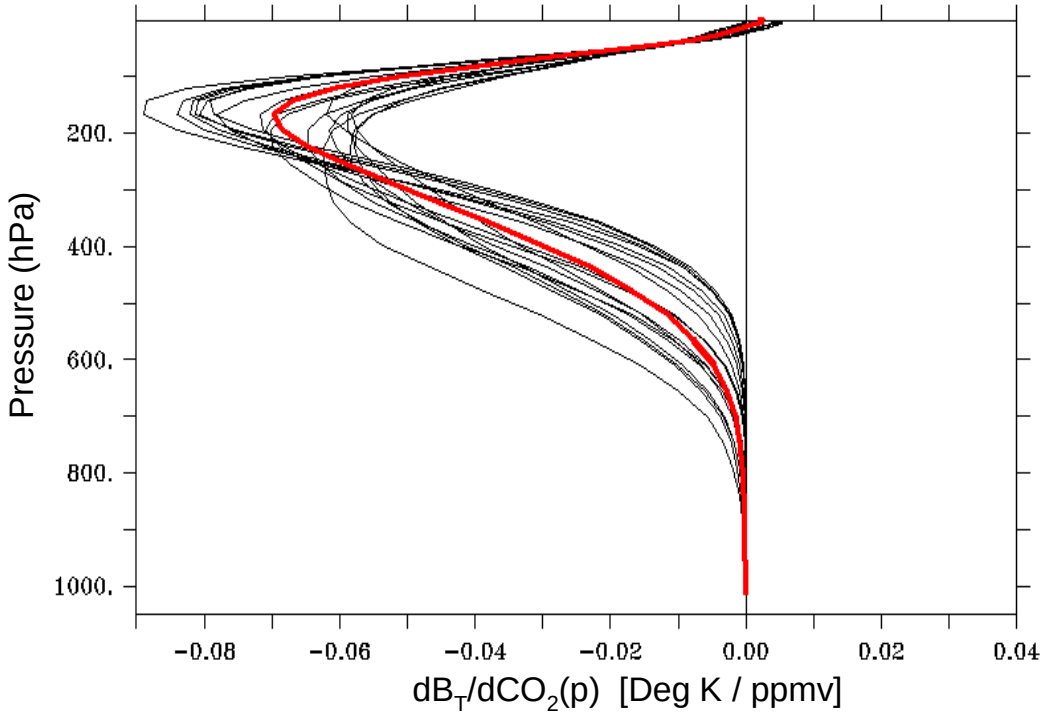

Figure 2.1: *Weighting function for the 18 channels (black) used to retrieve CO_2 (ppm) from AIRS data within the ECMWF weather forecast model, and the mean weighting function (red) used for weighting model concentrations for comparison with AIRS retrievals.*

2.2.1.2 AIRS characteristics and spatio-temporal retrieval coverage

AIRS was launched into a 705 km altitude polar orbit on the EOS Aqua spacecraft on May 4, 2002, and has an expected in-orbit lifetime of seven years. The instrument field of view is 1.1°, corresponding to a nadir footprint of 13.5 km on the surface. The scan angles vary from -49° to +49° [*Aumann et al.*, 2003]. The satellite crosses the equator at approximately 1:30 am and 1:30 pm, resulting in global coverage twice a day.

Most clouds are opaque at the radiance frequencies used in the CO_2 estimation. In order not to lose all information about the atmospheric profile in the presence of clouds, *McNally and Watts* [2003] developed a cloud detection scheme that identifies which

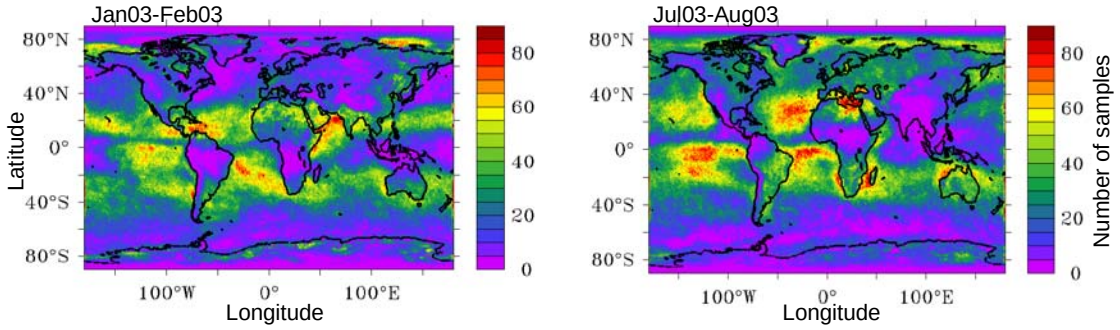

Figure 2.2a: *Number of AIRS retrievals per 1^0x1^0 grid box for two-month period*

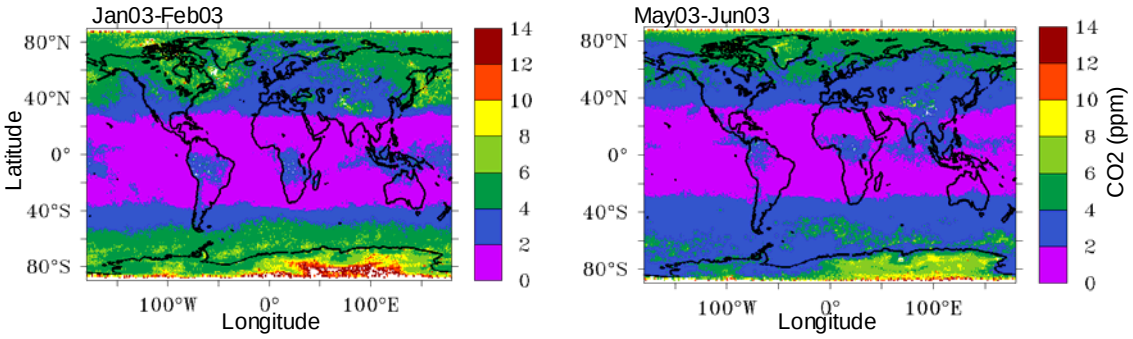

Figure 2.2b: *AIRS retrieval mean tropospheric error per 1^0x1^0 grid box for two-month period.*

channels are not affected by clouds. Within the ECMWF data assimilation system, this scheme identifies and removes those AIRS channels that are affected by clouds, and keeps only those channels which are cloud free. CO_2 estimates were only used when all 18 AIRS CO_2 channels were not affected by clouds. The typical number of uncontaminated data samples observed by AIRS is displayed in Figure 2.2a.

These sampling frequencies range from 10 to 90 per 1° x 1° grid box per month. As expected, the coverage is large in subsidence regions (~50 profiles per month) but very low in the ITCZ region (0-10 profiles per month). The month to month variability of data coverage is low.

2.2.2 Model predictions of atmospheric CO_2

Atmospheric CO_2 is predicted in this study by applying CO_2 fluxes estimated by *Rödenbeck et al.* [2003] as boundary conditions in the atmospheric transport models TM3 [*Heimann and Körner*, 2003] and LMDZ [*Sadourny and Laval*, 1984; *Hourdin et al.*, 1999]. The *Rödenbeck et al.* [2003] fluxes, based on 35 surface stations, cover the period from 1993 to 2001, and are resolved at monthly intervals. These fluxes have been extended to 2003 by averaging the 1993-2001 fluxes on a monthly basis. For the simulations both model simulations start in January 2000 and end in December 2003. For the comparisons, the last year of the simulations (year 2003) is used.

2.2.2.1 Atmospheric transport models

Both atmospheric transport models employed in this study solve the continuity equation for an arbitrary number of atmospheric tracers on a regular grid spanning the entire globe. The horizontal resolution of the TM3 model is 4° x 5° latitude by longitude with 19 sigma-coordinate layers in the vertical. Transport in TM3 is driven by meteorological fields derived from NCEP (National Center for Environmental Prediction) reanalysis [*Kalnay et al.*, 1996]. Tracer advection is calculated using the slopes scheme of *Russell and Lerner* [1981]. Vertical transport due to convective clouds is computed using the cloud mass flux scheme of *Tiedtke* [1989], and turbulent vertical transport is computed using the stability dependent vertical diffusion scheme of *Louis* [1979]. TM3 requires, as input, global fields of vertical diffusion coefficients and cumulus cloud transport fields. The cloud transport fields consist of entrainment and detrainment rates in updraft and downdraft, as well as updraft and downdraft mass fluxes. These are calculated in the preprocessing stage from meteorological analyses of geopotential height, surface pressure, horizontal wind, temperature, and specific humidity. Finally, surface fluxes of latent heat are used [*Heimann and Körner, 2003*] by TM3.

The second atmospheric tracer transport model used in this study is the LMDZ general circulation model (GCM), which is used here with a horizontal resolution of 2.5°x3.75° latitude by longitude and 19 sigma-coordinate layers in the vertical. The model solves the full dynamic equations for winds. The model-calculated winds are then relaxed towards ECMWF analyzed meteorology with a relaxation time of 2.5 hours, in order to force transport to reproduce the observed large scale advection [*Bousquet et al., 2005*]. The model uses the advection scheme of *Hourdin and Armengaud* [1999]. Deep convection is parameterized using the *Tiedtke* [1989] scheme, and turbulent mixing in the boundary layer is based on *Laval et al.* [1981]. The main differences between the two models are firstly the spatial resolution, with TM3 having a coarser resolution than the LMDZ model. Secondly, the LMDZ model is a full GCM that is used in a nudging mode, whereas TM3 is an off-line model which uses analyzed winds for time-stepping the discretized transport equation. The sub-grid scale parameterizations of the two models are rather similar.

2.2.2.2 Surface fluxes

The CO_2 surface fluxes of the *Rödenbeck et al.* [2003] atmospheric transport inversion study vary monthly, and are based on 20 years of atmospheric near surface CO_2 flask data from the NOAA/CMDL station network [update of *Conway et al.*, 1994]. The inverse calculations are based on the TM3 model, and have been regularized assuming exponentially decaying spatial a-priori correlations of the fluxes, in concert with prescribed prior fluxes in a Bayesian framework. The spatial resolution of the fluxes is 8°x10° latitude by longitude. More detailed information is available in the original manuscript [*Rödenbeck et al.*, 2003].

2.2.3 Specifics of model sampling for the comparison of retrieval model simulation

For all comparisons, we restricted ourselves to the latitude band between 60°N and 60°S, because the AIRS retrieval error estimates (Figure 2.2b) become very large at high latitudes, and thus are of limited use for constraining carbon sources and sinks at the surface. To perform a proper comparison between the retrieval and the model simulations, the simulations are sampled at the same locations and same times as the retrievals. For each

AIRS column observation, the model is sampled below the tropopause height because AIRS retrievals are mainly sensitive to the below-tropopause region of the atmosphere. Tropopause height is estimated using the algorithm employed by ECMWF, which is based on the WMO [1957] lapse-rate criterion as implemented by *Reichler et al.* [2003]. The samples are then weighted with the mean weighting function in Figure 2.1. The simulations permit comparison only up to a constant offset. The offset we added to the simulations is the difference between the annual mean AIRS signal and the annual mean weighted CO_2 simulation results, covering the 60° S to 60° N region of the globe.

2.3 Comparison of AIRS retrievals with model simulations

2.3.1 Expected signals and conceptualization of lower-to-upper troposphere transport in the models

The upper troposphere region (where AIRS is sensitive to CO_2) is only indirectly related to surface fluxes via lower troposphere transport, and thus the effect of surface fluxes on concentrations in this region is not entirely obvious. To gain intuition about the nature of signals that are likely to be seen by AIRS, and which transport routes are responsible, it is therefore instructive to consider model predictions. Specifically, we analyzed the latitude-height sections of atmospheric CO_2 for the four seasons (Figure 2.3), using both the TM3 and the LMDZ model. Similar to the situation near the earth's surface, upper troposphere CO_2 is dominated by the interplay between fossil fuel emissions, located mainly in the northern hemisphere mid-latitudes, and the seasonal cycle of carbon release and uptake by the land vegetation in the northern hemisphere. As a result, northern hemisphere upper troposphere concentrations exhibit a clear seasonal cycle that weakens towards the tropics and is largely absent in the southern hemisphere. Compared to the lower troposphere, signals are generally weaker and somewhat lagged, and the regions where N-S gradients are largest are shifted latitudinally compared to the surface region. In the upper troposphere, the largest gradients occur around 30° N and 30° S (this is particularly visible in the upper two panels of Figure 2.3a), while in the lower troposphere gradients are located more to the north at about 50° N. The shift of regions with the largest gradients is a reflection of the effect of tropospheric transport on surface concentrations.

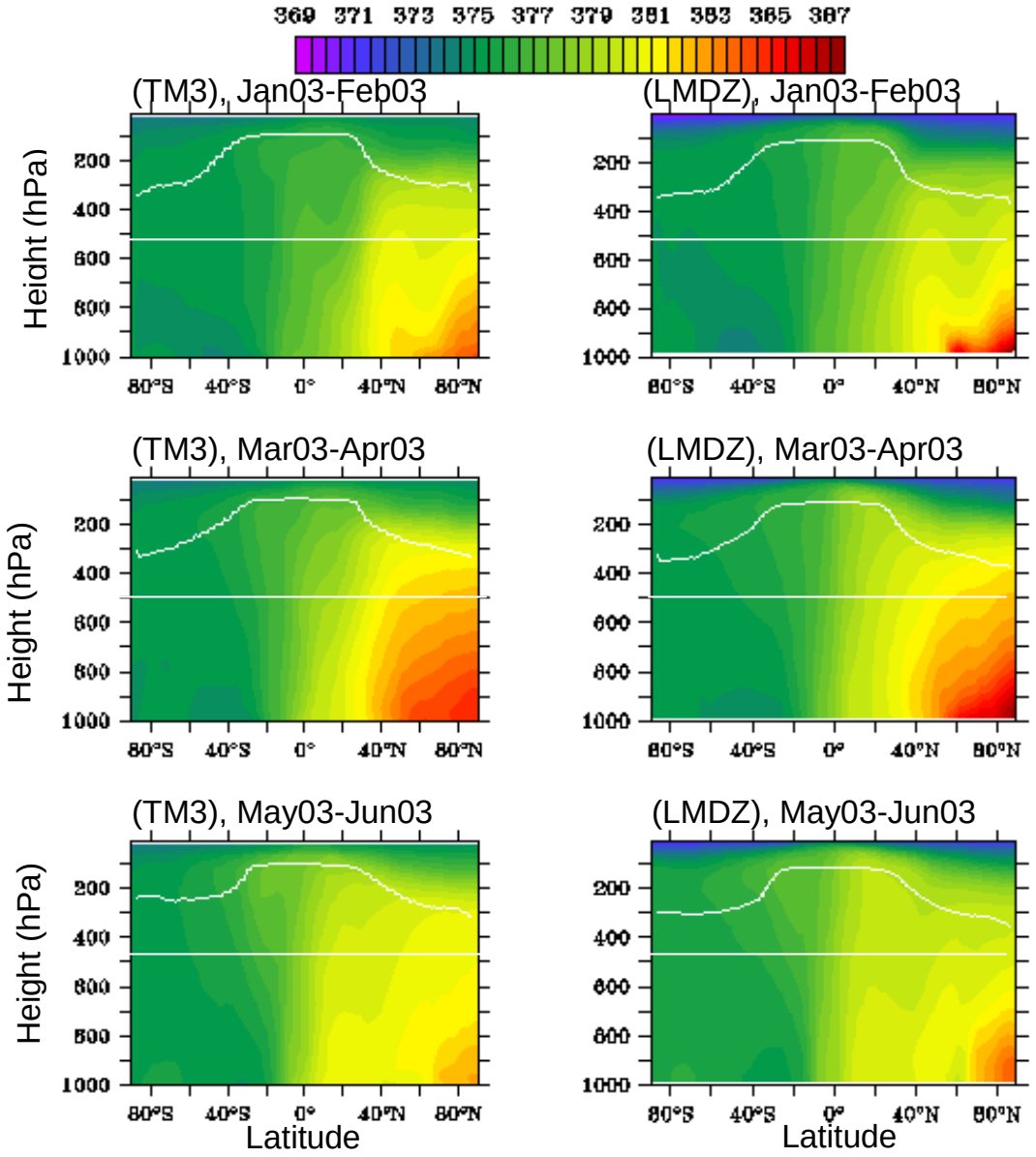

Figure 2.3a: *Vertical distribution of CO_2 mixing ratio (ppm) at 170^0 west longitude during first half of the year 2003 simulated by TM3 (left panels) and LMDZ (right panels). The upper white line delineate the tropopause height and the lower straight white line is the lower boundary to which AIRS CO_2 retrievals are mainly sensitive.*

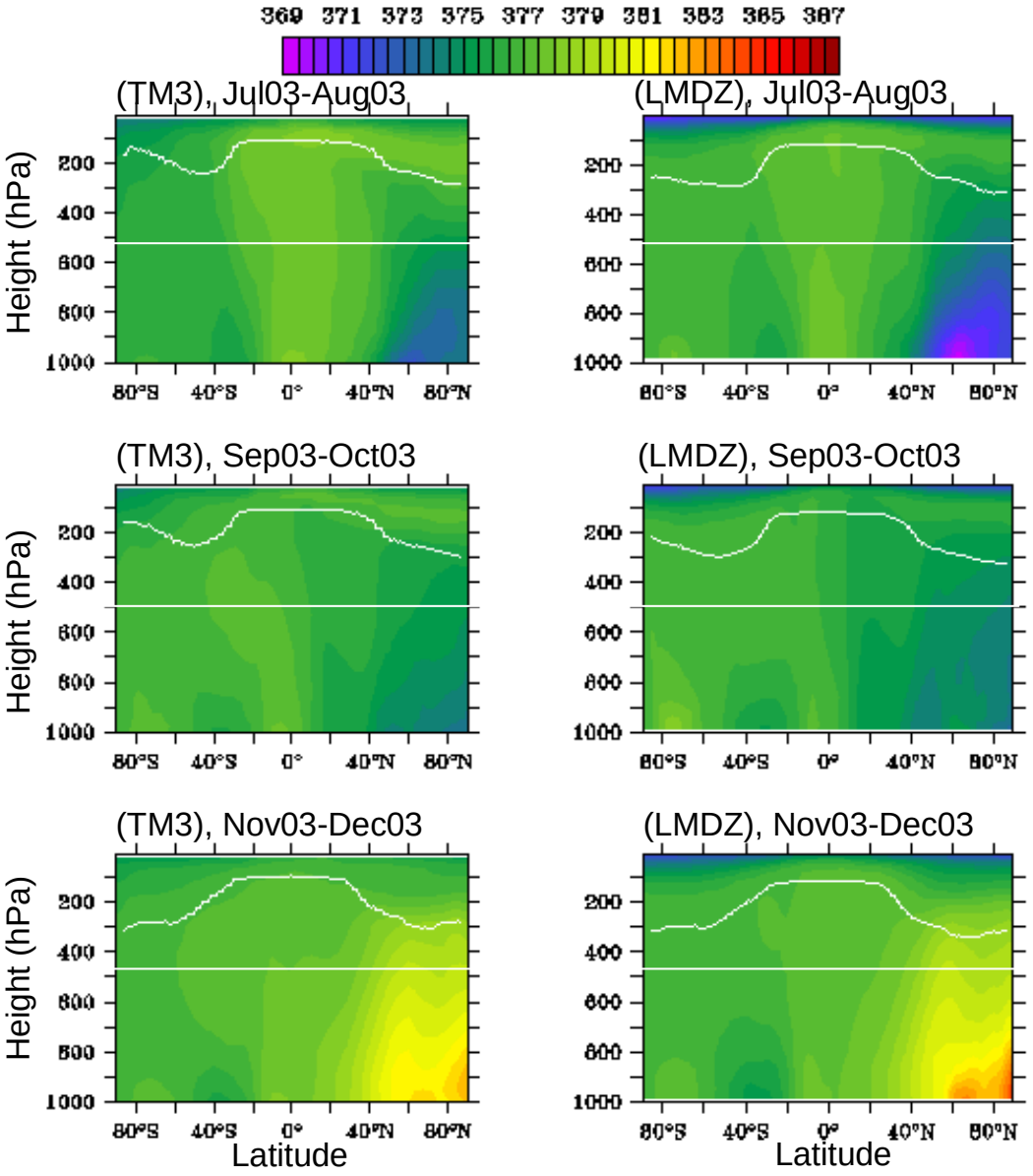

Figure 2.3b: *Same as Figure 2.3a but for the second half of year 2003.*

A tentative conceptual view of pathways from the surface to the upper troposphere in the northern hemisphere region is overlaid on top of isentropes (surfaces of constant potential temperature) calculated from the 2003 NCEP reanalysis [NCEP/NCAR reanalysis data provided at http://www.cdc.noaa.gov/] (Figure 2.4). A comparison with the CO_2 distributions in Figure 2.3 reveals that, in these models, CO_2 isosurfaces tend to be aligned with constant potential temperature surfaces, particularly during summer. This is a reflection that air parcel motion in the mid-to-high latitude free troposphere is, to first order, adiabatic. Equivalently, this indicates that tracer dispersion along isentropic surfaces is much faster than across isentropic surfaces. Largest concentration gradients in the upper troposphere indeed occur where the potential temperature surface curve the strongest, presumably because of the 'potential vorticity barrier' at this location [*Mahlman*, 1997].

A characteristic of the troposphere that is important for transport to the tropical upper troposphere is that potential temperature surfaces in the northern hemisphere mid-latitudes slope differently in the lower troposphere compared to the upper troposphere. As a consequence, one pathway for northern hemisphere mid-latitude air, laden with fossil fuel CO_2, to pass to the upper troposphere is via the northern high-latitudes. Lower troposphere air is dispersed towards the mid troposphere mainly along upward sloping constant potential temperature surfaces and to a lesser degree across isentropes. In the jet-stream region air-masses are mixed across isentropes (and across potential vorticity gradient) by breaking tropospheric cyclone waves where air parcels may disperse along potential temperature surfaces into the tropical upper troposphere [*Mahlman*, 1997].

An alternative pathway is the dispersal of CO_2 laden air in the Planetary Boundary Layer (PBL) towards the tropics, and subsequent transport to the upper tropical troposphere via deep convection. To obtain a measure of the roles played by parameterized tropical convection for lower troposphere – upper troposphere CO_2 transport we have repeated all the model simulations but with parameterized convective transport turned off. Surprisingly the lack of parameterized tropical convection did not change the CO_2 signatures in the upper troposphere to a great extent indicating that the pathway via northern hemisphere mid-to-high latitudes may be most important for lower-to-upper troposphere tracer transport from mid latitudes.

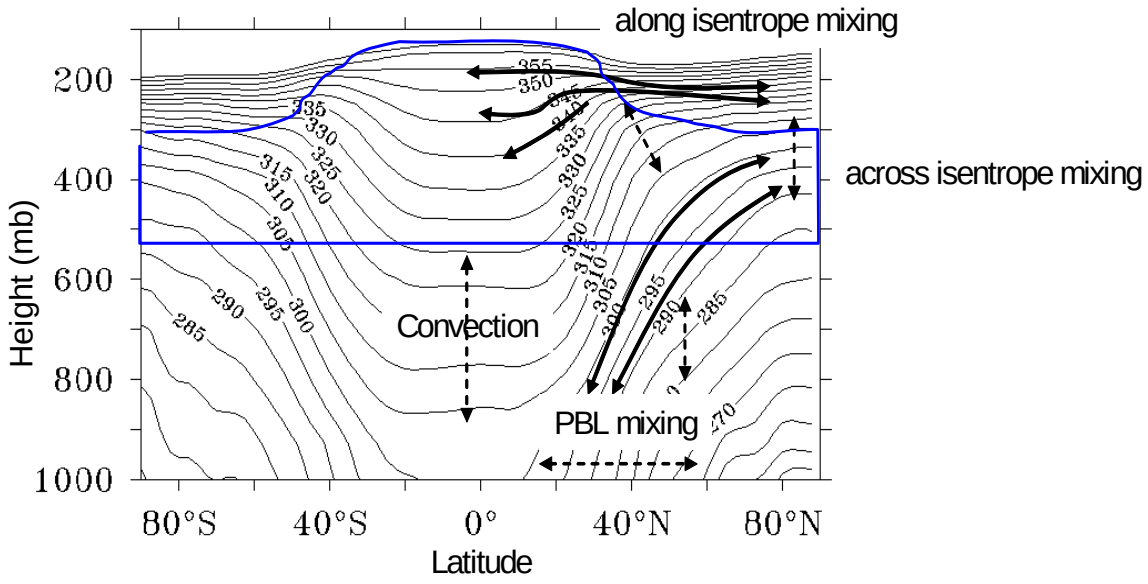

Figure 2.4: *Zonally averaged monthly mean potential temperature (K) for January 2003. Solid arrows show the mixing along the isentropes and dashed arrows show the mixing across the isentropes.*

In summary, from simulations we expect similar seasonality in upper troposphere CO_2 as is observed near the ground, but of a lower magnitude and with time delays compared to the timing of surface fluxes on the order of one month. We also expect the largest concentration gradients around 30° N, based on the atmospheric potential temperature distribution and the differences in simulated upper tropospheric CO_2. However, this result depends upon the relative roles of the two transport branches sketched above.

2.3.2 Comparisons

2.3.2.1 Temporal structure

The lowest order diagnostic, the spatially averaged CO_2 distribution (Figure 2.5), reveals overall a qualitatively good agreement between retrievals and models. The amplitude of the seasonal variation of the signals is very similar. There is a difference in the timing of the increase of carbon dioxide just after the phase of decrease due to summer drawdown, caused by photosynthesis on land. This may be an indication that the models exaggerate the upward propagation of surface signatures during late summer and autumn. Alternatively, surface fluxes may be biased in time, or there may be a bias in the retrievals. One

element that is absent in the AIRS retrievals is the trend caused by continuous burning of fossil fuels. Atmospheric surface concentration records from CMDL show that the growth of atmospheric CO_2 in 2003 was not unusually low. Furthermore, the observed stratospheric CO_2 growth rate generally follows closely the observed growth rate at the earth surface [*Boering et al.*, 1996]. Therefore, atmospheric data seem to support the model simulations rather than the retrievals in this regard.

In order to visualize the degree of agreement and disagreement on a finer, but still somewhat coarse, spatial scale, the monthly mean time-series for a few randomly selected land regions are displayed in Figure 2.6. For the Sahara and Indonesia regions, the agreement is again surprisingly good, while it is low for the Australian desert region. For the Sahara region, there is again somewhat a delay in the phases of increase and decrease associated with the upward propagating seasonal surface signal, compared to simulations. The AIRS-based signal over Australia is less smooth and its seasonality is less expressed. However, the magnitude of the signals is also only approximately half of the signal above the other regions. This may be an indication that time variability smaller than 0.5 ppmv, over regions of the size of the Sahara region, is not resolved by AIRS retrievals. Generally, model simulations are closer to one another than to AIRS retrievals.

Next, we compared zonal mean seasonal signals averaged over 5° latitude bands (Figure 2.7). Amplitudes of the seasonal signal, and its decrease with decreasing latitude, agree well between AIRS retrievals and model simulations. The amplitude of the retrievals tends to be slightly smaller, particularly in the tropics and southern hemisphere. There are, however, some differences in the phasing of the seasonal signals. The onset of the summer drawdown signal simulated by LMDZ in the northern hemisphere, between the equator and 25° N, precedes the retrievals by approximately one month. These, in turn, precede the TM3 simulations by one month.

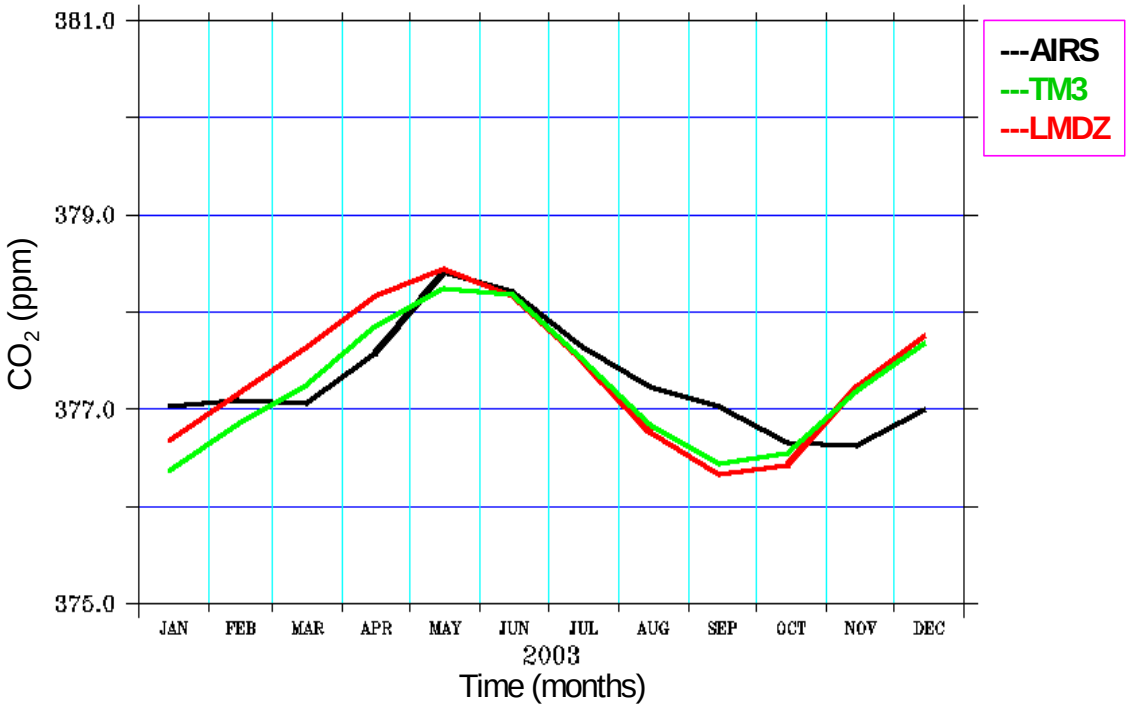

Figure 2.5: *Zonally averaged CO_2 (ppm) between 60^0S and 60^0N as retrieved by AIRS and simulated by TM3 and LMDZ.*

The reason for the different phasing between the models is likely due to differences in lower-to-upper troposphere transport. In particular, LMDZ may communicate surface fluxes too fast to the upper troposphere, while TM3 may be too slow. A possible explanation for model differences may be differences in across isentropical mixing, due to differences in the meteorological fields (NCEP versus ECMWF). A related, but somewhat different, reason may be that the LMDZ model is a full GCM used in a data-assimilation mode, while TM3 uses NCEP meteorological fields directly (i.e. without modifications).

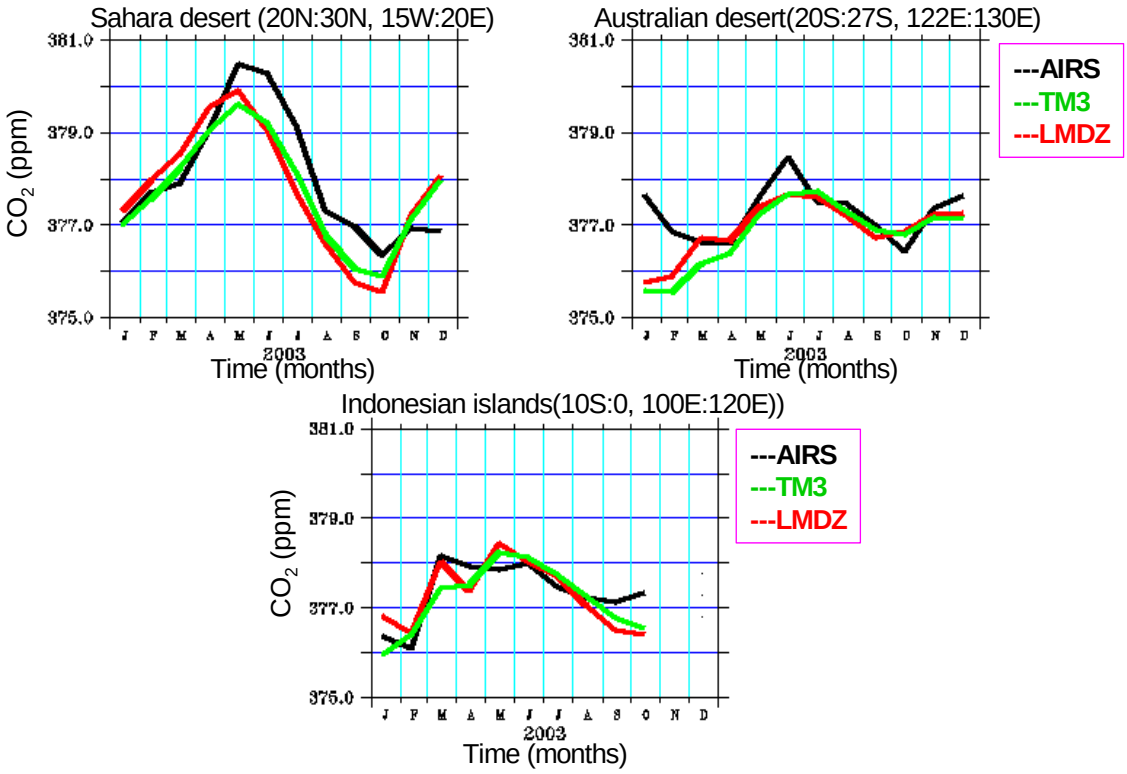

Figure 2.6: *Regionally averaged CO_2 (ppm) as retrieved by AIRS and simulated by TM3 and LMDZ for three selected regions.*

The point at which CO_2 begins to increase again in autumn agrees well between all estimates in the zone from the equator to 25° N, but retrievals lag both simulations by approximately 2-3 months in the tropics and in the southern hemisphere. This may partially be because the tropical and southern hemisphere signals are too small to be resolved by the retrievals. Alternatively, it could be an indication of misrepresentation of transport in the models. A lag is expected if the pathway of the northern hemisphere fossil fuel burning signal towards the tropics is via high latitudes, and subsequently the upper tropo-

sphere. On the other hand, if the northern hemisphere fossil fuel burning signal is dispersed latitudinally, by mixing in the planetary boundary layer first and then communicated to the upper troposphere by convection, the lag is likely to be smaller. This is particularly true in the tropics. It is interesting to note here that over the western Pacific the AIRS retrievals compare very well in terms of amplitude and phase with in-situ flight observations [*Engelen and McNally*, 2005]. A similar picture emerges when comparing zonal mean fields as a function of time (Hovmoeller plot, Figure 2.8). While there is a clear N-S propagation of the northern hemisphere spring maximum CO_2 signal discernible in the TM3 and LMDZ simulations, due to fossil fuel burning and the absence of photosynthesis on land in the winter, the AIRS retrievals reveal a maximum signal that occurs almost instantaneously over the entire latitude range (60°S-60°N). Model sampling sensitivity studies suggest that the difference between the model simulations and the AIRS retrievals could be that AIRS is actually more sensitive to above-tropopause CO_2 than would be indicated by the weighting functions in Figure 2.1. Further analysis of the AIRS estimates indicate that there is a potential for bias outside the tropical area. Depending on the difference between real stratospheric CO_2 values and stratospheric values used in the assimilation radiative transfer model, a bias of up to 2 ppmv can end up in the estimates. This suggests that the use of AIRS estimates outside the tropics has likely to be limited. An alternative explanation is that, in these models, the pathway of northern hemisphere mid latitude fossil fuel burning CO_2 to the upper tropical troposphere is biased towards the high latitude pathway at the cost of the convection mid and low latitude pathway.

2.3.2.2 Spatial gradients and patterns

As will be evident from the comparison of the 2-d spatial patterns, there is a land-sea contrast in the AIRS signals. We therefore consider not only the global zonal mean

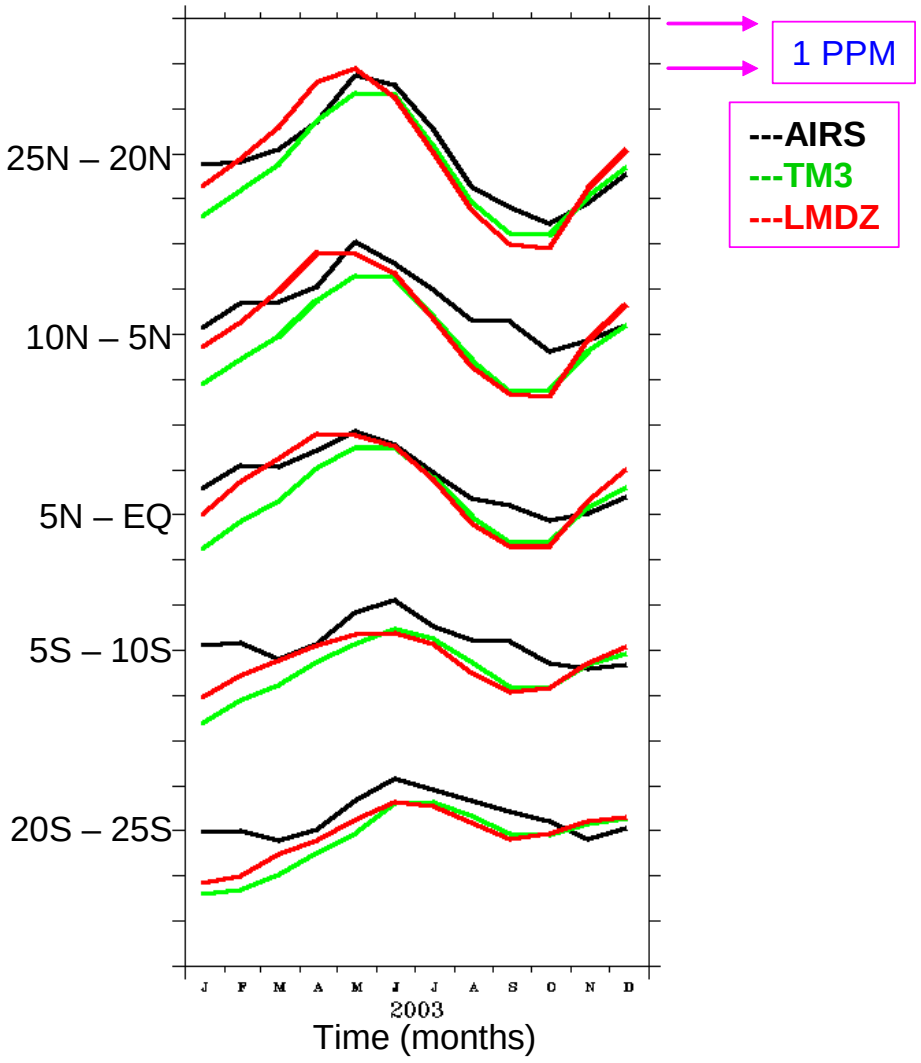

Figure 2.7: *Monthly mean CO_2 concentration (ppm) averaged zonally and over 5^0 latitudinal bands, as retrieved by AIRS and simulated by TM3 and LMDZ.*

gradients but also separately the mean gradients for land and ocean regions (Figure 2.9). Generally, as in the previous comparisons, the inter-model agreement is better than the agreement between the simulations and the AIRS retrievals. Also, differences between model predictions and retrievals are generally larger outside the tropical region extending approximately from 30° S to 30° N possibly because of the increase in retrieval biases outside the tropics mentioned earlier on. Looking into greater detail, there is quite good agreement in the latitudinal gradients during summer and autumn, but there is disagree-

ment north of 30° N during winter and spring, when simulations predict a strong increase around 30° N. The AIRS retrievals do not show such an increase. When comparing signatures over oceans versus land, the discrepancy is larger for ocean regions in the northern hemisphere, while it is larger for land regions in the southern hemisphere. The ocean-land separation reveals that AIRS retrievals are quite different over land compared to the oceans in the extratropics. Furthermore, the temporal variance of AIRS retrievals over land is generally substantially larger than over the oceans, a feature that is not expected from atmospheric transport considerations alone.

We also compared the simulated and retrieved spatial patterns for the four seasons, separately (Figure 2.10a/2.10b). The retrieved CO_2 fields have finer spatial structure and are much less zonally symmetrical than the model simulations, for the reasons mentioned above. During the first half of the year, the simulations exhibit a north-south gradient in the northern hemisphere, but the retrievals do not exhibit such a gradient. The gradient predicted by TM3 is somewhat larger than predicted by LMDZ, indicating that LMDZ is more diffusive than TM3.

There are also some specific features in the retrievals that are suspicious at first sight. During the first 8 months of the year, there is an elevation in CO_2 concentrations over North America that is not shown by the model simulations. Elevated CO_2 values are also seen to the west of Africa during May to June 2003, which is reminiscent of dust blown from the Sahara to the Tropical Atlantic. As already pointed out earlier, this increased CO_2 can either be due to biomass burning, or to an adverse effect of aerosol scattering on the CO_2 estimation. Extensive study of the retrievals in these areas did not reveal any obvious error sources. Further validation needs to be done, but little data for validation is available for these areas during 2003.

2.4 Summary and outlook

The comparisons presented here convey a somewhat mixed message regarding the use of CO_2 from AIRS observations for constraining carbon cycling. On the one hand, the good agreement of key large-scale signatures of atmospheric CO_2, like the seasonal cycle caused by the northern hemisphere land biosphere, or the decrease of the magnitude of this signal with latitude, is encouraging evidence that CO_2 from AIRS observations has

the potential to reveal new aspects of the carbon cycle. The comparisons also indicate that model simulations using two different transport models using the same extrapolated surface fluxes agree more closely with one another than with the retrievals. This raises the possibility that modeled transport is similarly biased in both models. To test this possibility, it is necessary to confront model predictions of upper troposphere tracer concentrations with independent observations. This calls for upper troposphere transport tracer data like SF_6 and APO (Atmospheric Potential Oxygen = O_2+1.1xCO_2), which are currently sparse. At the same time, it forces us to investigate tracer transport from the planetary boundary layer to the upper troposphere in more detail. On the other hand, there are features in the retrievals that cannot be easily explained, and this clearly requires further investigation as well.

CO_2 surface flux estimates based on inversions of atmospheric transport and atmospheric data are very sensitive to systematic errors in the data [*Gloor et al.*, 1999]. The sensitivity to data errors grows strongly with the decrease in the strength of the CO_2 signal, and thus with height above ground. Because of the dilution of surface sources and sinks due to mixing in the troposphere, their signature is substantially degraded in the upper troposphere compared to the planetary boundary layer. As a consequence, surface fluxes estimated using upper troposphere CO_2 will be particularly sensitive to retrieval biases, and therefore any significant bias in the AIRS retrievals are deleterious to the quality of surface flux estimates. We therefore conclude that CO_2 retrieved from space will eventually help to constrain carbon cycling, and will help improve the modeling of transport in the mid and upper troposphere. However, further improvements in the retrievals in concert with independent evaluation of lower-to-upper troposphere transport modeling are a prerequisite.

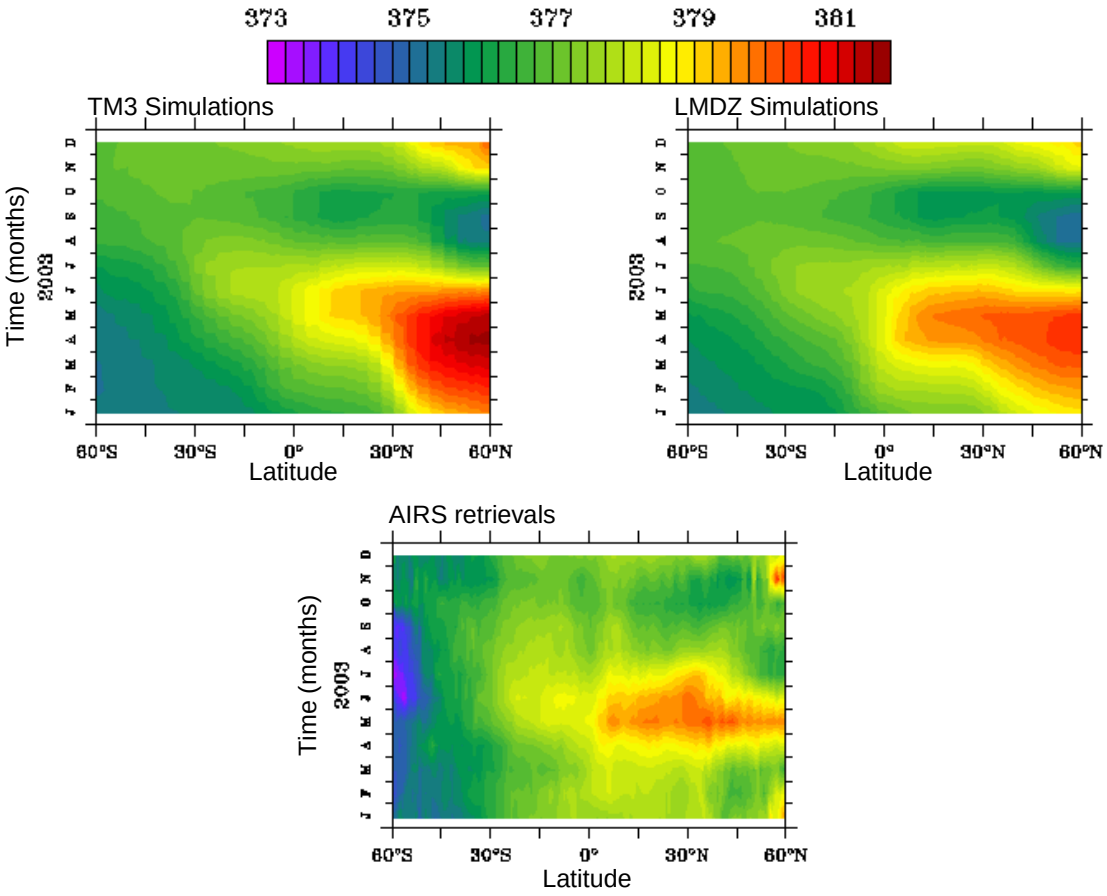

Figure2.8: *Zonal mean CO_2 concentration (ppm) versus time as retrieved by AIRS and simulated by TM3 and LMDZ.*

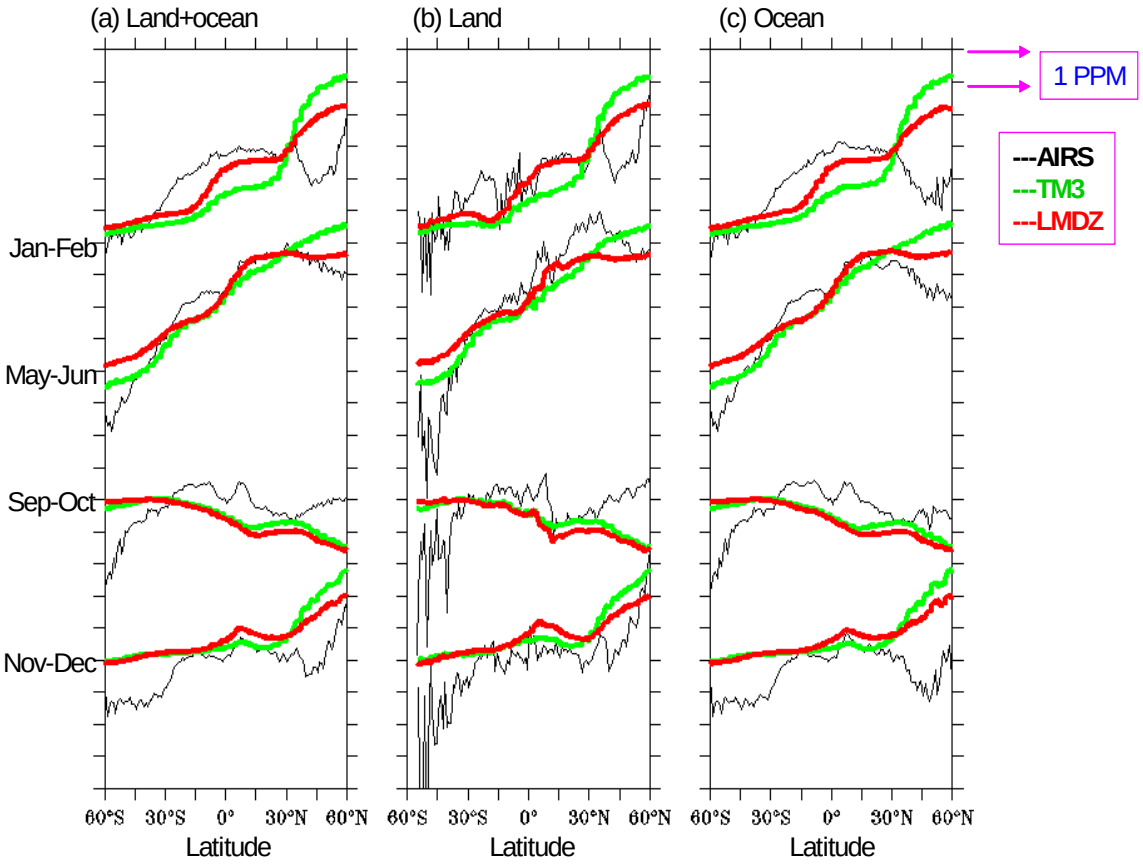

Figure 2.9: *Zonal mean latitudinal variation of two month average CO_2 concentration(ppm) over (a)land and ocean (b)only over land and (c)only over ocean, as retrieved by AIRS and simulated by TM3 and LMDZ.*

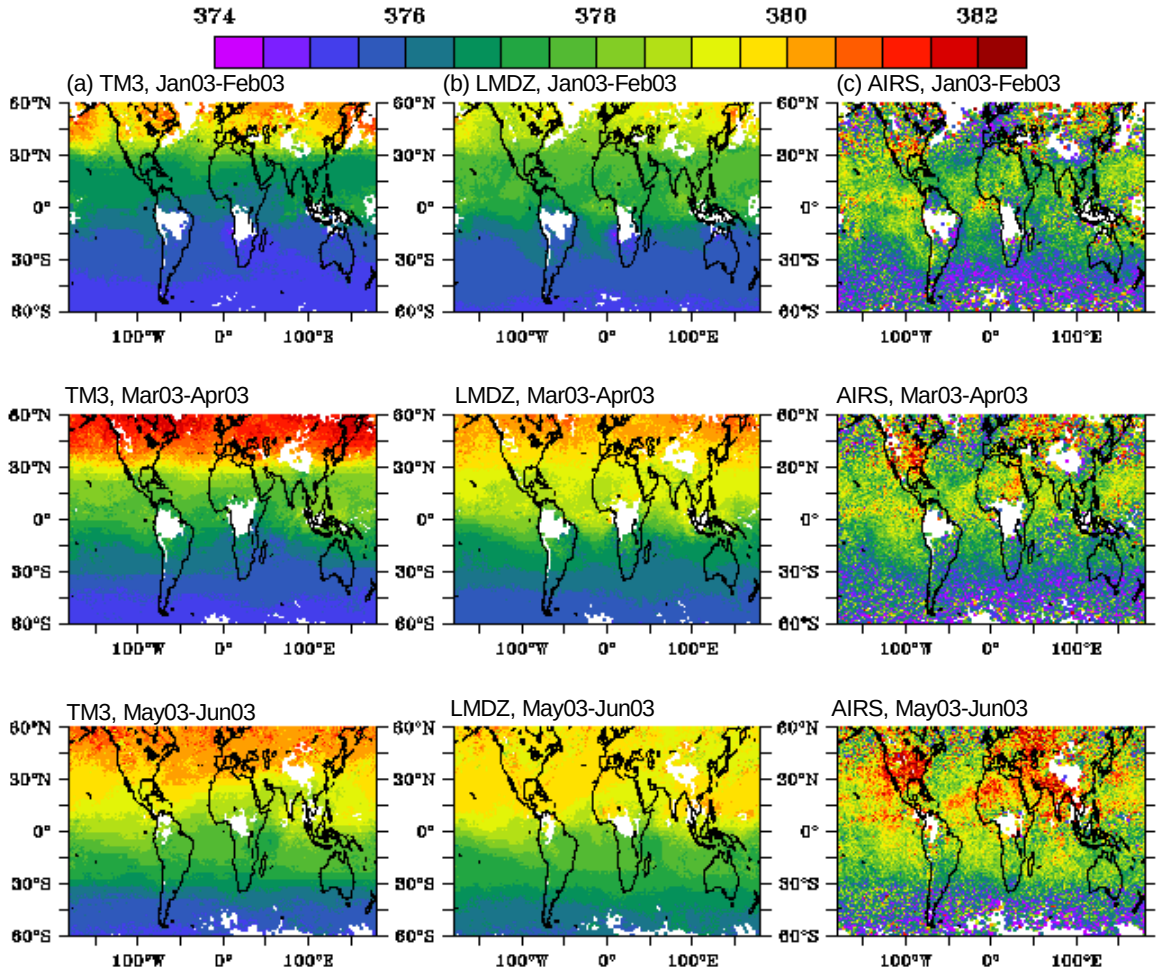

Figure 2.10a: *Two month mean maps of upper tropospheric CO_2 concentration (ppm) as simulated by (a)TM3, (b)LMDZ and (c)retrieved by AIRS.*

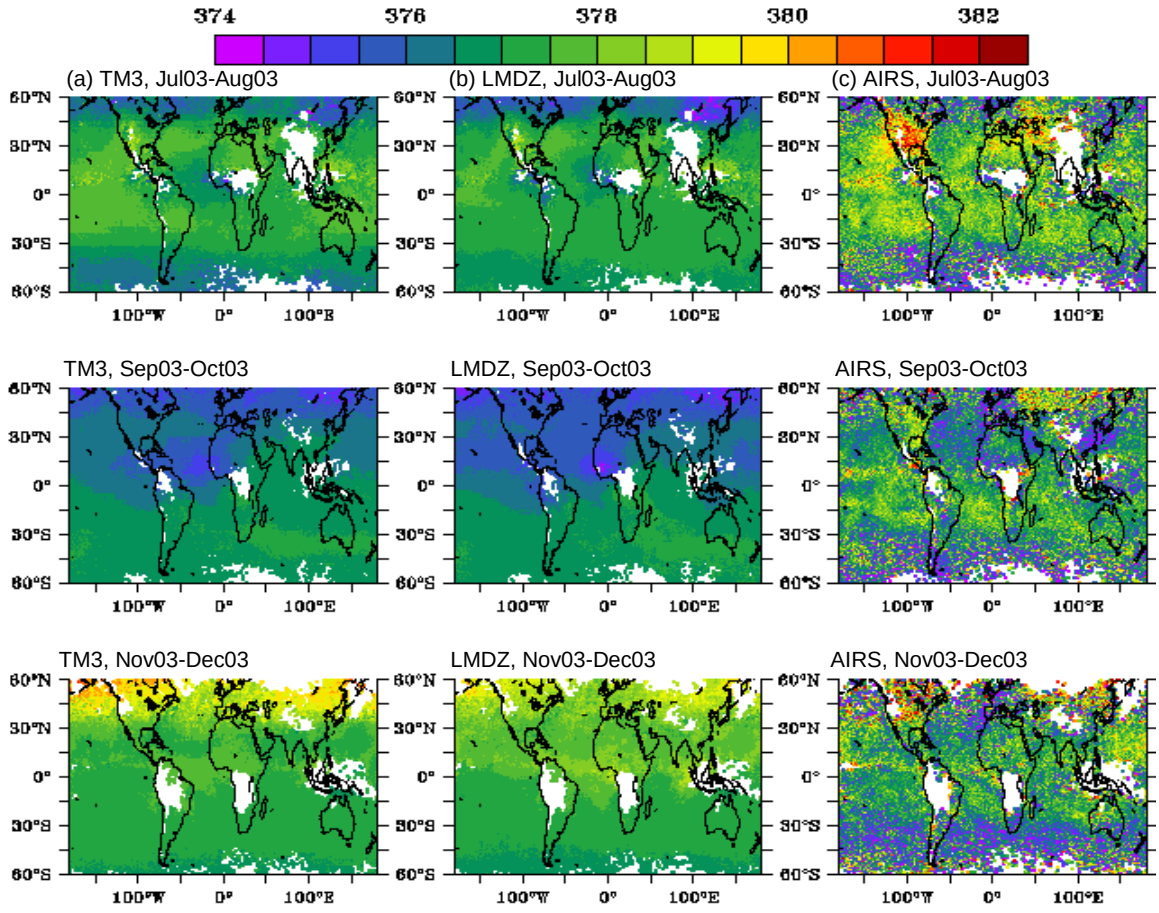

Figure 2.10b: *Same as Figure 2.10a, but for the second half of year 2003*

Chapter 3

Evaluation of TOVS space-borne CO_2 estimates using model simulations and aircraft data

Abstract

CO_2 mixing ratio estimates derived from spaceborne measurements of the TOVS instrument onboard NOAA-10 available for the time period 1987-1991 are evaluated against modeling results and aircraft based measurements. The model simulations are based on two transport models and two sets of surface flux boundary conditions which have been estimated with inverse calculations of atmospheric transport and near surface atmospheric concentrations.

In the tropics, the zonal mean annual cycle and the concentration growth rate of the satellite product are consistent with those of the models. On the other hand, spatial distributions for a given month show large differences. There are large longitudinal gradients that can reach 7 ppm in the satellite retrievals that are absent in the model predictions. The RMS differences between the two models and the satellite product are around 1.7 ppm.

One time series of the model CO_2 trend is used to extrapolate in time to the airborne measurement period both for the satellite and the monthly mean model products. The RMS difference between the airborne measurements and the extrapolated model predictions is on the order of 1 ppm, while it is 2 ppm for the satellite estimate. These compari-

sons suggest that the large longitudinal variation of the satellite retrievals reflect substantial biases and uncertainties in the retrievals which need to be reduced before remotely sensed CO_2 will help constrain carbon cycling.

3.1 Introduction

Determining the spatial and temporal structure of surface carbon fluxes has become a major scientific, but also political, issue during the last decade. In the so-called *bottom-up* approach, sparse observations of surface fluxes are up-scaled in space and time with biogeochemical models. In the so-called *top-down* or *inverse* approach, observed atmospheric concentration gradients are used to unravel surface fluxes, given some description of the atmospheric transport. This approach has been widely used to invert concentration measurements from global surface networks [*Globalview*, 2005] to estimate the spatial distribution of annual mean surface fluxes [*Gurney et al.*, 2002; *Fan et al.*, 1998] and their inter-annual variability [*Bousquet et al.*, 2000; *Rödenbeck et al.*, 2003].

Major limitations of the inverse approach are the uncertainties in atmospheric transport and mixing as well as the low density of atmospheric CO_2 concentration measurements. The current observation network consists of about 100 stations. With such a coarse network, the uncertainty in the retrieved surface fluxes on sub-continental (or regional) scales is too large both for monitoring purposes as well as making progress in our understanding of the carbon cycle. As a consequence, the density of CO_2 in-situ observations, including regular aircraft profiles, has increased in recent years. Another new perspective has arisen with the possibility to measure atmospheric CO_2 from space. Satellite-based observations of CO_2 have the potential to dramatically increase the spatial and temporal resolution of the fluxes. On the other hand satellite products are vertically integrated concentrations rather than point-wise measurements which are well linked to the fluxes of interest. Several retrieval methods have been proposed to optimize the use of existing or forthcoming satellite observations. The first CO_2 estimate derived from spaceborne measurements was obtained using the Television Infrared Observation Satellite (TIROS-N) Operational Vertical Sounder (TOVS) [*Chédin et al.*, 2003]. Other similar products [*Engelen et al.,* 2005; *Crevoisier et al.*, 2004] are based on data from the Atmospheric Infra-Red Sounder (AIRS). The information content of the retrieved products is unclear

at this stage. Validation of these satellite retrievals is therefore of interest both to see if these data can improve our current knowledge of the carbon cycle but also help design upcoming dedicated missions. Such missions include the CO_2 Orbiting Carbon Observatory (OCO) and the Greenhouse gases Observing Satellite (GOSAT).

The purpose of this paper is to assess the accuracy and information content of the first satellite estimate of CO_2 concentration, retrieved from the TOVS instrument data for the period July 1987 to June 1991, in the tropical zone (20^0N-20^0S). A first qualitative evaluation of this product has been presented by *Chédin et al.* [2003] and focused on zonal means and on comparisons with upper tropospheric CO_2 measurements made on board commercial aircraft over the Western Pacific between 1993 and 1999 [*Matsueda et al.,* 2002]. Here we extend this study by comparing TOVS retrievals with simulations of the full three-dimensional CO_2 field based on two independent model simulations. We include in the analysis also comparisons with aircraft measurements other than the *Matsueda et al.* [2002] data which so far have not been used to assess CO_2 retrievals from space. The model simulations rely on two different transport models, TM3 or LMDZ, and two different sets of surface fluxes previously optimized towards atmospheric observations close to the surface through an inverse procedure. The use of two different models with different estimates of the surface fluxes provides a rough indication of the current uncertainties in the atmospheric concentration in the upper troposphere. The aircraft data provide in-situ "truth" although over a limited spatial and temporal scale and a different time period compared to the TOVS retrievals.

In the following, we first describe the model and data used for this validation exercise. We then compare the satellite and model CO_2 concentrations at different spatial and temporal scales. In section 3.4, we use airborne data to compare the accuracy of the model and satellite estimates.

3.2 Data description

3.2.1 Satellite estimates

The retrievals analysed here are derived from a retrieval method proposed and applied to TOVS data by *Chédin et al.* [2003]. The main mission of TOVS is to measure atmospheric temperature and moisture profiles at the global scale. The National Oceanic and

Atmospheric Administration (NOAA) polar meteorological satellite series has provided continuous observation of the Earth atmosphere and surface since 1978 [*Smith et al.*, 1979]. This series of satellites carry TOVS, which is a multi-sensor package, composed of the High resolution Infrared Radiation Sounder (HIRS-2), the Microwave Sounding Unit (MSU) and the Stratospheric Sounding Unit (SSU). In the 13µm to 15 µm range and around 4.3 µm with CO_2 absorption, HIRS radiances depend mostly on the atmospheric temperature profile along the view of sight but also on the CO_2 concentration and its vertical profile as well as the concentrations of other greenhouse gases (O_3 around 13 µm, N_2O and CO around 4.3 µm) [*Chédin et al.*, 2002]. The observations made simultaneously by MSU in the microwave absorption band of oxygen, also strongly depend on temperature, but are neither sensitive to CO_2, nor to other greenhouse gases. Thus, the combination of MSU and HIRS data permits in principle to differentiate between the temperature and CO_2 concentration signatures in the HIRS radiances.

The approach developed in *Chédin et al.* [2003] is based on a neural network technique. The neural network was trained with the results from radiative transfer simulations for a large set of representative atmosphere profiles. It was then applied to radiances observed on NOAA-10, between July 1987 and June 1991, in the tropical zone (20^0N-20^0S). Higher quality retrievals are expected in the tropical area compared to the extra-tropics because of the comparably high tropopause height and low variability of temperature profiles. There is the potential for an extension of the method to data from other NOAA satellites, which would provide a time series covering a period of more than 20 years. The retrieval algorithm described in *Chédin et al.* [2003] underwent some improvements which led to a significant reduction in the magnitude of the retrieved regional CO_2 gradients, as described in *Chedin et al.* [2005].

Individual cloud-free retrievals at a spatial resolution of 1°x1° were binned into monthly fields and then smoothed with a boxcar averaging procedure with 15°x15° resolution over the latitude band extending from 20^0S to 20^0N. To compare the satellite product to model simulations, it is necessary to properly assess the vertical weighting function of the retrieval algorithm. The weighting function was determined through radiative transfer simulations based on the atmospheric profiles of the "Thermodynamic Initial Guess Retrieval" (TIGR) database [*Chédin et al.*, 1985]. A uniform perturbation of CO_2 mixing

ratio δq_i (ppm) was applied sequentially to each of the 40 layers (i) of the TIGR database. The perturbed atmospheric profiles were then used as input to a radiative transfer model to simulate TOVS radiances. The neural network was then applied to these radiances to obtain the theoretical change of the column mean apparent mixing ratio $\delta q_i^{NeuralNet}$ given a mixing ratio perturbation δq_i in layer i:

$$F_i = \frac{\delta q_i^{NeuralNet}}{\delta q_i} \text{ [ppmv/ppmv]} \qquad (3.1)$$

In order to use these weights with any given vertical profile of mixing ratios, it is necessary to normalize for the layer thickness ΔP_i. In practice, we need to translate this vertical weighting function to the vertical discretization of each model. Because F_i is not independent of the thickness (or equivalently the mass) of the TIGR layers, it is necessary to express F_i in units of δ (number of CO_2 moles in air column) / δ (number of CO_2 moles in layer i). This results in the quantity

$$G_i = \frac{\sum_l \Delta p_l}{\Delta p_i} F_i = \frac{p_{surf}}{\Delta p_i} F_i \quad \text{(mol/mol)} \qquad (3.2)$$

The 40 G_i values are independent of the layer thickness and they can be interpolated to any vertical layer distribution. There are 7 different sets of G_i depending on the satellite observation view angle. Figure 3.1 displays the vertical weighting function derived from this procedure for nadir viewing. Because 80% of the CO_2 concentration sensitivity is between 90 and 440 hPa, the TOVS measurement processed through the neural network is only sensitive to the upper troposphere concentration. It is not sensitive to the boundary layer mixing ratio.

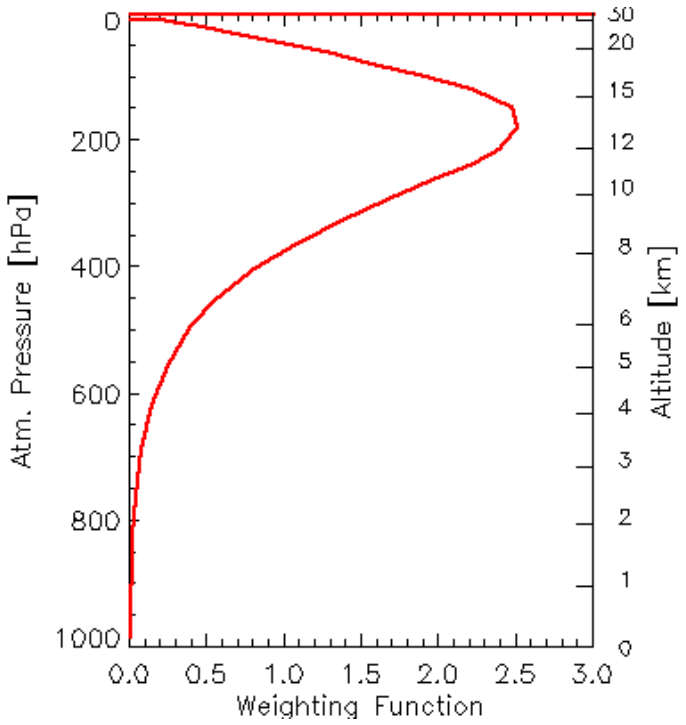

Figure 3.1: Vertical weighting function of TOVS (as implemented in LMDZ and TM3) as a function of altitude.

3.2.2 Model simulations

We performed two simulations of atmospheric CO_2 concentration for the period 1987-1991, using the LMDZ and the TM3 transport models. Differences between the transport models include analyzed wind fields, parameterizations of subgrid-scale processes and the numerical methods used to solve the advection equation. The transport models are forced with carbon fluxes as boundary conditions. These have been previously estimated by inversions of atmospheric transport that use surface concentrations as input. Because the data used are mainly from the surface one expects that these model simulations represent the lower troposphere concentrations fairly well.

The LMDZ simulation uses the general circulation model of the Laboratoire de Météorologie Dynamique, LMDZ [*Sadourny and Laval*, 1984] with a spatial resolution of 3.75° x 2.5° longitude by latitude with 19 vertical levels. Although the model computes its own dynamics and mass transport, the simulated winds and temperature are nudged toward the analyzed fields of ECMWF with a time constant of 2.5 hours. We use

the proper winds for each year of the simulation, starting in 1985 to allow for a two years spin-up period. Large-scale advection of trace species follows the Eulerian framework described by *Hourdin and Armengaud* [1999]. Deep convection is parameterized according to *Tiedtke* [1989] and the turbulent mixing in the boundary layer is based on *Laval et al.* [1981]. The optimized CO_2 fluxes are taken from *Peylin et al.* [2005] inverse study. They are based on 15 years of atmospheric near surface CO_2 observations from a network of 76 stations. The monthly fluxes include both the natural and anthropogenic components.

The horizontal resolution of the TM3 model [*Heimann et al.*, 2003] is 4^0x 5^0 latitude by longitude with 19 sigma-coordinate vertical layers. Transport in TM3 is driven by meteorological fields derived from the NCEP (National Center for Environmental Predictions) reanalysis [*Kalnay et al.*, 1996]. Tracer advection is calculated using the slopes scheme of *Russell and Lerner* [1981]. Vertical transport due to convective clouds is computed using the cloud mass flux scheme of *Tiedtke* [1989] and turbulent vertical transport by the stability dependent vertical diffusion scheme of *Louis* [1979]. The CO_2 surface fluxes used as boundary conditions in the TM3 simulations are from the *Rödenbeck et al.* [2003] atmospheric transport inversion study. They are based on 20 years of atmospheric near surface CO_2 flask data from the NOAA/CMDL station network and vary with monthly timestep. The spatial resolution of the fluxes is 8^0x10^0 latitude by longitude. For more information we refer to the original manuscript.

Significant differences between the two simulations can be expected both at the surface in regions that are poorly sampled and in the upper atmosphere. In the context of the present work, the differences between the two simulations provide a rough estimate of the uncertainty in the CO_2 concentration field. For the comparison between the model results and the satellite data, we paid particular attention to potential sampling errors. The models outputs were sampled collocated in space and time with the TOVS measurements (nearest grid point). The model vertical profiles were averaged with the weighting function described above, accounting for the satellite viewing angle. The model results extracted with this procedure were then averaged to monthly means and smoothed spatially (15°x15°) with exactly the same procedure as the satellite data.

3.2.3 Airborne campaigns

Although sparse in time and space, in-situ aircraft measurements are useful to evaluate both TOVS-CO_2 retrievals and model simulations. We use available measurements from regular programs of atmospheric observations or from several short-term research campaigns that were not designed to principally study atmospheric CO_2. We only consider here the data that cover the tropics and extend from the mid to the upper troposphere (from 5 to 12 km above ground). Table 3.1 gives the period, location, and references for each of these campaigns. The resulting dataset covers approximately half the altitude range covered by the satellite retrieval weighting function.

Most airborne data used in this study were collected several years after the satellite measurements used here. For the purpose of this comparison we therefore had to apply a time extrapolation method of the satellite data to the period of in-situ measurements (see section 3.4). Note that the spatial coverage of the campaigns is biased towards the Pacific. Only few flights (CARIBIC campaigns) with CO_2 measurements exist over continental landmasses (see Figure 3.2).

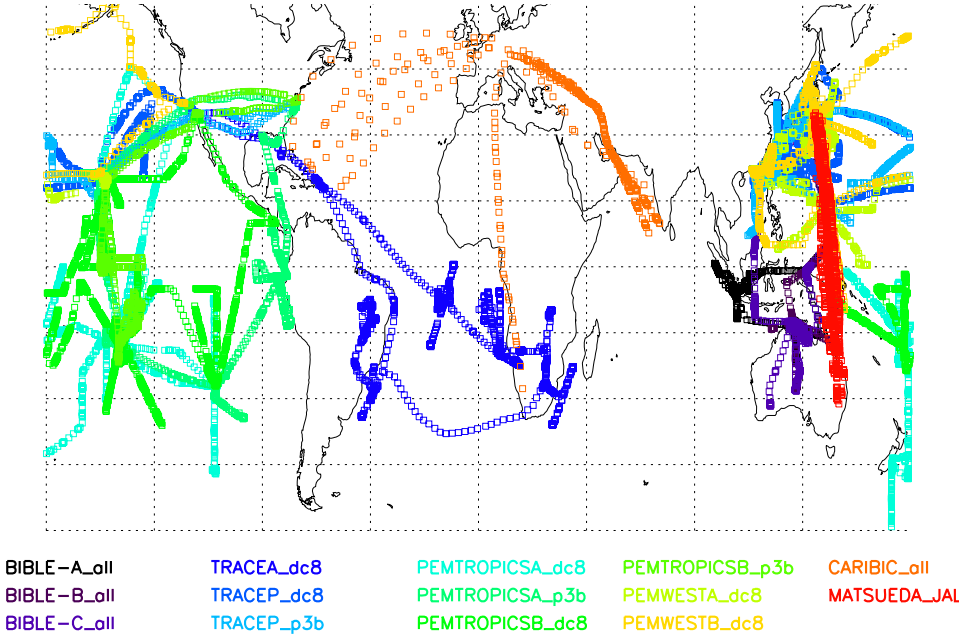

Figure 3.2: Spatial distribution of the airborne measurements used in this chapter

Table 3.1: Aircraft campaigns used to compare with model simulations and TOVS estimates.

Mission / reference	Period	Location	Frequency
Specific campaigns			
PEM-WESTA (*Newell at al.*, *1996*)	09-10/1991	North western Pacific	15 flights; 1 Hz
PEM-WESTB (*Hoell et al.*, *1997*)	02-03/1994	North western Pacific	14 flights; 1 Hz
PEM-TA (*Hoell et al.*, *1999*)	08-10/1996	Tropical Pacific	34 flights; 1 Hz
PEM-TB (*Raper et al.*, *2001*)	03-04/1999	Tropical Pacific	36 flights; 1 Hz
TRACE-A (*Andreae et al.*, *1994*)	09-10/1992	Brazil, S. Atlantic, SW Africa	18 flights; 1 Hz
TRACE-P (*Jacob et al.*, *2003*)	02-04/2001	North western Pacific	38 flights; 1 Hz
BIBLE-A (*Machida et al., 2003*)	09-10/1998	Western Pacific	14 flights; 1/60 Hz
BIBLE-B (*)	08-09/1999	Western Pacific	12 flights; 1/60 Hz
BIBLE-C (*)	11-12/2000	Western Pacific	16 flights; 1/60 Hz
Regular aircraft observations			
JAL (*Matsueda et al., 2002*)	1993-2003	North Australia to Japan	Weekly flights; 1/2 h
CARIBIC (*Brenninkmeijer et al., 1999*)	1997-2001	South India/Africa to Germany	32 flights; ~1/2 h

** see http://www.eorc.nasda.go.jp/AtmChem/GLACE/bible/BIBLE.html for detail*

3.3 Comparison between TOVS and Models estimates

3.3.1 Zonal means

Figure 3.3 compares the time evolution (from June 1987 to July 1991) of the three different fields (TOVS, LMDZ, and TM3) for 5 degrees zonal means from 20^0N to 20^0S. At first sight, the trend and seasonal cycles appear rather similar for the three products, especially in the northern hemisphere where the CO_2 signal is larger. The main cycles are in phase and with similar amplitude for the three curves. On the other hand, the model time series are very smooth in time while TOVS shows large month-to-month fluctuations (up to 2 ppm) with strong inter-annual variations. In the southern hemisphere, the two simulations produce a much weaker seasonal cycle than in the northern hemisphere, while TOVS depicts large variations but with no clear seasonal cycle. Note that high altitude in situ measurements from *Matsueda et al.* [1996] show a complicated seasonal cycle with two maxima around June-July and Nov.-Dec. In order to quantify the differences between the three time series, we computed the amplitude of the seasonal cycles (decomposing each time series into its trend and seasonal component with the curve fitting procedure of *Thoning et al.* [1994]) and the root mean square value (RMS) of the pair differences, for each zonal band (Table 3.2).

In the northern hemisphere, the large seasonal cycle of the land biosphere flux drives the CO_2 concentration in the boundary layer, which then propagates under attenuation into the upper troposphere. This results in a cycle with a maximum concentration in the spring, and yearly amplitude on the order of 4 ppm (Table 3.2). The land biosphere signal is much weaker in the southern hemisphere and surface stations see a seasonal cycle that is only around 1 ppm [*Globalview*, 2005]. Other factors also have a noticeable impact. In particular, the northern hemisphere seasonal cycle influences that of the south through atmospheric transport across the Inter Tropical Convergence Zone. Although these influences may impact the seasonal cycle in the upper troposphere in ways that are not well modelled, the large monthly excursions of TOVS in the southern hemisphere appear truly suspect. The amplitudes of the seasonal cycles only significantly differ between the two models in the southern tropics (up to 20%), a situation corroborated by the RMS of the model differences that increase from north to south (Table 3.2). The magnitude of these

model-to-satellite and model-to-model differences will be further analyzed when we will discuss the information content of TOVS (section 3.5).

Table 3.2: Seasonal cycle amplitude (in ppm) of TOVS-data and model simulations for different latitude bands, together with the RMS value of the differences computed from the zonal mean time series of Figure 3.3

Latitude band	Seas. Cyc. amplitude TOVS / LMDZ / TM3	RMS of differences TOVS-LMD / TOVS-TM3 / LMD-TM3
15N – 20N	4.80 / 3.46 / 3.26	0.92 / 1.08 / 0.31
10N – 15N	4.31 / 3.28 / 3.17	0.86 / 0.89 / 0.31
5N – 10N	3.88 / 2.89 / 2.91	0.99 / 0.95 / 0.29
0 – 5N	3.47 / 2.37 / 2.47	0.99 / 0.97 / 0.29
5S – 0	3.13 / 1.87 / 2.01	1.02 / 1.06 / 0.30
10S – 5S	2.86 / 1.48 / 1.78	1.14 / 1.23 / 0.33
15S – 10S	2.46 / 1.30 / 1.61	1.34 / 1.24 / 0.36
20S – 15S	2.69 / 1.19 / 1.48	1.34 / 1.39 / 0.38

Figure 3.4 shows, for the three datasets, the evolution of the monthly mean North-South gradients averaged over the four years analyzed here. While the two models show similar gradients, the one retrieved from the satellite data is very different. The large difference with the model results, and the strong excursions (~0.5 ppm around 10° North or South), which cannot be easily linked to physical processes, tend to indicate an error in the satellite product. The large variations observed on monthly curves tend to cancel out when averaged so that the yearly mean TOVS gradient is similar, although not alike, the model results.

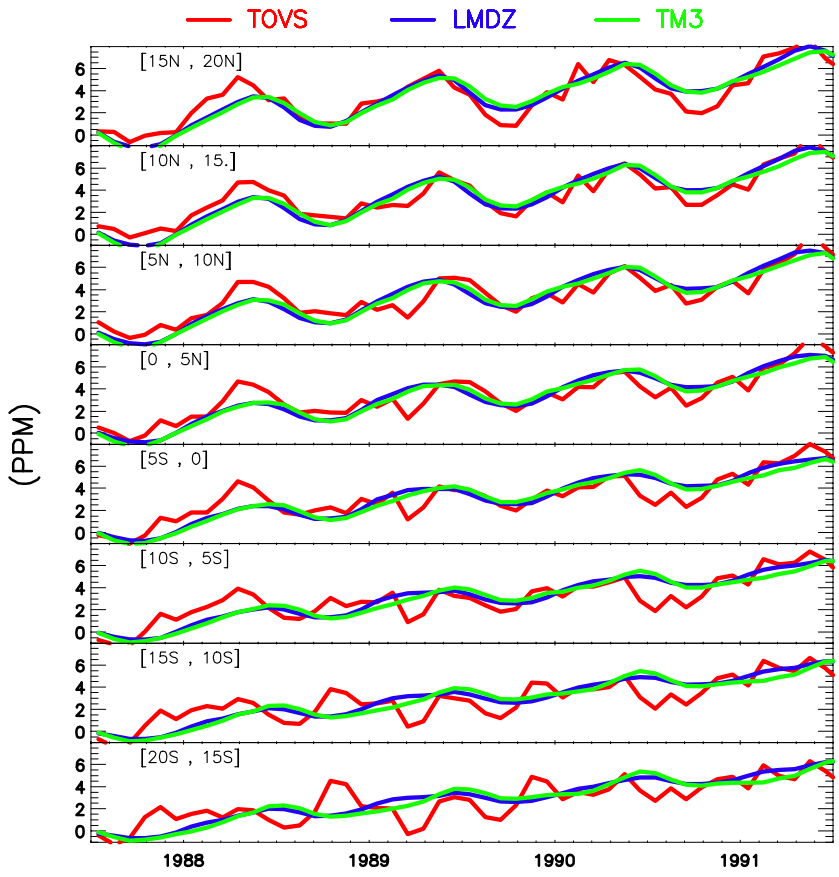

Figure 3.3: Time evolution of the zonal mean concentration anomalies for the two models (LMDZ in blue, TM3 in green) and TOVS data (red), for different latitude bands (5° bands).

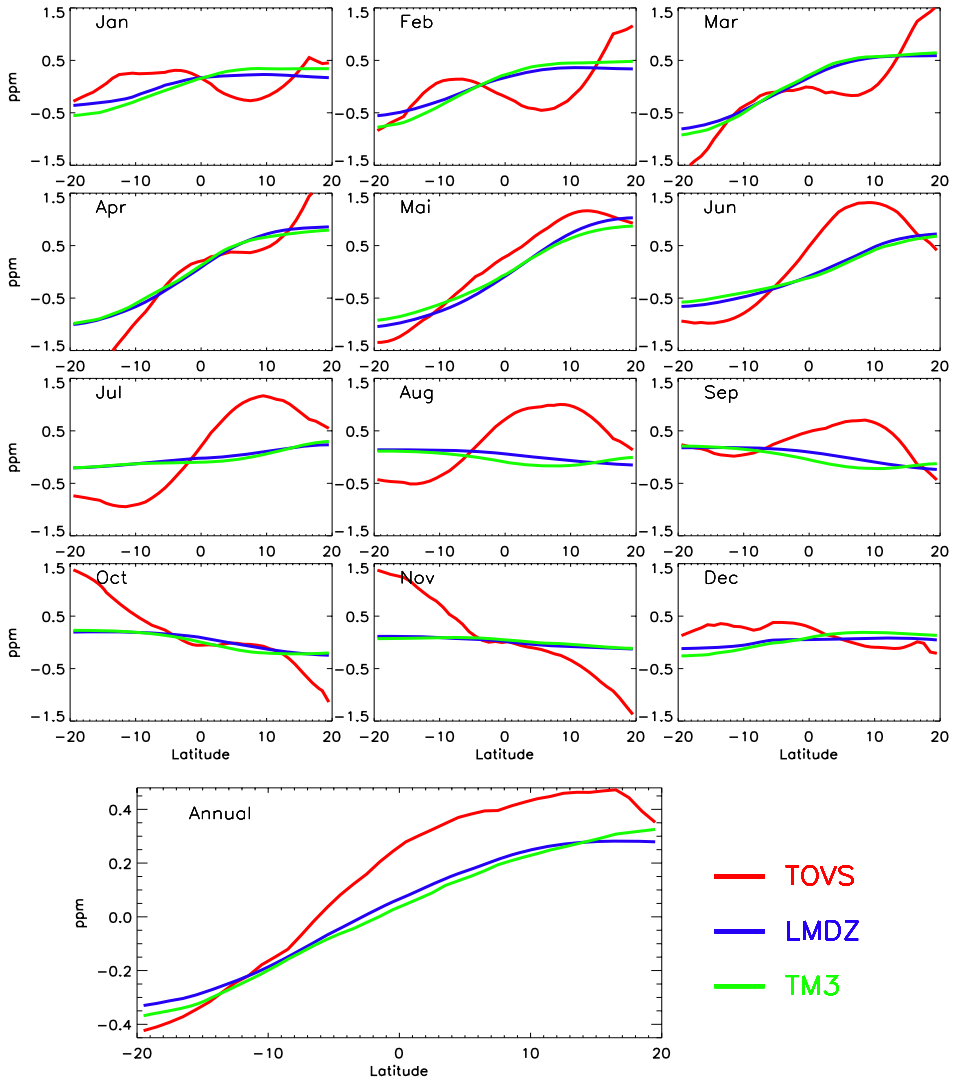

Figure 3.4: Monthly mean North to South concentration gradients for the three estimates (TOVS, and the two model simulations), averaged over the period July-87 to June-91. The annual mean gradient is also added.

3.3.2 Regional patterns

We now analyze the spatial patterns of the monthly mean CO_2 column weighted concentrations, with monthly mean subtracted (and a spatial smoothing to a 15°x15° longitude by latitude box). These patterns are shown in Figure 3.5a. The white zones on the maps correspond to areas with less than 275 satellite measurements per grid cell and month. Only the year 1990 is shown, as inter-annual variations for both model and satellite data are small compared with the difference between the satellite and model results. The colour scales have been limited such that 90% of the data is covered. There are some large and unexpected spatial structures in the TOVS retrievals. The range of the estimated values, on a monthly time scale, is close to 7 ppm, a value much larger than that of the models (~ 1.7 ppm). In addition, most of the gradients in the model are zonal, while the satellite product also varies strongly with latitude. As a consequence, not only the magnitude of the structures but also the spatial patterns are different.

During the first half of the year, both model simulations exhibit a distinct zonality with CO_2 concentrations decreasing from North to South. This zonal gradient increases from January to May (see Figure 3.5a) and starts to decrease in June. It results from the interplay of anthropogenic emissions of which the main share originates from the northern extra-tropics and the seasonal cycle of biospheric CO_2 uptake and release. TOVS retrievals do not show the same zonal structure. East-West variations are of the same magnitude as North-South variations. The origin of the longitudinal variations, partly associated to land sea contrast, is unclear. We have not been able to relate them to known biogeochemical or anthropogenic surface flux patterns, nor to characteristics of atmospheric transport. They are therefore rather suspicious especially since the vertical weighting function of the CO_2 concentration is significant in the mid to upper troposphere only, where gradients caused by surface fluxes are expected to be diluted by mixing in the atmosphere.

The picture is slightly different for the model simulation results during the second half of the year. During the boreal late spring and summer, the biospheric sink more than cancels the anthropogenic source to the atmosphere. As a consequence, the zonal gradient is much smaller than during previous months (see Figure 3.5b), and therefore longitudinal variations emerge. Note that the amplitude of these structures are somewhat affected by

the sampling of the model: monthly means based on a similar procedure but using all grid points rather than those observed by the satellite show the same patterns but with smaller amplitudes. The monthly spatial patterns are somewhat different for the two models with differences up to 1 ppm. The most striking difference is observed in the southern hemisphere in October and November when LMDZ shows a positive anomaly over Africa, while TM3 points to a local maximum over South America. These differences result from differences in the flux field that reflect our poor knowledge of the tropical CO_2 flux in particular over land areas with biomass burning fluxes. This is due to a lack of ground stations in the tropics. The TOVS patterns have an amplitude that is much larger and not significantly correlated with the prediction of any of the two models. However, as explained in *Chedin et al.* [2005], the 12-hours difference between day time and night-time retrievals (NDD) are expected to reflect biomass burning activities over the tropics. Such NDD product is in favor of a larger biomass burning activity in Africa than in South America for this two month period (their figures 3.3 and 3.4).

3.4 Statistical comparison with aircraft measurements

As just discussed, differences between satellite CO_2 estimates and the two model simulations are much larger than the difference between the two model results. As also pointed out, there is no obvious explanation based on missed surface flux processes or shortcomings in atmospheric transport modelling. A tempting explanation of the differences between the model and the satellite products is therefore that they are due to noise and biases in the latter.

However, model simulations have so-far only been validated at a few selected surface locations, while no similar effort has been made for the upper atmosphere. There are potential causes for biases in the modeled fields, linked to uncertainties in the current parameterization of the vertical convection and vertical diffusion in the models. Besides, surface fluxes are also poorly constrained in the tropical zone. Thus, before jumping to conclusions the realism of high altitude model transport needs to be assessed. For this purpose we rely here on a comparison with the airborne in-situ measurements. The validation procedure implies the comparison of point data to vertically averaged, spatially smoothed, monthly mean fields, which is a potential cause for differences. As the result-

ing noise will be the same for the satellite and model fields, our conclusions will therefore not be affected by this problem.

Because the satellite CO_2 product is available from July 1987 to June 1991, while the airborne campaigns happened all after September 1991, it is necessary to extrapolate TOVS and model CO_2 concentration in time for the comparisons. As time series of monthly mean upper troposphere CO_2 are dominated by the secular trend and the seasonal cycle this can be achieved approximately in the following manner. A secular trend expressed as function of year *y*, month *m* and location *x*, *Tr(y,m,x)*, is calculated for the upper troposphere tropical region sampled by TOVS for 1990 to 2003 based on the LMDZ simulation. The TOVS or model seasonal signal for 1990 is then *S(m,x) = C(1990,m,x) - Tr(1990,m,x)* where *C(y,m,x)* is the monthly mean concentrations for year *y* and locations *x*. The extrapolated TOVS and model values are then given by

$$C_{ext}(y,m,x) = Tr(y,m,x) + S(m,x) \qquad (3.3)$$

We choose the year 1990 as reference (largely unaffected by an El-Nino event) but checked that the results remain similar when using 1988 or 1989. The statistical differences between the airborne measurements and either the satellite product or the model simulations are summarized in Table 3.3 in terms of mean bias, and root mean square value (RMS) for each campaign. We also derive a global mean value by sub-sampling uniformly the different campaigns in order to give a similar weight to each of them. Note that because many campaigns last less than a month and cover only a limited region, the statistical comparison with monthly satellite or model products should be interpreted with great care.

The overall biases (last line in Table 3.3) are similar for the three estimates, i.e. 0.3 ppm or less. On the other hand, the individual bias for each campaign can be much larger, up to 1 ppm for the models and 3 ppm for the satellite product. In general, the bias is larger (in absolute value) for the satellite product than for the models, with mean absolute values of 0.4, 0.5 and 1.1 ppm for LMDZ, TM3, and TOVS, respectively. Recall however that for the short period campaigns (last less than a month), there are few independent

model or satellite estimates so that it is difficult to clearly distinguish bias and random error.

The RMS provides a complementary measure of the differences between the estimate and the true value. All campaigns combined, the RMS error is on the order of 1 ppm for the models, and 2 ppm for the satellite product. Campaign by campaign, the picture is rather similar; the two models behave similarly with typical RMS errors on the order of 1 ppm and differences in this parameter are less than 0.1 ppm, while the satellite product shows significantly larger RMS except for two campaigns, “PEMTROPICSB_p3b” and “PEMWESTA”. Note that the statistical results for the “MATSUEDA” and “CARIBIC” campaigns are more robust as these campaigns cover several years.

The typical value of 1 ppm for the RMS error for both model simulations is a rough indication of the model performance in the high troposphere of the tropics. Such a value is probably an overestimate of the modeling error as it includes the impact of temporal averaging and extrapolation and spatial smoothing. The actual performance of models in the upper troposphere depends on their ability to model the upper troposphere synoptic variability. Such analysis is beyond the scope of this paper.

The above 2 ppm RMS error for TOVS versus 1 ppm for the models confirms that the model simulations are closer to the truth than the satellite product is. The difference between the monthly mean satellite product and the two model equivalents can be larger than 5 ppm locally (figure 3.5a), while the RMS difference is on the order of 1.7 ppm in both cases with variations from 1.4 to 2.2 ppm depending on the months. These statistical results (satellite vs. in-situ data and satellite vs. model simulations) indicate 1) that the RMS error of the satellite monthly mean product (15°x15°) is on the order of 2 ppm, 2) that the striking structures observed on TOVS retrievals (at a spatial scale of few thousand kilometers, figure 3.5a) and not resolved by the model are suspicious and likely related to some biases in the retrieval method, and 3) that these errors can be larger than 5 ppm. Further analysis is needed to explain the origin of these biases.

Table 3.3: Summary of the differences between model/TOVS estimates and the in-situ observations in (ppm), expressed in terms of mean bias and root mean square.

	LMDZ_integr		TM3_integr		TOVS	
	Bias	Rms	Bias	Rms	bias	Rms
BIBLE-A_all	-0.71	0.95	-0.74	1.01	-0.38	1.02
BIBLE-B_all	-0.96	1.12	-1.05	1.21	-1.70	1.77
BIBLE-C_all	-0.66	0.81	-0.59	0.74	3.15	3.73
CARIBIC_all	0.77	1.42	0.61	1.34	1.61	2.64
MATSUEDA_JAL	-0.08	0.83	0.01	0.88	0.30	1.88
PEMTROPICSA_dc8	-0.01	0.47	-0.22	0.51	-1.32	2.07
PEMTROPICSA_p3b	-0.14	0.51	-0.39	0.78	-1.49	1.88
PEMTROPICSB_dc8	0.68	0.93	0.51	0.92	1.37	1.79
PEMTROPICSB_p3b	-0.19	0.91	-0.36	1.02	0.16	1.03
PEMWESTA_dc8	0.77	1.26	0.84	1.32	0.83	1.32
PEMWESTB_dc8	-0.23	0.61	-0.55	0.75	0.61	1.31
TRACEA_dc8	-0.27	1.78	-0.70	1.85	1.62	2.40
TRACEP_dc8	-0.05	1.08	-0.59	1.22	-0.60	2.14
TRACEP_p3b	0.03	0.84	-0.48	0.92	0.47	1.96
All	-0.10	0.96	-0.27	1.04	0.30	2.03

3.5 Discussions

Based on our comparisons TOVS CO_2 retrievals appear to capture the mean atmospheric CO_2 trend (around 1.5 ppm/year) and the predominance of a large seasonal cycle in the northern hemisphere (amplitude ~4 ppm), when averaged over large regions like 5 degrees latitude bands. These results have been initially pointed out in *Chédin et al.* [2003] and also notified in *Chevallier et al.* [2005]. This result is encouraging as it is the first quantitative retrieval of atmospheric CO_2 concentration, and it is based on an instrument that was not designed for that purpose. However, an important question is whether these estimates can bring new information to the carbon cycle and, if so, at what spatial and temporal scales. To answer that question, we compare below an estimation of the accu-

racy that we currently need on atmospheric CO_2 mixing ratios to improve our knowledge of the atmospheric CO_2 variations to an evaluation of the noise in the satellite data.

We propose successively two methods to estimate the accuracy needed, depending on the scale considered and based on our model simulations. First, we simply use the "mean difference" between the two simulations used in this paper as an overall target. Second, we consider local features (in space and time) and define the accuracy need with either the largest concentration difference between the two simulations or an estimation of the local impact of a relatively "poorly constrained" process, such as biomass burning, using one atmospheric transport model.

At monthly time scales, the two simulations show mostly similarities (Figure 3.5a) and the RMS error of the differences is around 0.30 ppm over the year and ranges from 0.21 ppm in August to 0.39 ppm in May. Thus, at the 15 degrees spatial scale the mean accuracy requirement (or signal to be detected) is on the order of 0.3 ppm. On the other hand, the RMS of the differences between TOVS and the two models are on the order of 1.7 ppm. Because such a high value results from large coherent spatial structures in TOVS that cannot be related to any known transport or biophysical process and because the validation with airborne samples has demonstrated a typical error of that magnitude, the 1.7 RMS value can be taken as an estimation of the noise in the current satellite retrieval. Such value is then roughly 6 times the required accuracy defined above.

If we now consider the zonal means (5° zonal bands of Figure 3.3), the model-to-model RMS differences are around 0.30 ppm in the zonal bands north of the equator and around 0.35 to the south (Table 3.2). As before, we can use these values as a mean accuracy requirement for satellite data to reduce the uncertainty in the zonal mean upper troposphere CO_2. On the other hand, the RMS differences between the satellite and model time series are close to 0.95 ppm in the north and 1.25 ppm in the south. If we assume again that this is mostly a result of noise of the satellite retrievals, one can find a ratio close to 3 between the noise and the signal for both hemispheres. The situation is thus more favorable at the zonal scale.

At this point the noise in the monthly TOVS product (15° x 15°) appears prohibitive to provide valuable information on atmospheric CO_2 mixing ratio variations. Such result has been confirmed by *Chevallier et al.* [2005] in an attempt to estimate surface CO_2 fluxes

from this dataset. However this result is a mean result based on the use of the whole dataset. We will thus now briefly consider the same analysis using maximum absolute differences instead of mean RMS values and investigate the specific case of local (in space and time) biomass burning signals.

At the regional scale (Figure 3.5a), the maximum model to model difference is on the order of 1.4 ppm for few months, while the maximum satellite to model difference is around 6 ppm. This gives us a ratio between a need in accuracy and the satellite noise close to 4. At the zonal scale of figure 3.3 the same approach based on maximum differences led to a similar ratio as with the RMS differences (~3), and the smallest value is only 2.4 for the [10^0N-15^0N] zonal band. Let us now consider biomass burning fluxes in the tropics, which are at present still poorly constrained. These events, intense and sporadic in nature, are a major source of uncertainty in the description of the surface CO_2 fluxes. We use an up-to-date estimate of the biomass burning CO_2 flux that combines information on the space-time location of the fires (using space measurements) and on the amount of burned carbon (using the CASA biogeochemical model; *Van der Werf et al.*, [2003]). The mean flux for the 1997-2001 period was transported by the LMDZ model, using the 1990 meteorology. The resulting monthly mean concentrations, processed consistently with the satellite measurements (spatio-temporal sampling, weighting function, smoothing procedures) are shown in figure 3.6. The impact on the upper troposphere concentration is significant over several regions, up to about 1 ppm. This number gives an order of magnitude of the biomass burning signal, although such signal critically depends on the amount of biomass that is burned, and on the representation of vertical mixing processes that may be specific over large fires. Note that the monthly concentration changes at the lowest level of the model only reaches 3 ppm for the strong events in September and October, a value that can considered as an upper limit. The need in accuracy to clearly detect the upper troposphere CO_2 increase from biomass burning fluxes is thus on the order of 1 or 2 ppm, like for the maximum model differences. Such value is still very low compared to the estimated noise for TOVS. The spatial patterns in figure 3.6 from biomass burning can also not be directly related to those of TOVS retrievals (Figure 3.5a). However, as established by *Chedin et al.* [2005], the 12-hour difference between day time and night time retrievals is more directly linked to biomass burning events. Such

new product is probably less sensitive to regional biases and it therefore constitutes a potential source of additional information.

Overall our analysis of accuracy need versus noise, although quite crude and only based on two model simulations, highlights the inability of the current TOVS retrievals to enhance our knowledge about the spatio-temporal variations of the atmospheric CO_2 mixing ratio. The errors in the satellite product are not purely random as the patterns spread over spatial scales larger than the smoothing grid box of 15^0. Besides, several coherent patterns are observed at the same place for several months in a row, or during the same month of several years (not shown). These consistent patterns likely result from signals other than CO_2 that bias the current retrieval. Potential causes for biases are the ozone and water vapor concentrations that affect the TOVS channels used in the retrieval, as well as the temperature profiles that strongly affect the measured radiances. The exact identification of the causes for biases in the retrieval is beyond the scope of this paper (Serrar et al., in preparation).

3.6 Summary and Conclusions

In *Chédin et al.* [2003] measurements from the TOVS instrument, onboard the NOAA-10 satellite, have been used to produce the first estimate of atmospheric CO_2 concentration from space-borne observation. Although this instrument was never designed for that objective, this pioneer work has demonstrated that there is a CO_2 signature in the measured radiances. Indeed, the estimate of CO_2 concentration, derived using a neural network technique, reflects several well-known feature such as the general growth rate of around 2 ppm per year, and the seasonal cycle of about 4 ppm in the northern hemisphere.

On the other hand, global maps of retrieved CO_2 concentration show features that are unexpected. We have therefore evaluated the product against both model simulations and airborne measurements. These comparisons suggest that the satellite retrieved CO_2 concentration patterns, with an amplitude of several ppm, result from noise and biases in the method rather than being a real signal. Both comparisons to the modeling results and to in-situ measurements suggest RMS errors of the TOVS monthly mean 15^0x15^0 product on the order of 2 ppm. These errors are not random as they extend over several thousand

of kms and have similar patterns during succeeding years. However, the night-minus-day differences of TOVS retrievals (NDD, *Chedin et al.* [2005]) are probably less sensitive to these biases and they have been linked to the biomass burning activity at the regional level. Such product is thus worth further exploitation.

On the other hand, the two models investigated here show very consistent results with RMS differences of 0.3 ppm, and a maximum RMS difference of 1.3 ppm over land areas with regular biomass burning. The comparison of modeling results to airborne measurements shows an RMS difference on the order of 1 ppm. More upper-air data, especially over the continents, would be very useful to assess more conclusively the performances of the models and a larger ensemble would also provide a better assessment of the current knowledge on upper air CO_2 concentration. Based on this limited set of airborne observation and model simulations, we have estimated that the error (random and bias) in the TOVS monthly product is roughly 6 times the accuracy needs to improve our knowledge of the atmospheric CO_2 mixing ratio variations.

The 1 ppm model uncertainty is relevant in the context of accuracy requirements for future satellite CO_2 mission like OCO and GOSAT. It is a rough minimal requirement for accuracy and precision of monthly mean CO_2 estimates over scales of 10° x 10° longitude by latitude. Any bias close or larger to 1 ppm would definitely hamper the use of these products. However, regionally and for particular periods, those constraints might be slightly relaxed if the “synoptic” or “sub-monthly” events can produce larger signals, which may be expected with a vertical weighting function that probes not only the upper but also the lower troposphere.

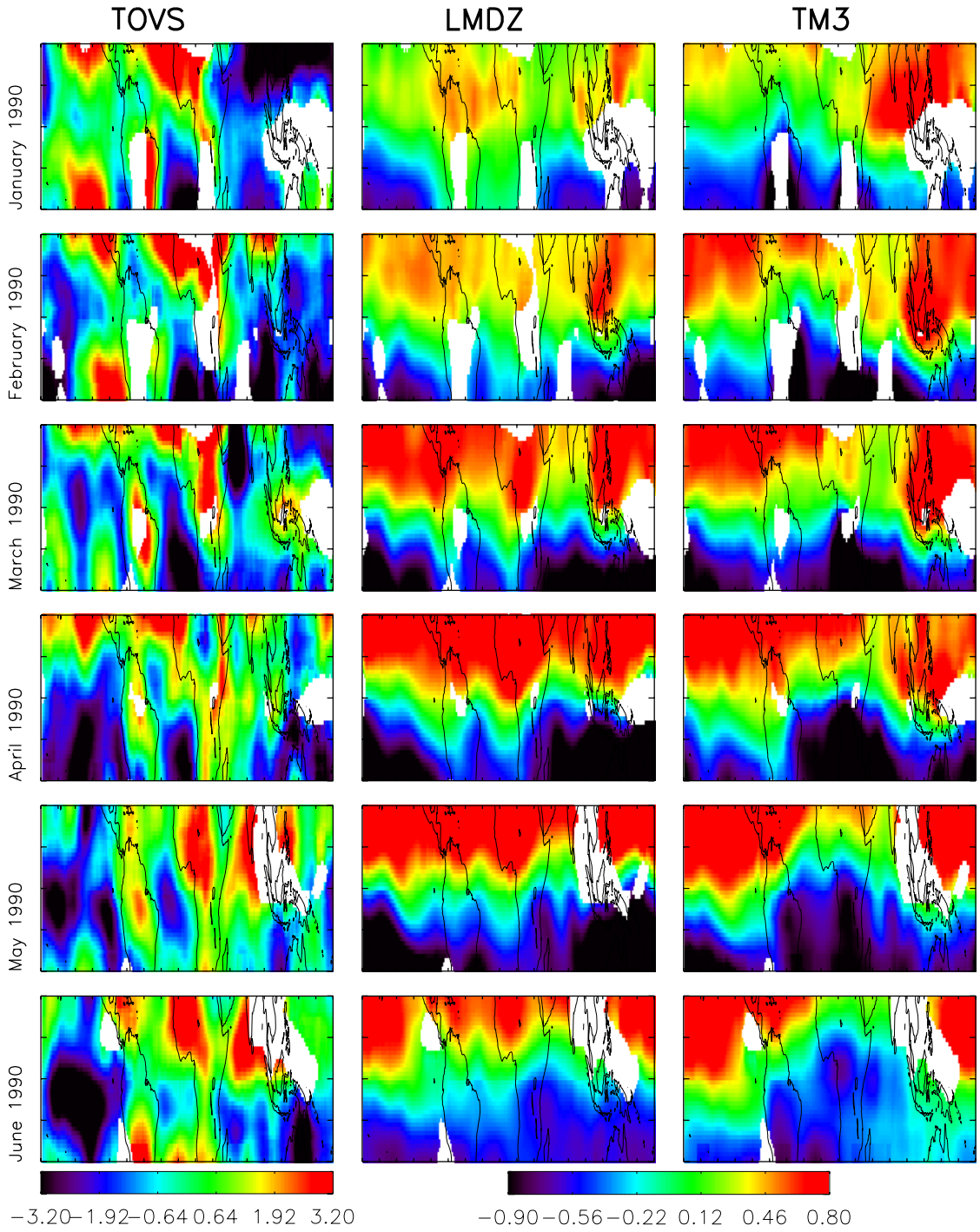

Figure 3.5a: Monthly mean CO_2 concentration anomaly maps over the tropics, for TOVS and LMDZ, TM3 model simulations, for January to June 1990. We use two color tables, one for TOVS and one for both models, and adjusted the range of the tables to truncate 5% of the minimum and maximum values.

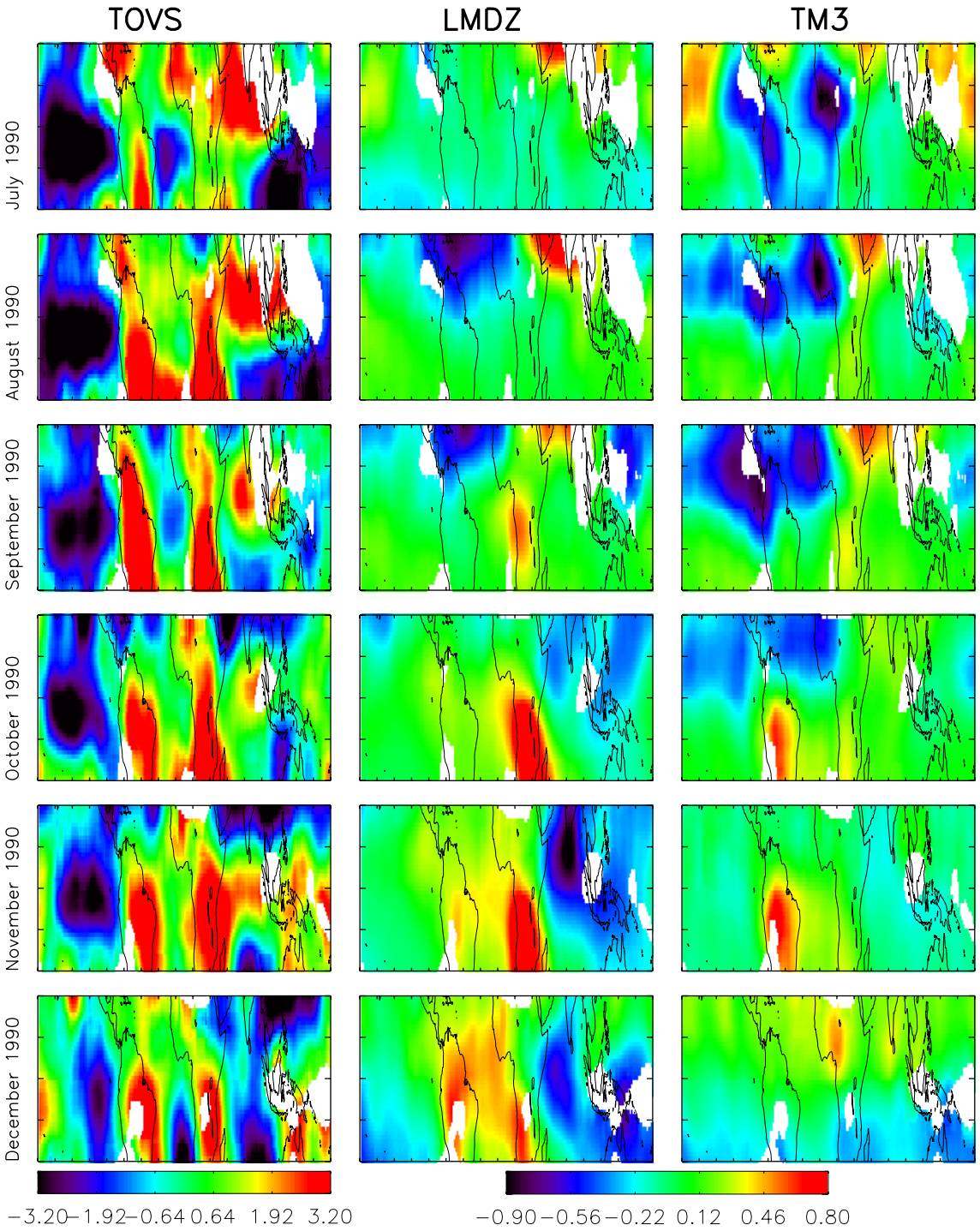

Figure 3.5b: same as Figure 3.5a but for July to December 1990.

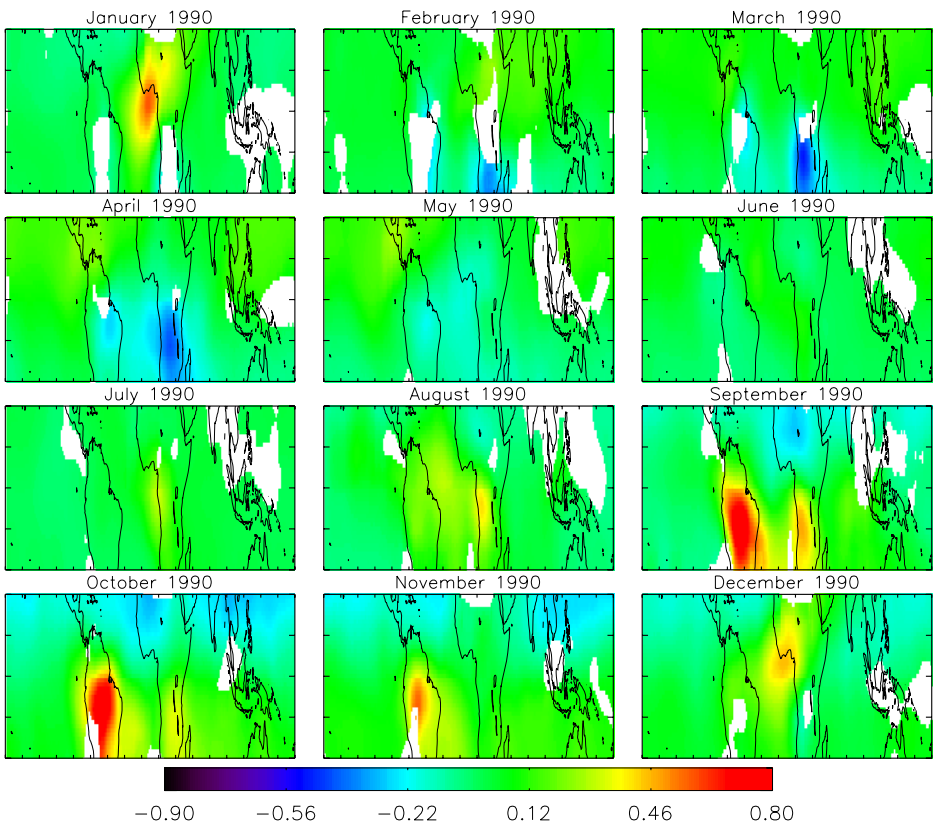

Figure 3.6: Monthly CO_2 concentration anomaly maps due to the Biomass-Burning effect using the LMDZ transport model for 1990 and the sources estimated from Randerson et al. (1999) that combine satellite observations and a biogeochemical model (CASA). We use the same color table as in figure 3.5 for the model outputs.

Chapter 4

Evaluation of model simulated lower-to-upper troposphere transport for purpose of constraining surface sources and sinks using remotely sensed upper troposphere CO_2

Abstract

Atmospheric CO_2 can in principle be used to constrain surface CO_2 sources and sinks using inverse modeling. However since atmospheric sampling is still sparse such estimates are currently of a more qualitative than quantitative nature. Recently first upper troposphere CO_2 estimates from remote sensing (AIRS instrument on AQUA satellite) have become available and may have the potential to substantially reduce current uncertainties of the atmospheric approach by closing observational gaps. However two conditions need to be met before these upper troposphere data can be used to constrain carbon sources and sinks: biases and uncertainties in retrievals must be understood and small (~ <0.3 ppm) and lower-to-upper troposphere air mass transport must be represented realistically by the transport models used for the inversions. Results in a precursor study revealed substantial differences between simulated and remotely sensed upper troposphere CO_2 with two possible mutually non-exclusive explanations. Either lower-to-upper troposphere model transport or remotely sensed CO_2 is biased. This study is dedicated to address the first of the two hypotheses by comparing model predictions of

upper troposphere CO_2 with available observations from aircraft from the BIBLE and PEM campaigns, and the JAL, CARIBIC and Cape Grim continuous aircraft programs. We find good agreement both in temporal, meridional and vertical structure between simulations and observations (RMS ~ 0.4 ppm) with the exception of the tropics during autumn where differences are often up to 2 ppm. As vertical structure agrees well between observations and simulations we attribute this tropical bias to biases in the surface fluxes rather than model transport. Comparisons between aircraft observations, model simulations and AIRS retrievals reveals better agreement between simulations and observations compared to retrievals. Together with the small model-observation RMS difference this indicates that model transport error cannot explain the differences between AIRS retrievals and simulations and thus these must rather be due to biases in the retrievals.

4.1 Introduction

Determining the magnitude and cause of continental-scale carbon sources and sinks is important to advance our current understanding of the carbon cycle and to permit more accurate prediction of its future behavior. Carbon sources and sinks at the earth surface can in principle be estimated from atmospheric concentrations by inverting atmospheric transport [*e.g. Keeling and Heimann 1989, Tans et al. 1990, Fan et al. 1998, Bousquet et al. 2000, Rödenbeck et al. 2003*]. However these calculations are quite uncertain as they are inherently unstable, atmospheric sampling is coarse and model transport may be unrealistic. Satellite CO_2 data have the potential to substantially reduce uncertaintites of the atmospheric inversion approach to estimate carbon sources and sinks because of the dense spatial and temporal resolution of the retrievals. However before these data can be used uncertainties and biases of the retrievals as well as of simulated lower-to-upper troposphere transport must be quantified. A first comparison study between model simulations and recent satellite retrieval [*Tiwari et al.,* 2005, in press] indicates systematic differences between simulations and retrievals. The study used two different global tracer transport models forced with the same surface flux as a boundary condition and compared them with recent CO_2 satellite retrievals from the AIRS instrument on the AQUA satellite. The retrievals have been obtained by *Engelen et al.* [2004] using a

retrieval algorithm embedded in the 4D Var data-assimilation system of the ECWMF weather forecast model. The study finds that the two model predictions of upper troposphere CO_2 are closer to each other than to the retrievals. There are two possible explanations. Either both simulations are equally biased particularly with respect to model transport or the retrievals are biased. This study addresses the first of the two explanations by comparing model simulations with in-situ upper air observations of CO_2. Several airplane campaigns have been conducted in the past and recent past which measured atmospheric CO_2 mixing ratios at high altitude. Some programs were regular and some were campaign based. These data have not been used in inversions so far and will serve as a basis to answer the question posed.

The same modeling framework as in *Tiwari et al.* [2005] is used here. Atmospheric CO_2 for the period from 1991 to 2001 is predicted using the atmospheric transport model TM3 forced with monthly surface fluxes estimated by *Rödenbeck et al.* [2003] using inverse methods. The meteorological transport fields are derived from the NCEP (National Center for Environmental Predictions) reanalysis [*Kalnay et al.*, 1996]. In the following we first describe the airplane campaigns and then we give a brief description of the TM3 model and surface fluxes applied. We then discuss the comparison results and finally we conclude.

This chapter is part of an article which is in preparation by the author. In that article we will use a second global tracer transport model similarly as *Tiwari et al.* [2005], and more airplane data from all over the globe to obtain better spatial coverage and better statistics. We will also look in more detail at lags between surface signals and upper troposphere signals.

4.2 Methods

4.2.1 Airplane observations

Airplane observations from five measurement programs are used in this study. The programs are selected such that they cover a large part of the globe.

4.2.1.1 Japan AirLines (JAL) campaign, 1993-2003

Since the details of the JAL observations are given elsewhere [*Matsueda el al.*, 2002] here we describe JAL observation only in brief. Onboard the north-bound (Sydney,

Australia to Narita, Japan) Japan Airline Boeing 747 passenger aircraft flask samples were collected at an interval of 30-40 minutes which corresponds to a latitudinal interval of 5^0-6^0 from April 1993 onwards. To minimize storage time of air samples and thus contamination samples were taken only during the return flight from Sydney to Narita, Japan. The flight frequency was maximally three times per month. The observations cover the latitude band from 34^0S to 35^0N [Figure 4.1(a)].

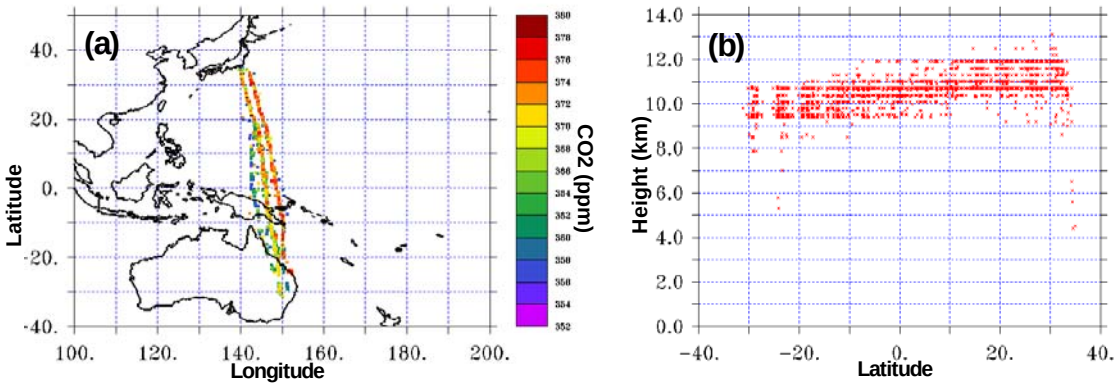

Figure 4.1: JAL (Japan AirLines) 1993-2003 flight track(a) and cruising altitude(b).

At a few times the flight destination in Australia has changed but that did not affect the observation locations [*Matsueda et al.*, 2002]. The air samples were collected at cruising altitude of 9-12 km [Figure 4.1b]; also few samples were collected below 8 km while the aircraft was descending before landing at the Narita airport. Flask CO_2 analysis was performed at the MRI (Meteorological Research Institute), Japan, using a nondispersive infrared gas analyzer (NDIR). Details of the instrument and measurement techniques are given in *Matsueda et al.* [2002].

4.2.1.2 Cape Grim/Bass Strait airplane observations, 1991-2000

CSIRO (Commonwealth Scientific and Industrial Research Organization) Atmospheric Research has carried out air sampling by aircraft in the southeast Australian region since 1972. The original aim was to monitor atmospheric CO_2 concentration, describe the movement of CO_2 in the atmosphere and the exchanges between various carbon

reservoirs [*Pearman et al.*, 1983]. Concentration analysis of flasks was done at the Global Atmospheric Sampling Laboratory (GASLAB) [*Francey et al.*, 1996, 1999b]. A new, more powerful light aircraft with a dedicated air sampling inlet system was installed in April 1992. The sampling altitude increased accordingly from 0.3km- 4km to 0.15km-8km. Flask samples were analyzed at the GASLAB within 10 days after flask samples have been taken. Most of the profiles are located close to 40^0S, 144^0E, approximately 35 km west Cape Grim [Figure 4.5a(i)]. For this study airplane observations conducted during 1991-2000 with sampling altitude between 4 km to 8 km [Figure 4.5a(ii)] are used. Details of this campaign and the sampling method and analytical techniques are described in *Pak* [2000].

4.2.1.3 BIBLE (Biomass Burning and Lightning Experiment) Airplane Campaign, 1998-2000

The BIBLE campaign was carried out in three phases: BIBLE-A was conducted during September-October 1998, BIBLE-B during August-September 1999 and BIBLE-C during November-December 2000. At present only the BIBLE-A campaign data is published in *Machida et al.* [2003] but the sampling and data analysis method are similar for BIBLE-B and BIBLE-C campaigns [*T. Machida*, personal communication]. The main aim of the BIBLE campaigns was to investigate the impact of biomass burning and lightning on tropospheric gas composition. These campaigns were conducted between Japan and Australia [Figure 4.6(a)] and atmospheric CO_2 mixing ratios were measured continuously onboard the aircraft. During the BIBLE-A campaign fifteen flights were conducted using a continuous measurement system with a nondispersive infrared analyzer (NDIR) onboard the airplane [*Machida et al.*, 2003]. The cruising altitude during the flights varied between the surface to 13 km [Figure 4.6(b)].

4.2.1.4 CARIBIC (Civil Aircraft for the Regular Investigation of the atmosphere Based on an Instrument Container) airplane observations, 1998-2001

CARIBIC phase I campaigns were conducted between November 1997 and April 2002 onboard passenger flights between Germany and India, and between Germany and the Caribbean islands [see figure 4.15b,c,d]. Observations were resumed in December 2004,

as a phase II experiment. The phase-I campaign was based on a Boeing 767 passenger aircraft from German Lufthansa with cruising altitude between 9-11 km [Figure 4.15b,c,d]. During each flight, 12 flask samples were collected for laboratory analysis of CO_2 and other trace gas concentrations. In this study we use data from the phase-I campaign and the years 1998, 1999 and 2001. The information that phase-I delivered has been partly published (*caribicatmospheric.com*). The experimental details and analytical methods are described in *Brenninkmeijer et al*. [1999] and *Zahn et al*. [2002].

4.2.1.5 PEM-Tropics (Pacific Exploratory Mission) airplane campaign, 1996 & 1999

PEM-Tropics airplane observations were conducted in the southern tropical regions of the Pacific Ocean, extended zonally across the entire Pacific basin and meridionally from Hawaii to Southern New Zealand (Figure 4.10). PEM-Tropics-A was conducted during August-September 1996 and PEM-Tropics-B during March-April 1999. The PEM-Tropics-A observations (August-October, 1996) coincide with the period when biomass burning reaches its seasonal maximum in the southern tropics [*Kirchhoff et al.,* 1996]. PEM-Tropics-B was conducted during March-April 1999 which corresponds to the wet season. The two aircraft used in these campaigns were P3B and DC8. Observations onboard P3B covered the altitude from the surface to 8 km and observations onboard DC8 were taken at 12 km. Both aircraft were equipped with instrumentation which measured various trace gases including CO_2. The DC8 and P3B CO_2 data were measured with a LI-COR non-dispersive infrared gas analyzer. The details about analysis technique and instrument are given in *Vay et al.* [1999]. In total 34 flights were conducted during the PEM-Tropics-A and 35 flights during the PEM-Tropics-B.

4.2.2 Model Simulations

4.2.2.1 Atmospheric Tracer Transport Model, TM3

Most of the model simulations used in this study have been described in *Tiwari et al.* [2005]. Here we will review briefly some aspects necessary to understand the results. Atmospheric CO_2 is predicted by TM3 [*Heimann*, 1996], a global atmospheric tracer transport model, by applying CO_2 fluxes estimated by *Rödenbeck et al.* [2003] as a boundary condition. The model solves the continuity equation for an arbitrary number of

atmospheric tracers on a regular grid spanning the entire globe. The horizontal resolution of TM3 is 4^0 latitude x 5^0 longitude with 19 sigma-coordinate layers in the vertical. Transport in TM3 is driven by meteorological fields derived from NCEP (National Center for Environmental Predictions) reanalysis [*Kalnay et al.*, 1996].

4.2.2.2 Surface Flux

The CO_2 surface fluxes applied in TM3 as a boundary condition are described in *Rödenbeck et al*. [2003]. The fluxes are resolved monthly and are based on 20 years of atmospheric near surface CO_2 flask data from the NOAA/CMDL station network [update by *Conway et al.*, 2004]. The inverse calculations are based on the TM3 model. The *Rödenbeck et al*. [2003] fluxes used in this study are based on 26 surface stations and cover the period from 1991 to 2001. The spatial resolution of the flux is 8^0 latitude x10^0 longitude. Details of the flux and its estimation method are given in *Rödenbeck et al*. [2003].

4.3. Comparison and Results

4.3.1 Upper Troposphere longterm time series

4.3.1.1 Time extrapolation of surface fluxes and detrending and deseasonalizing of time-series

Surface fluxes used as surface boundary conditions in the simulations of atmospheric CO_2 span the period 1991-2001. To compare the simulations with observations after 2001 we have extended the *Rödenbeck et al.* [2003] data to 2003 by averaging the 1991-2001 fluxes on a monthly basis. The 2002-2003 fluxes thus represent a climatological mean only.

To permit an analysis of events in the time-series we decompose them into trend, seasonal cycle and residual variation by fitting a function of the form

$$CO_2^{model}(t) = \underbrace{a_0 + a_1 t + a_2 t^2}_{trend} + \underbrace{\sum_{n=1}^{4}[b_n \cdot \sin(2\pi n\omega t) + c_n \cdot \cos(2\pi n\omega t)]}_{seasonal\ cycle} \qquad (4.1)$$

to the data where t is time and ω=1 yr^{-1} (e.g. *Keeling and Heimann*, 1989). Residual variability may be related to climate oscillations like El Nino or may be due to shorter term events like deep convection.

In all the comparisons discussed below the model is sampled at the same time and same location as the observations.

4.3.1.2 JAL data (Japan-Australia flights)

Figure 4.2a shows observed CO_2 time-series during the JAL flights cruising between Japan and Australia together with simulated CO_2 ordered into latitude bands. Agreement is generally very good (Tables 4.1 and 4.2). Both phase and amplitude of the seasonal cycle as well as short term variance are quite well captured.

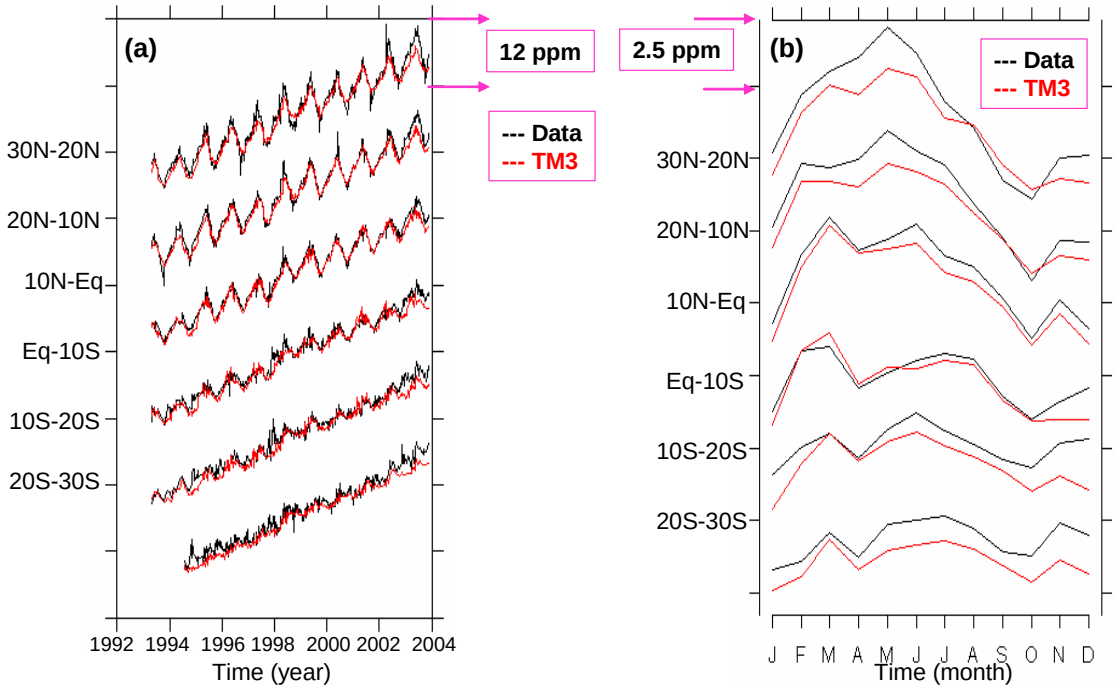

Figure 4.2: (a) CO_2 concentration (ppm) averaged over 10^0 latitudinal bands as observed by (Japan Airlines) JAL (black) and simulated by TM3(red) for the period 1993-2003; (b) Monthly mean CO_2 concentration (ppm) for 10^0 latitude bands as observed by JAL (black) and simulated by TM3(red) for the same period 1993-2003.

The simulations tend to underestimate maxima in winter and to a lesser extent minima in summer in the northern hemisphere. This may be a reflection that surface fluxes are resolved only on a monthly basis. The simulations also tend to underestimate short term variance in Southern hemisphere records (particularly 20^0S-30^0S) which may indicate shortcomings of transport modeling in this region. Agreement is less good at the end of the record (years 2002 and 2003) as expected as surface fluxes used for the simulations have been extrapolated to these years as explained above. Mean annual cycles (Figure 4.2b) confirm the previous remark that maxima in seasonal cycles in the northern hemisphere are underestimated in the models by up to 2 ppm. Also both at northern and southern hemisphere subtropical latitudes the upper troposphere CO_2 value is smaller than observed by approximately 1 ppm while the agreement in the tropical upper troposphere is very good. The mean annual cycles reveal three maxima in CO_2 during the year in the tropics and southern hemisphere subtropics in contrast to the northern hemisphere with only one annual maximum Residuals for four selected latitude bands (Figure 4.3) shows that the magnitude of observed maximal residuals is larger by approximately a factor 1.5 indicating that transport events probably related to convection are more vigorous in nature than modeled. The comparison also shows that surface flux anomalies like the one during the 1998 El Nino event are reflected both in observations and simulations with very similar magnitude. Often events of shorter duration are correlated quite well between observations and simulations which is somewhat surprising and very encouraging with regards to our capability to represent atmospheric transport with models. This can be made more quantitative by calculating correlations between observed and simulated residuals and examining significance of the correlation coefficients (Figure 4.4). Correlation coefficients R^2 vary between 0.1 and 0.27 and all are significant at the 95% significance level according to a t-test. The regression line (red line in Figure 4.4) indicates that there is variability in the observed residuals but the variability in the simulated residual is small.

.

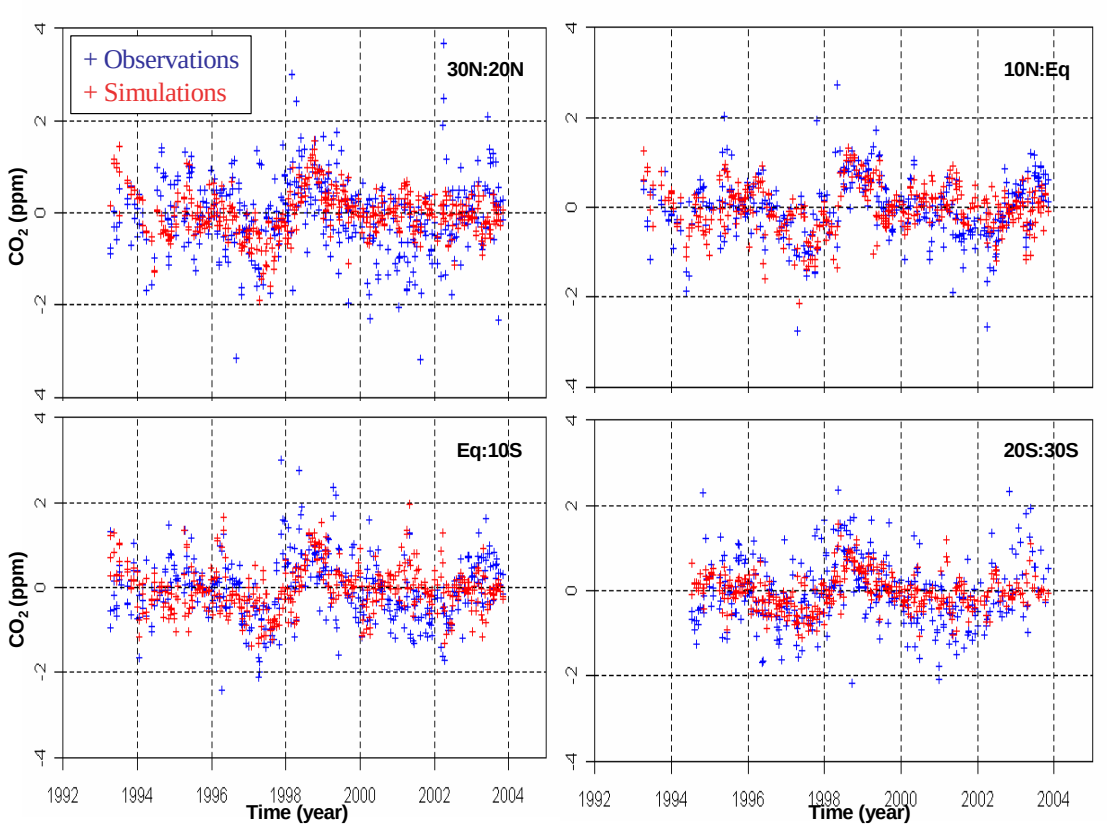

Figure 4.3: Deviations from the global mean for 10^0 latitude bands as observed by (Japan AirLines) JAL (blue) and simulated by TM3(red) between period 1993-2003.

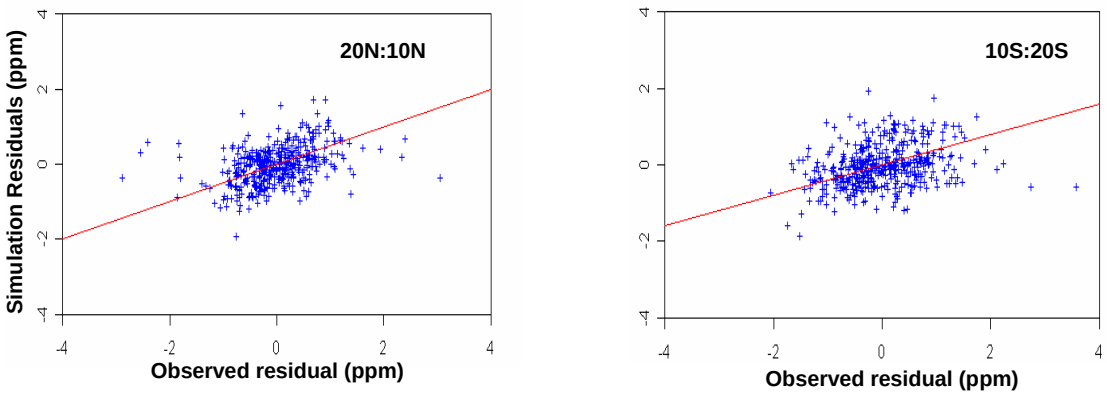

Figure 4.4: Correlation between simulated and observed residuals (deviations from the global mean) for two 10^0 latitude bands along the (Japan AirLines) JAL observation flight track between period 1993-2003. Red line indicates regression line

Table 4.1: 10 year mean difference of JAL observed minus model simulated CO_2 mixing ratio (ppm) along JAL flights (Japan-Australia).

Latitude Band	Difference (full signal) = JAL observed - simulated (ppm)	Difference (Seasonal cycle) = JAL observed - simulated (ppm)	Difference (residual) = JAL observed - simulated (ppm)
40N:30N	-0.2	0.4	-0.5
30N:20N	0.3	0.4	0.0
20N:10N	0.4	0.4	0.0
10N:0	0.3	0.4	-0.1
0:10S	0.3	0.4	-0.1
10S:20S	0.5	0.4	0.1
20S:30S	0.7	0.4	0.3
30S:40S	0.3	0.3	0.1

Table 4.2: RMS difference between JAL observed and model simulated CO_2 mixing ratio (ppm) for the years 1993 to 2003.

Year	$RMS_{deviation}$
1993	0.59
1994	1.01
1995	0.83
1996	0.53
1997	0.60
1998	0.67
1999	0.29
2000	0.39
2001	0.26
(2002	0.95)
(2003	1.66)

4.3.1.3 Cape Grim/Bass Strait airplane observations

Airplane observations over Cape Grim/Bass Strait [Figure 4.5a(i)] have been carried out during 1991-1998. The altitude of these observations ranges from the surface to 8 km. Since in this study we are concerned with a mid-to-upper troposphere airplane-model comparison we are focusing on data between 4 km to 8 km split into two altitude ranges (4-6 km and 6-8 km). Comparison of data and simulations reveals again agreement both in phasing and amplitude. Observed values are approximately 0.4 ppm higher than simulated ones (Table 4.3) which may indicate some systematic bias in transport and fluxes. Inspection of residuals shows again good correlation between observations and simulations particularly with respect to longer-term anomalies on the order of a half to one year but shorter term events are sometimes captured as well. Correlations are again significant.

Table 4.3: RMS (Root Mean Square) difference between Cape Grim airplane observed and model simulated CO_2 mixing ratios (ppm) for the years 1991 to 1998.

Year	$RMS_{deviations}$
1991	0.44
1992	0.44
1993	0.50
1994	0.75
1995	0.58
1996	0.34
1997	0.40
1998	0.37

4.3.2 Vertical profiles of atmospheric CO_2 concentration (ppm)

In the following we are comparing vertical profiles of CO_2 observations extending from the surface to the mid/upper troposphere from 5 campaigns, as the vertical profile structure contains information about transport processes. A representative set of vertical profiles is shown for each campaign ordered by latitude with profiles at the top of the figures corresponding to the northernmost profiles.

One diagnostic for comparing observed and simulated vertical profiles used in the following is a very rough vertical gradient (VG) of atmospheric CO_2, which we compute as follows

$$VG = Mean(C_{(5km\ to\ top\ of\ profile)}) - Mean(C_{(surface\ to\ 5\ km)}) \quad (4.2)$$

The 5 km boundary is chosen because the aim of the study is to validate model simulation at those heights where satellite retrievals are most sensitive. The retrievals which are used in this thesis (in previous chapters) are most sensitive well above 5 km altitude (Chapter 2).

4.3.2.1 BIBLE campaigns

There were three BIBLE campaigns conducted during September-October 1998, August-September 1999 and during November-December 2000 (Figure 4.6). Because of their timing and location the data should contain the biomass burning signal from the rainforests particularly during the 1998 El Nino event.

The profiles from the 1998 campaign (Figure 4.7) reveal good agreement with simulations in the subtropics particularly over the oceans. This concerns both the vertical structure as well as absolute magnitude. There is however a large difference along the equator where the models strongly underestimate concentrations between 0 and 4 km height and to a lesser extent at higher altitude. The reason is unlikely due to transport deficiencies but reflects that the surface fluxes of *Rödenbeck et al.* [2003] did most likely not capture properly the biomass burning signal from the region because of insufficient data coverage. This indicates that surface fluxes in this region and possibly throughout the tropics may be severely underestimated by the *Rödenbeck et al.* [2003] study. It also shows that enhanced observational coverage of lower troposphere CO_2 in the tropics would strongly enhance our capability to constrain a very important component of the carbon cycle – tropical land.

Observation simulation comparison for the 1999 campaign (Figure 4.8) reveals very good agreement for the northern hemisphere subtropics however there is substantial disagreement in the tropics and the southern subtropics. This is again most likely a reflection of much better data coverage in the northern hemisphere compared to the

Southern hemisphere and their effect on the surface flux estimates of *Rödenbeck et al.* [2003]. Finally for the 2000 campaigns (Figure 4.9) there is stunningly good agreement between simulated and observed profiles.

Table 4.4 summarizes the difference between simulations and observations for all BIBLE vertical profiles stratified by latitude bands and height range above ground. When averaged in this way a more detailed picture emerges. In the northern hemisphere subtropics CO_2 seems to be somewhat trapped in the lower 2 km while concentrations are underestimated between 2 and 4 km but match well in the upper troposphere. This indicates that ventilation of the PBL over land during winter is not always efficient enough, however upper troposphere values are not affected – likely because they are not directly linked to PBL – free troposphere exchange. Again very large differences emerge in the tropics throughout the air column indicating strong underestimation of surface fluxes from this region during Northern hemisphere winter months. This is likely again not an indication of flaws in transport but rather surface fluxes. As a consequence other tracers like SF_6 need to be considered to constrain model transport in the tropics.

Table 4.4: CO_2 concentration difference in (ppm) between airplane observations during BIBLE and TM3 simulated CO_2 (ppm) averaged over 10^0 latitude bands and at selected altitude ranges.

Difference = BIBLE observed - simulated			
Latitude Band	Altitude		
	0 to 2 km	2 km to 4 km	5 km to 12 km
40N : 30N	0.8	-0.3	0.0
30N : 20N	0.6	-0.4	-0.2
20N : 10N	-0.1	0.3	0.4
10N : 0	2.6	2.7	1.4
0 : 10S	2.3	1.5	1.5
10S : 20S	1.3	0.9	1.2
20S : 30S	0.0	0.8	1.0
30S : 40S	-0.3	0.4	0.6

Table 4.5: Vertical gradients (for definition see equation 4.2) of the observed and simulated CO_2 (ppm) for each air-borne campaign.

Air Plane Campaigns	Vertical gradient (VG) correlation coefficients (R^2)	Significance (p value)
BIBLE-A (1998)	+0.026	0.79
BIBLE-B (1999)	+0.76	**0.01**
BIBLE-C (2000)	+0.94	**0.0003**
PEM-Tropics-A-DC8 (1996)	+0.61	**0.04**
PEM-Tropics-A-P3B (1996)	+0.23	0.23
PEM-Tropics-B-DC8 (1999)	+0.73	**0.0004**
PEM-Tropics-B-P3B (1999)	+0.080	0.42

4.3.2.2 PEM-Tropics observations

The observations from the PEM campaigns add two additional components to the picture. First not only autumn and winter profiles have been measured but also spring profiles and second the Eastern Pacific troposphere is sampled across a wide latitude range (Figure 4.10). In agreement with the BIBLE data the PEM profiles reveal a substantial underestimation of tropical CO_2 throughout the air column during autumn and winter while the vertical structure of the profiles matches well with observations (Figures 4.11, 4.12). In contrast during the March-April campaigns agreement is generally good both with regards to absolute magnitude and vertical structure. A quantitative assessment of the agreement between vertical gradients is given in Table 4.5.

Table 4.6: Difference between PEM airplane observed data and TM3 simulated CO_2 (ppm), averaged over 10^0 latitude bands for selected altitude regions.

Difference = PEM observed - simulated			
Latitude Band	Altitude		
	0 to 2 km	2 km to 4 km	5 km to 12 km
40N : 30N	-0.01	0.46	-0.22
30N : 20N	-0.57	0.09	-0.02
20N : 10N	-0.19	-0.22	-0.07
10N : 0	0.43	0.56	-1.43
0 : 10S	0.20	0.12	0.13
10S : 20S	-0.25	0.14	0.04
20S : 30S	-0.31	0.26	0.05
30S : 40S	0.14	0.43	0.25

It is interesting to note that in Figure 4.13 for each profile over the tropical Pacific there is a surface and mid-to-upper troposphere CO_2 maximum that gradually decreases with height. This feature is due to release of CO_2 at the ocean surface in the tropical oceanic areas [e.g. *Gloor et al.,* 2003]. Surface measurement of $^{13}C/^{12}C$ ratio have also demonstrated that the source can be attributed to the release of CO_2 from sea water along the equator where the north and south equatorial currents from each hemispheres meet causing a divergence or upwelling [e.g. *Gruber et al.,* 2001].

Mean differences across all PEM vertical profiles are summarized in Table 4.6. While generally agreement is very good (<= 0.5 ppm) the tropics are again an outlier particularly in the upper troposphere. We tend to interpret this as deficiencies in surface fluxes rather than transport but we cannot definitely answer this question.

4.3.3 Seasonal Cycle of upper troposphere meridional CO_2 gradients

4.3.3.1 CARIBIC and JAL campaign observations versus model simulation and AIRS retrievals

The JAL observation program has been introduced already (Figure 4.1). CARIBIC was in operation during 1997-2002 using a Boeing 767-ER (phase 1), and resumed

measurements in December 2004, using an Airbus A340-600 (phase 2) [*Brenninkmeijer et al.*, 2005]. In this study we use part of CARIBIC (phase 1) campaign (1998-2001). The comparisons focus on the meridional gradient in CO_2 and its seasonal cycle imprinted by the seasonal cycle of the northern hemisphere land biosphere with large carbon uptake during spring and summer and carbon release during the rest of the year. The meridional structure and particularly the amplitude of these signals in the upper troposphere is an indicator whether lower-to-upper troposphere transport in models is realistic.

Focusing first on JAL observations (Figure 4.15a) for two years we find good agreement for 1999 but less agreement in 2003. Since we only use climatological mean fluxes in 2003 as explained earlier on the 2003 simulations should be given less weight. The 1999 gradients reveal the expected picture. From January to July Northern hemisphere CO_2 is ramping up as a consequence mainly of fossil fuel emissions and respiration of the land biosphere. The signal is also seen in the Southern hemisphere but with much smaller amplitude, particularly to the South of 15^0S. From July onwards there is a steep decrease in the North-South gradient due to photosynthetic carbon uptake by the Northern hemisphere land vegetation. In November the gradient starts to steepen again in accordance with the end of the growing season at this time. It is interesting to notice that the CO_2 maxima during the first half of the year are located between 25^0N and 30^0N which is further to the South than expected from fossil fuel emissions. It may thus be a reflection of transport to the upper troposphere (see Chapter 2). This feature is stronger in the data than in the simulations. Also the total seasonal amplitude in the gradient is somewhat smaller in the simulations indicating that transport of surface signatures to the upper troposphere is somewhat less efficient than expected, likely because the diffusive component of transport is somewhat exaggerated in the model.

Comparison of the annual cycle of North-South gradients in upper tropospheric CO_2 for the CARIBIC campaigns confirms this latter assertion (Figures 4.15b,c,d). The amplitude of the annual cycle in North-South gradients as predicted by the simulations is too small by up to a factor 2. This is particularly pronounced along the flight tracks from Germany to Arabia. There are also differences in phasing which suggest that there are issues with transport representation in the models.

Finally for both CARIBIC flights we have also extracted the CO_2 signatures recorded by AIRS. While phasing of the seasonal cycle in North-South gradients is captured the amplitude of the drawdown signal is smaller than the simulated amplitude which itself is smaller than observed. This shows that simulated signatures are close to observations than to AIRS retrievals.

4.4 Summary

The potential of the global tracer transport model in the upper troposphere and lower to upper troposphere transport can be determined by closely comparing model simulations with upper troposphere in-situ observations. In this study airplane observations from 5 observation programs are compared with the model simulated CO_2 mixing ratio, sampled at the same time and location as the observations. We have looked at three diagnostics: upper troposphere long-term time-series, vertical structure of profiles extending from the ground to the upper troposphere and upper troposphere meridional gradients and their seasonality. Long term time-series at various latitudes between Japan and Cape Grim, Australia reveal generally good agreement (Northern hemisphere RMS=0.3 ppm, Tropics and Southern hemisphere RMS=0.5-0.6 ppm). At northern hemisphere mid latitudes summer maxima are underestimated possibly because they are not properly communicated from the surface to the upper troposphere. Possibly there is a relation to mixing related to breaking of Rossby waves in the upper troposphere and associated mixing which may be too weak or not well represented in the models. Similarly short term events possibly due to convection are smaller in the simulations compared to observations by approximately a third of the signal indicating again that surface signals are communicated too weakly to the upper troposphere even though the events themselves are often well captured by the transport model.

Vertical profiles above Indonesia and Indo-china reveal generally good agreement in the vertical structure of the profiles however there are large differences (~ 2 ppm) in magnitude in autumn 1998 and 1999 in the tropics. A similar picture emerges from the profiles measured above the Eastern Pacific in 1996 where observed tropical concentrations during autumn are also substantially larger than simulated ones. While the good agreement in vertical structure gives trust in the transport abilities of the model the

differences in magnitude in the tropics indicate that the *Rödenbeck et al.* [2003] fluxes underestimate fluxes from the tropics to the atmosphere most likely related to biomass burning (particularly 1998). This is not a surprise as there are very few surface stations in the tropics which enter these inverse calculations. Nonetheless it indicates that the results on tropical sources and sinks in the *Rödenbeck et al.* [2003] need likely to be substantially revised.

Comparison of meridional structure and seasonality of meridional upper troposphere gradients across the North Atlantic, Europe and Arabia, and Japan and Australia reveal quite good agreement. The total amplitude of the annual cycle tends to be too small in the simulations particularly for the Europe to Arabia transect indicating that surface signals may not be quite communicated properly in the models. Comparison with observations from AIRS reveals that models are in closer agreement with observations than the satellite retrievals.

In summary we find that agreement between upper troposphere simulations and observations both with regards to vertical and temporal phasing are in good agreement within RMS ~ 0.4 ppm. Nonetheless signals tend to be communicated from the surface to the upper troposphere in somewhat too diluted form for reasons that need to be investigated using possibly other tracers than CO_2. Altogether this indicates that differences found in a precursor paper between AIRS retrievals and simulations of atmospheric CO_2 based on the *Rödenbeck et al.* [2003] fluxes are unlikely due to deficiencies in model transport but rather biases in the retrievals.

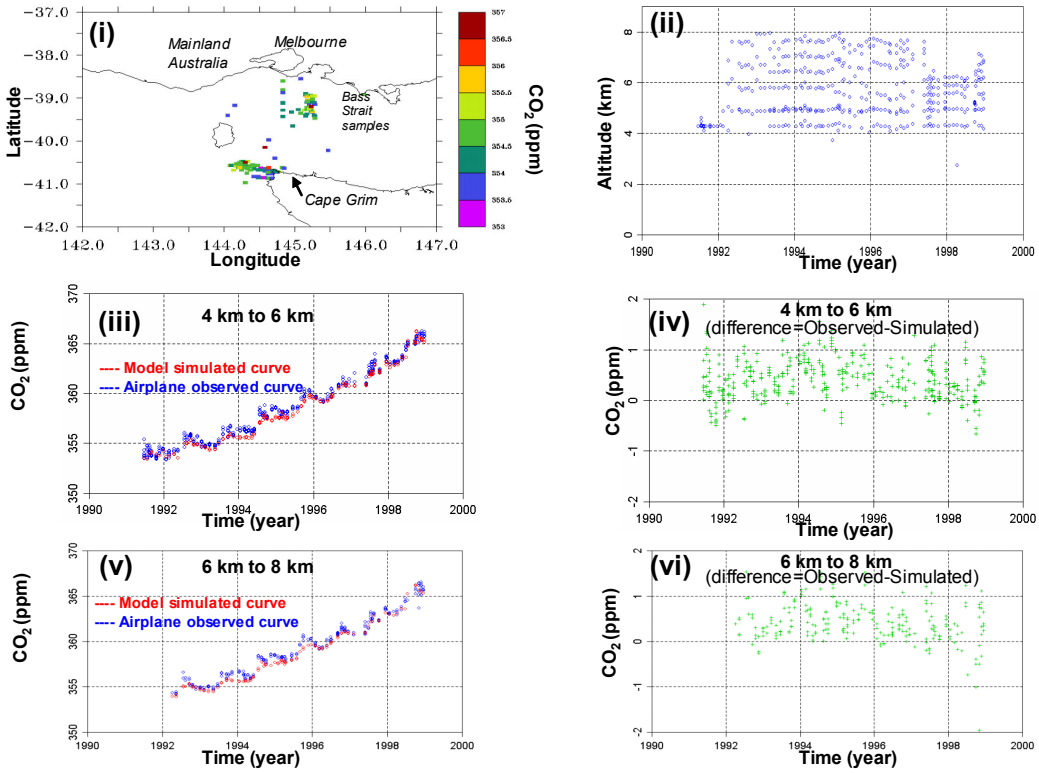

Figure 4.5a: Cape Grim/Bass Strait airplane observations 1991-2000 (i)locations; (ii) cruising altitude as a function of time; (iii) CO_2 concentration timeseries for airplane observations(blue) and TM3 simulations(red) between 4km to 6km; (iv) observation minus simulation between 4km to 6km height; (v) CO_2 concentration timeseries for airplane observations(blue) and TM3 simulations(red) between 6km to 8km height; (vi) observation minus simulation in 6km to 8km height

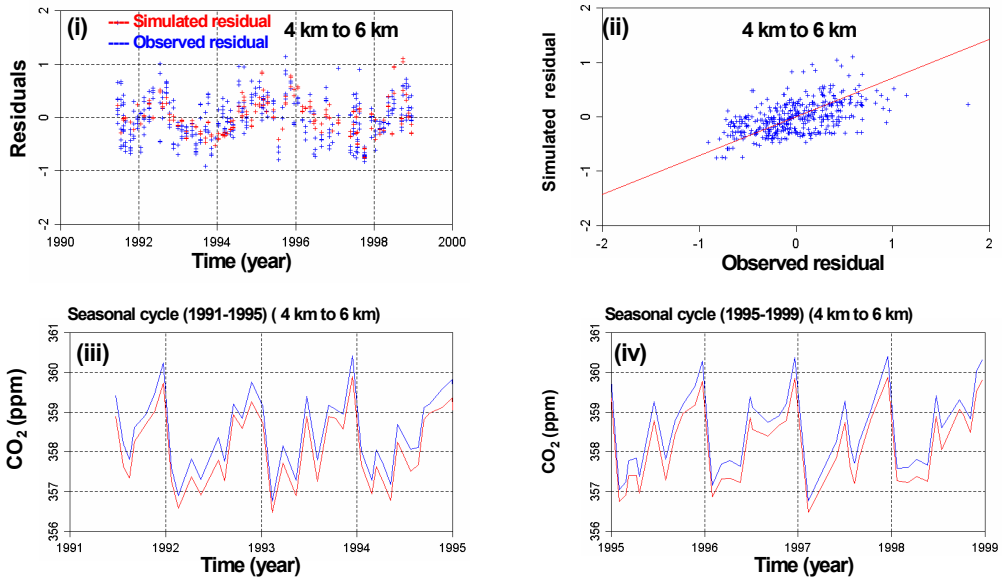

Figure 4.5b: Cape Grim/Bass Strait airplane observations 1991-2000 : (i) observed (blue) and simulated (red) residuals between 4km to 6km height; (ii) correlation between observed and simulated residuals between 4km to 6km height, red line indicates regression line; (iii)seasonal cycle for observations (blue) and simulations (red) during 1991-1995 at 4km to 6km height; (iv) seasonal cycle for observations (blue) and simulations (red) during 1995-1999 between 4km and 6km height.

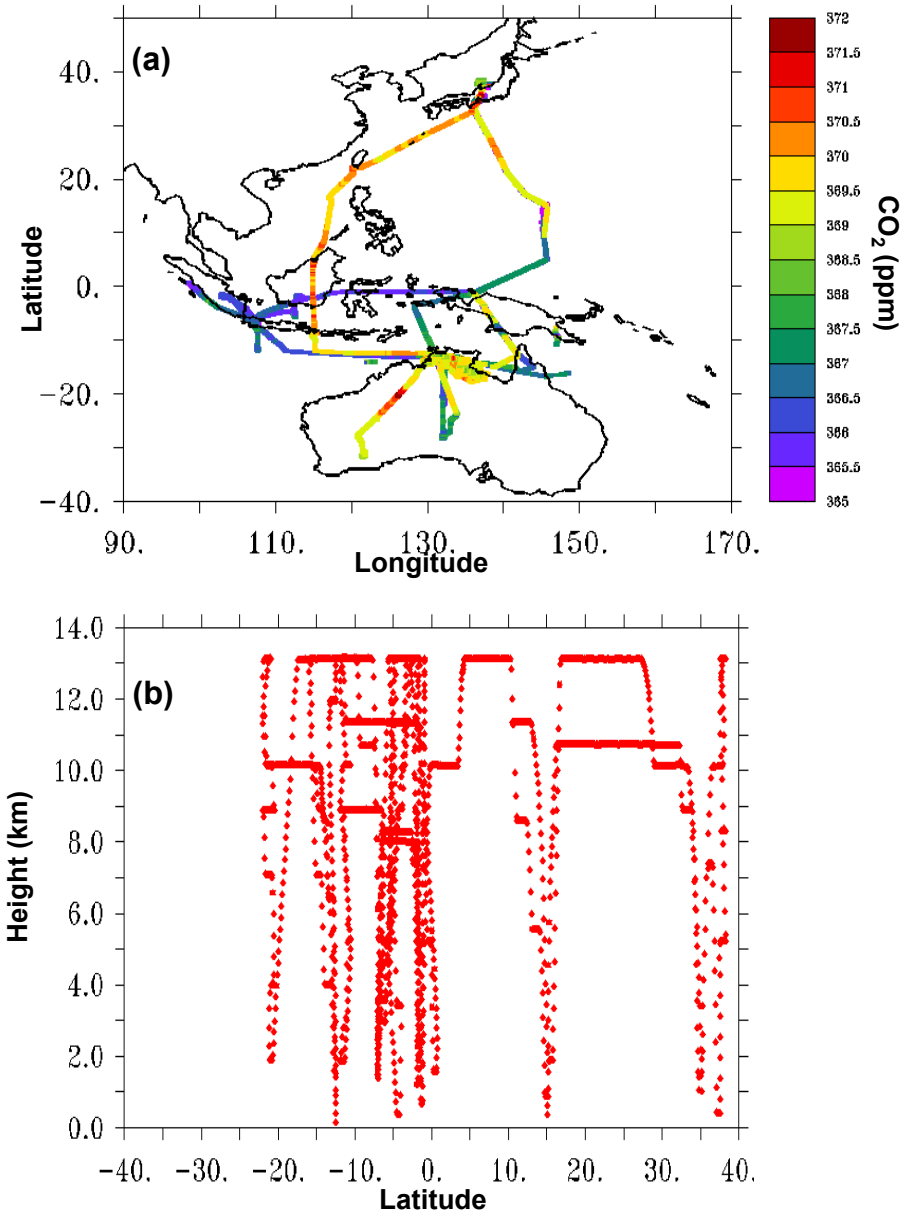

Figure 4.6: BIBLE airplane observations of CO_2 concentrations in along 1998-2000 airplane tracks (a) and cruising altitude as a function of latitude (b) during these flights.

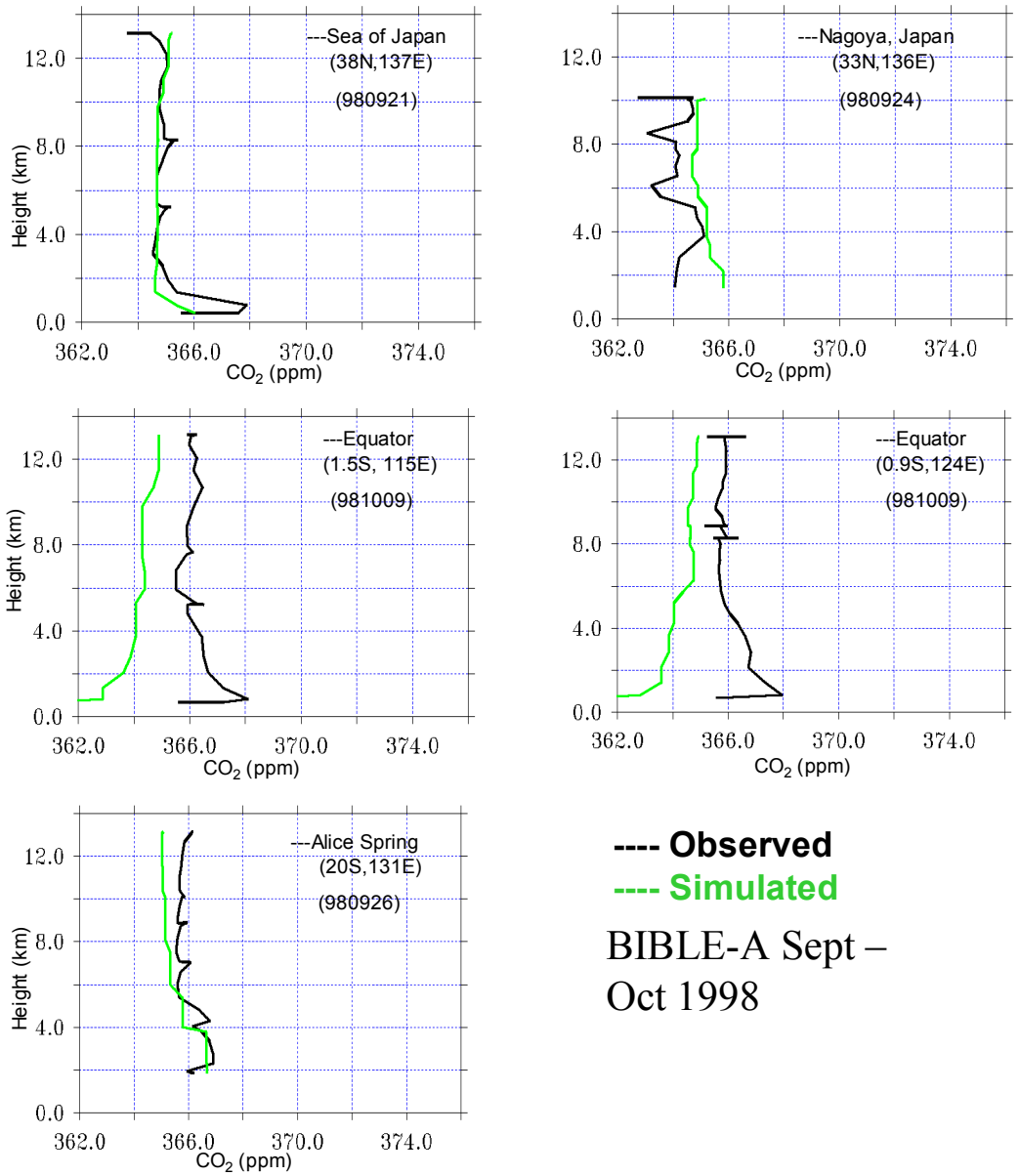

Figure 4.7: Vertical distributions of CO_2 (ppm) at selected locations, as observed by BIBLE-A airplane observations (black) and TM3 simulations(green) during 1998.

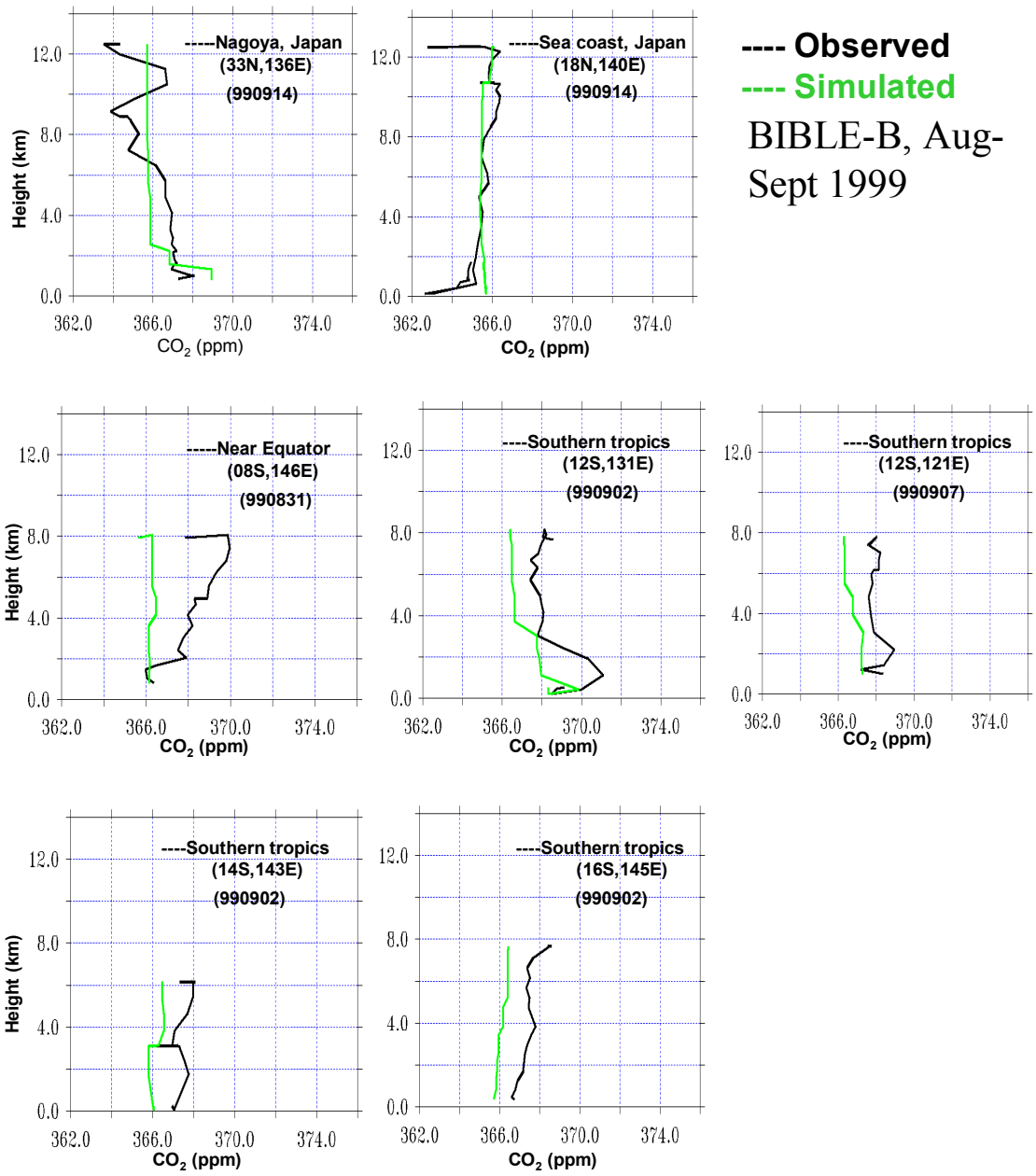

Figure 4.8: Vertical distributions of CO_2 (ppm) at selected locations, as observed by BIBLE-B airplane observations (black) and TM3 simulations(green) during 1999.

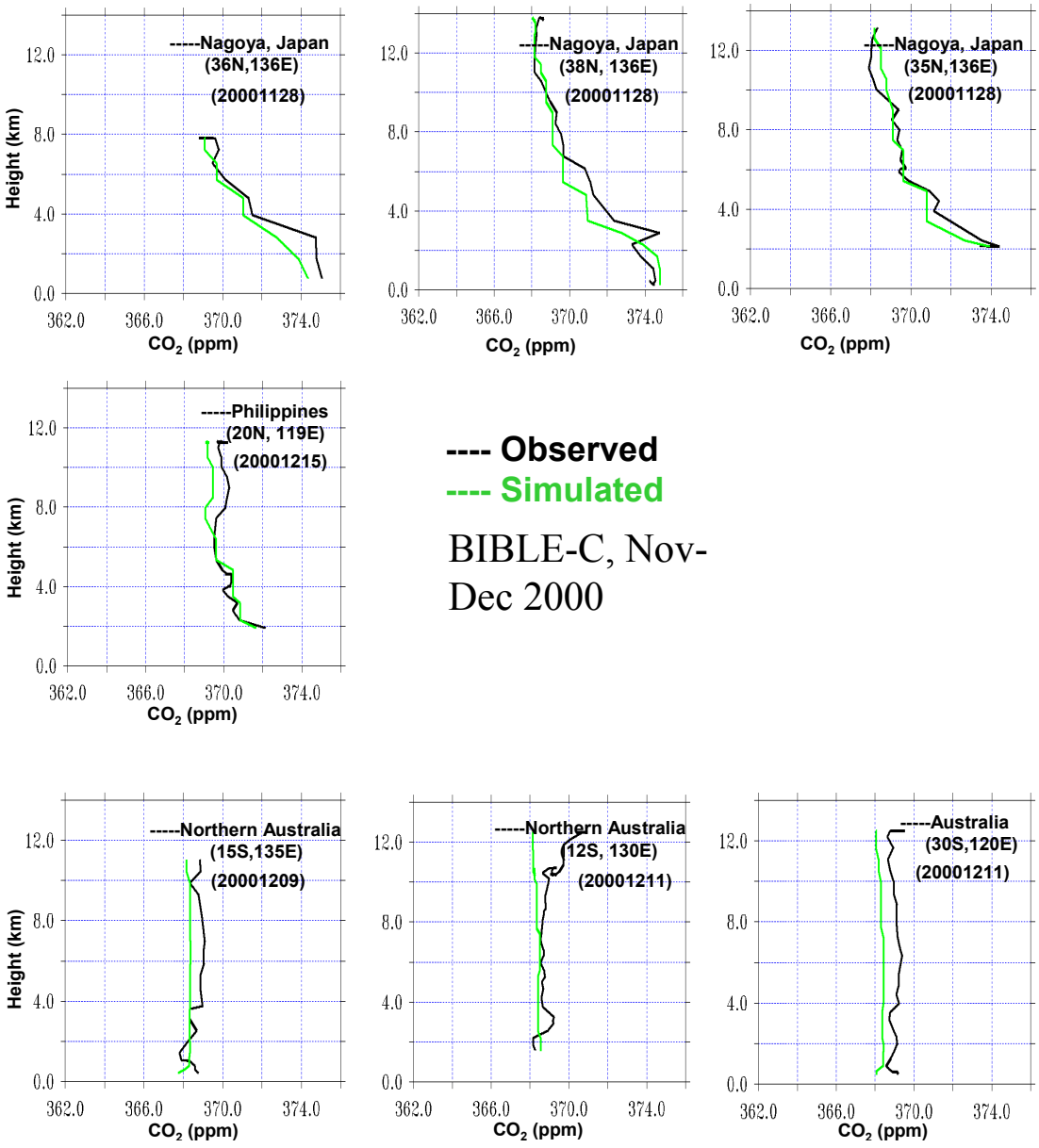

Figure 4.9: Vertical distributions of CO_2 (ppm) at selected locations, as observed by BIBLE-C airplane observations (black) and TM3 simulations(green) during 2000.

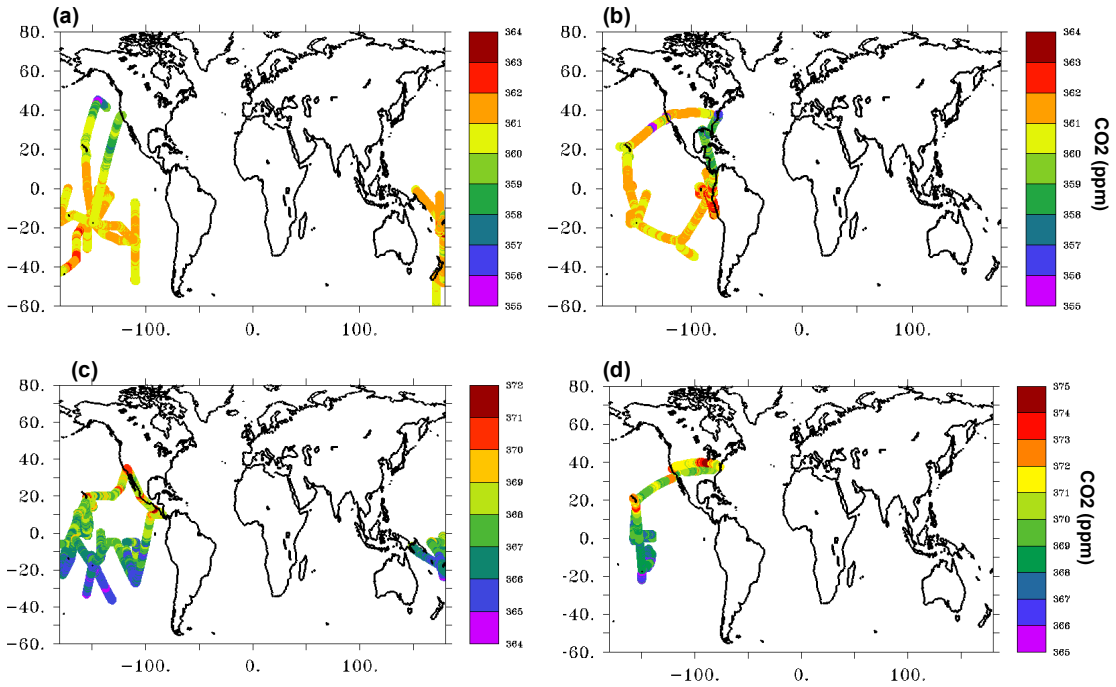

Figure 4.10: PEM air-borne observations: (a) PEM-Tropics-A-DC8, 1996 ; (b) PEM-Tropics-A-P3B, 1996; (c) PEM-Tropics-B-DC8, 1999; (d) PEM-Tropics-B-P3B, 1999.

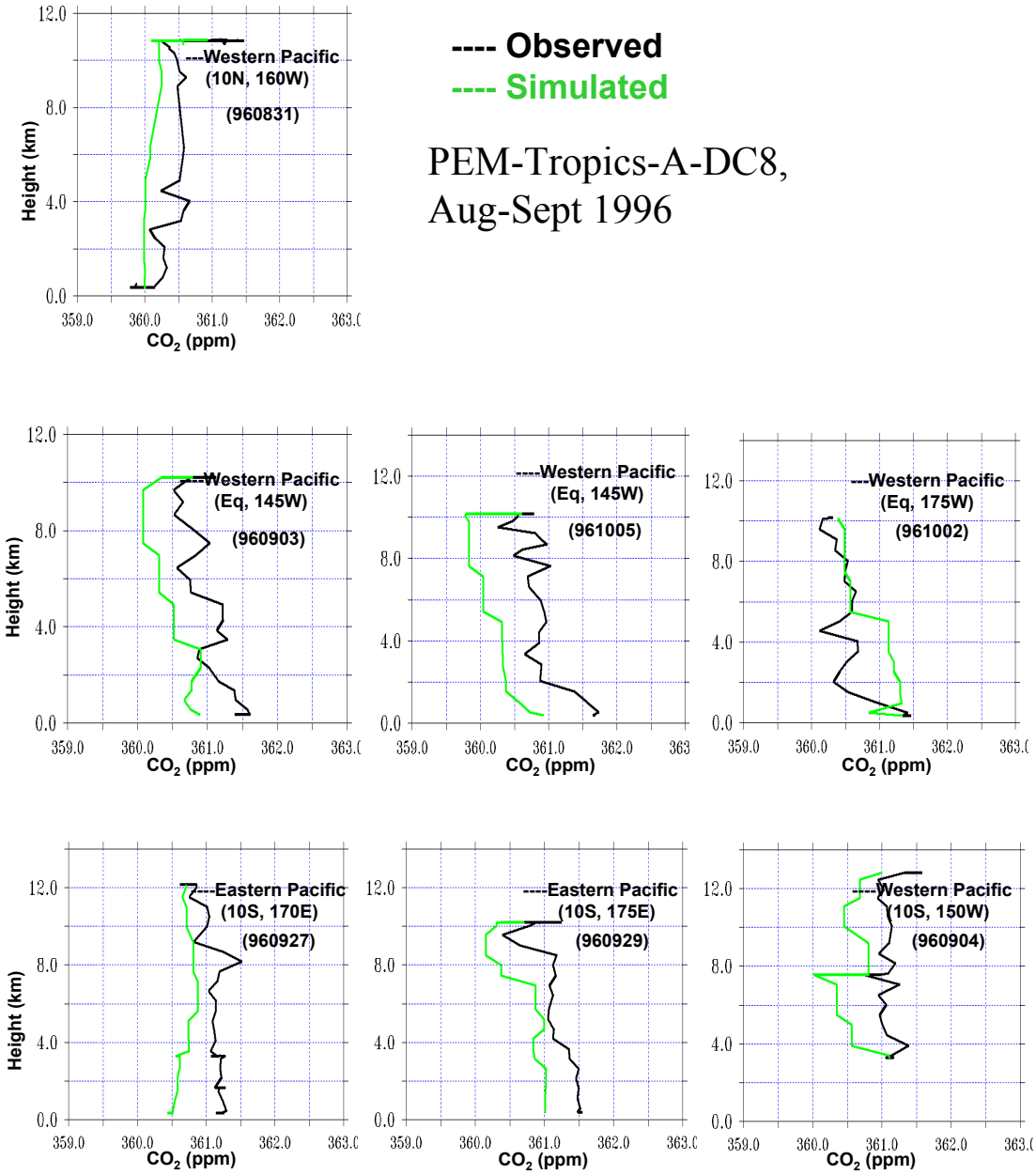

Figure 4.11: Vertical distributions of CO_2 (ppm) at selected locations, as observed by PEM-Tropics-A-DC8 airplane observations (black) and TM3 simulations (green) during 1996.

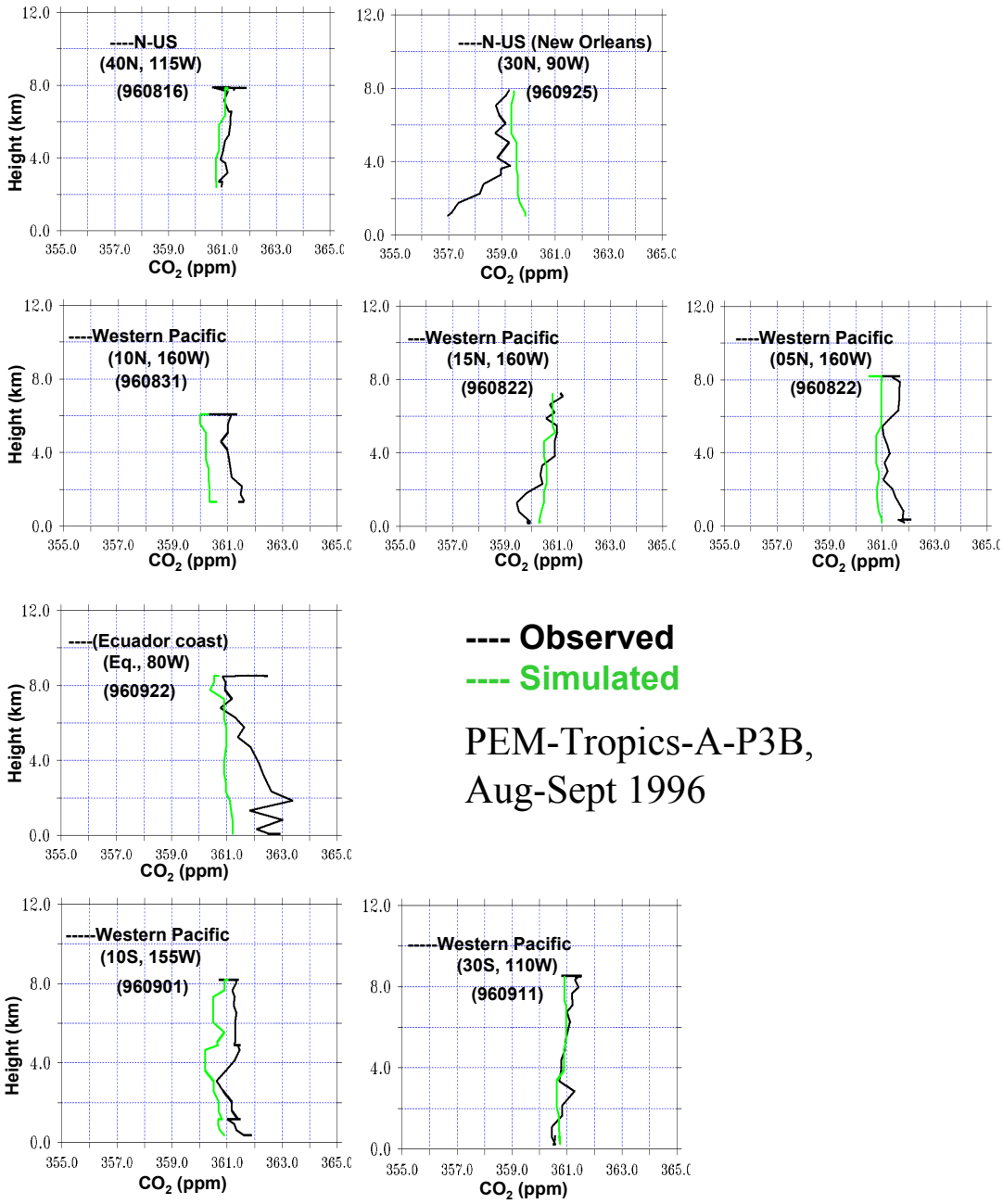

Figure 4.12: Vertical distributions of CO_2 (ppm) at selected locations, as observed by PEM_tropics-A-P3B airplane observations (black) and TM3 simulations(green) during 1996.

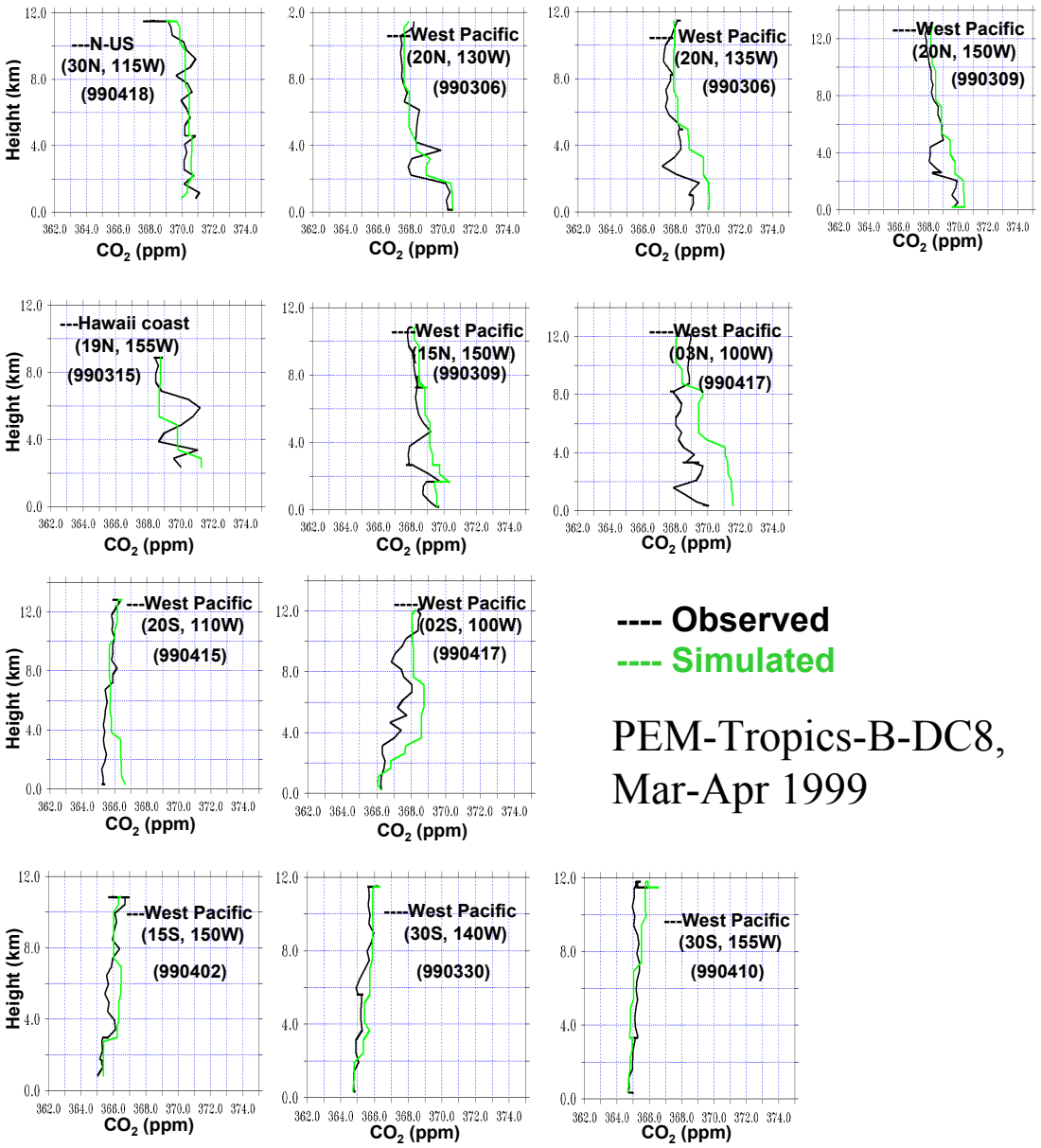

Figure 4.13: Vertical distributions of CO_2 (ppm) at selected locations, as observed by PEM-Tropics-B-DC8 airplane observations (black) and TM3 simulations(green) during 1999.

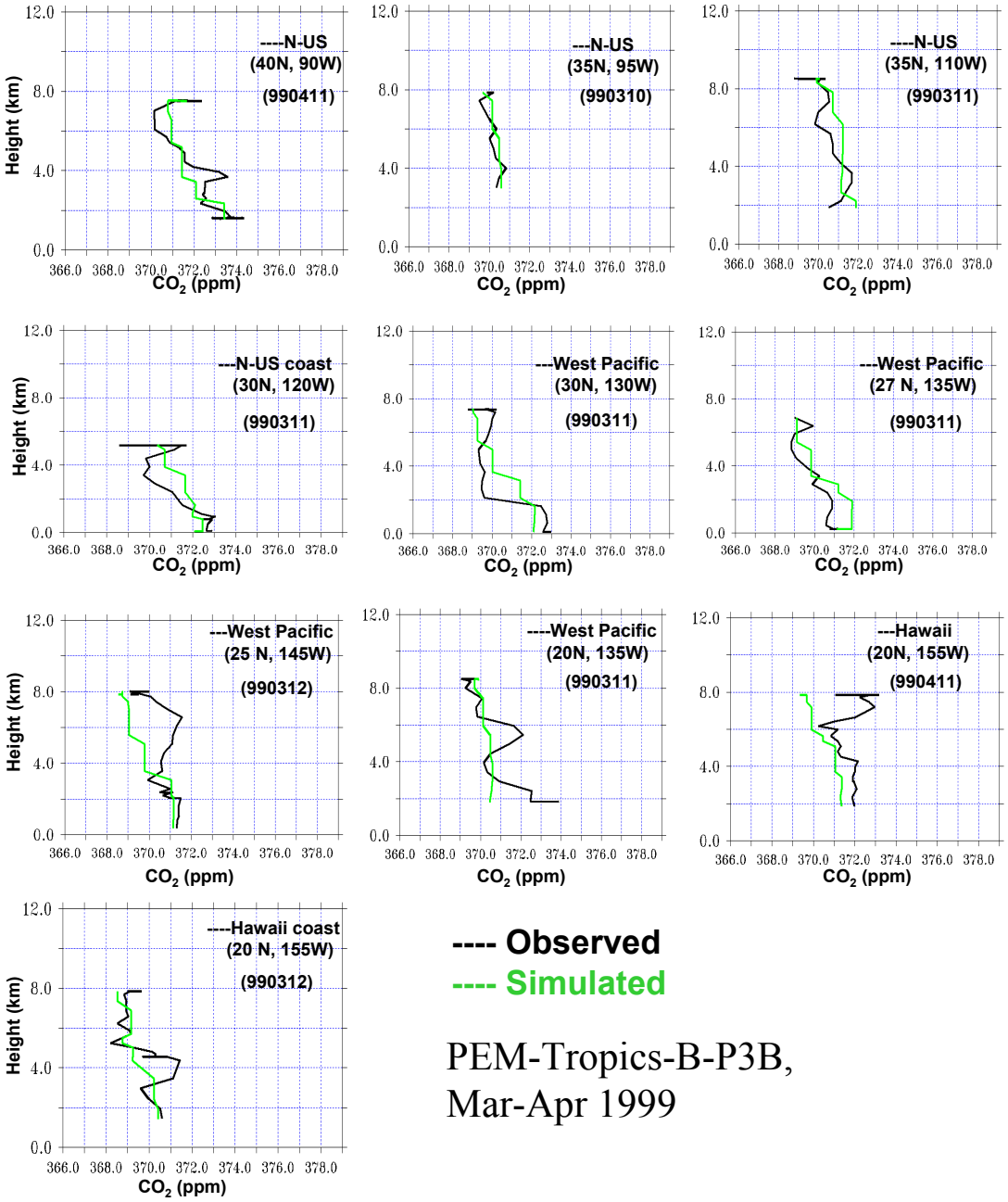

Figure 4.14: Vertical distributions of CO_2 (ppm) at selected locations, as observed by PEM-Tropics-B-P3B airplane observations (black) and TM3 simulations(green) during 1999.

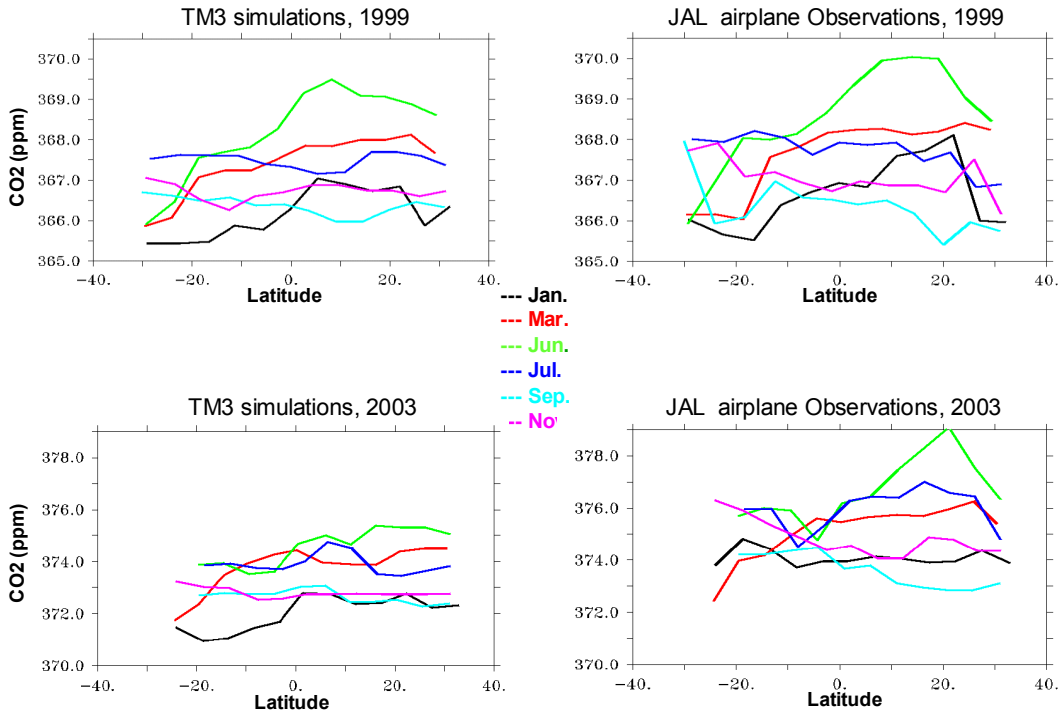

Figure 4.15a: Monthly mean latitudinal variation of CO_2(ppm) as observed by Japan Airlines(JAL) and TM3 simulations during 1999 and 2003.

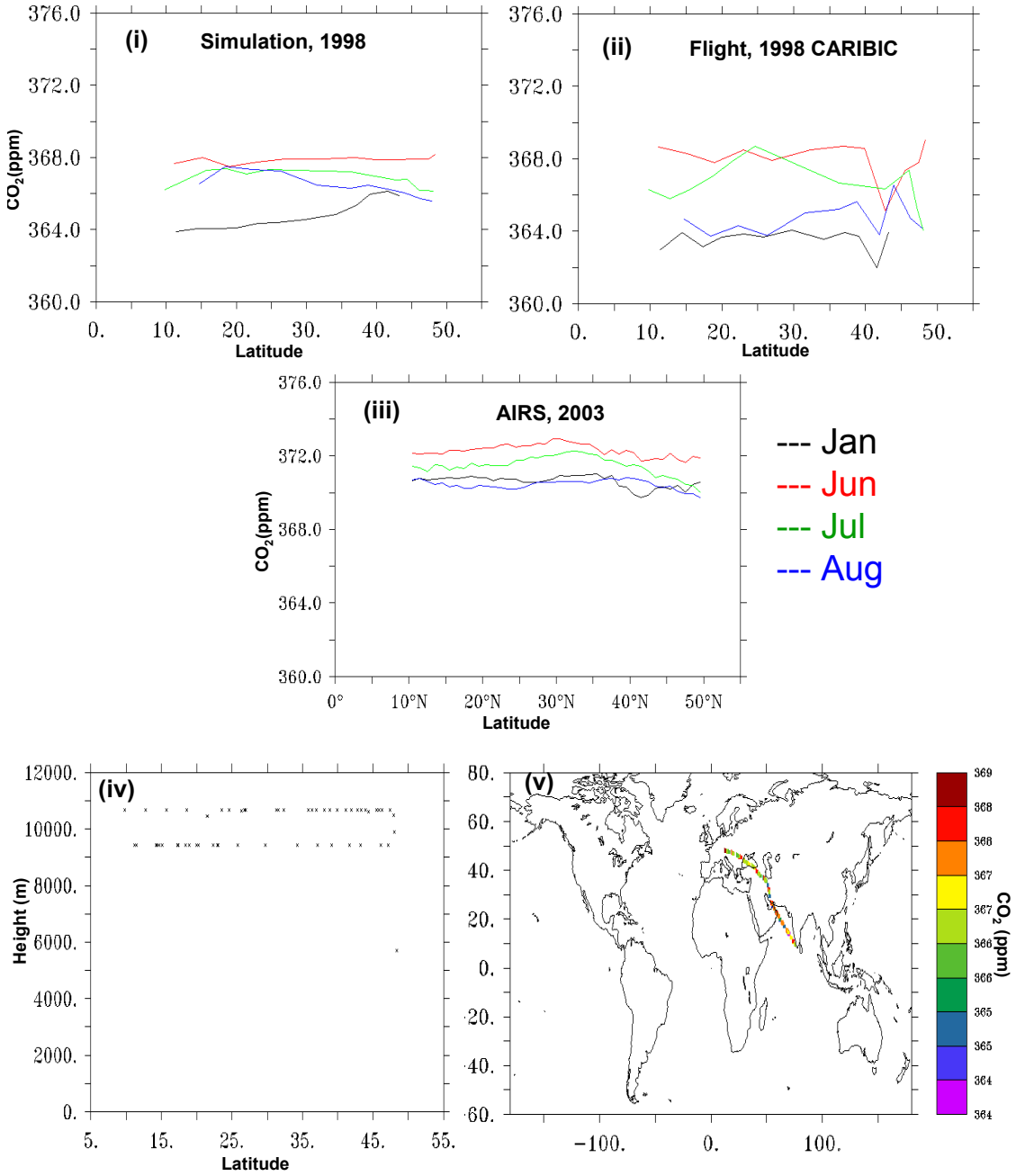

Figure 4.15b: Monthly mean latitudinal variation of CO_2(ppm): (i) as simulated by TM3 during 1998; (ii) observed by CARIBIC, 1998; and (iii) retrieved by AIRS during 2003; (iv) cruising altitude as a function of latitude; (v)CO_2 concentration along flight track.

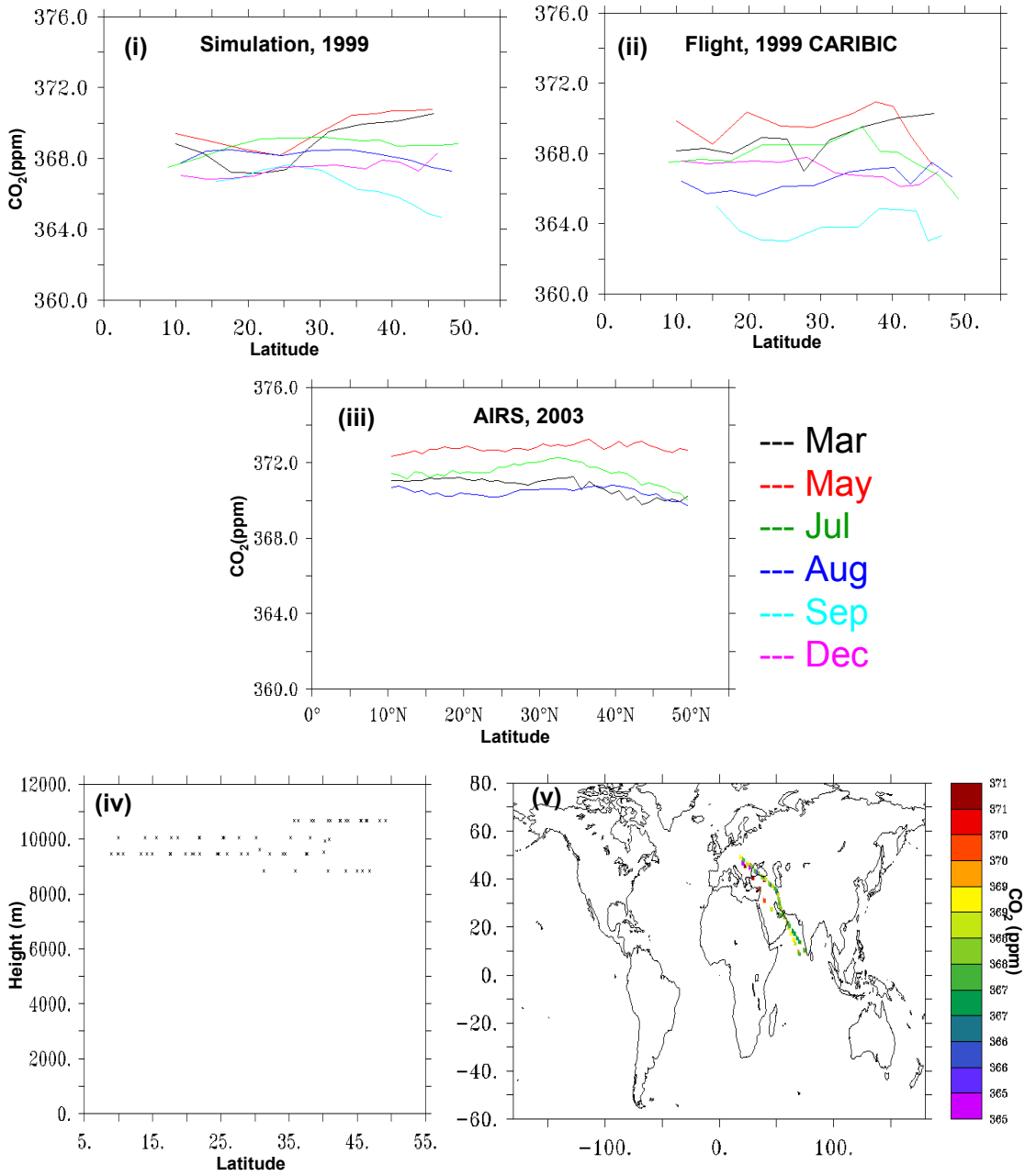

Figure 4.15c: Monthly mean latitudinal variation of CO_2(ppm): (i) as simulated by TM3 during 1999; (ii) observed by CARIBIC, 1999; and (iii) retrieved by AIRS during 2003; (iv) cruising altitude as a function of latitude; (v)CO_2 concentration along flight track

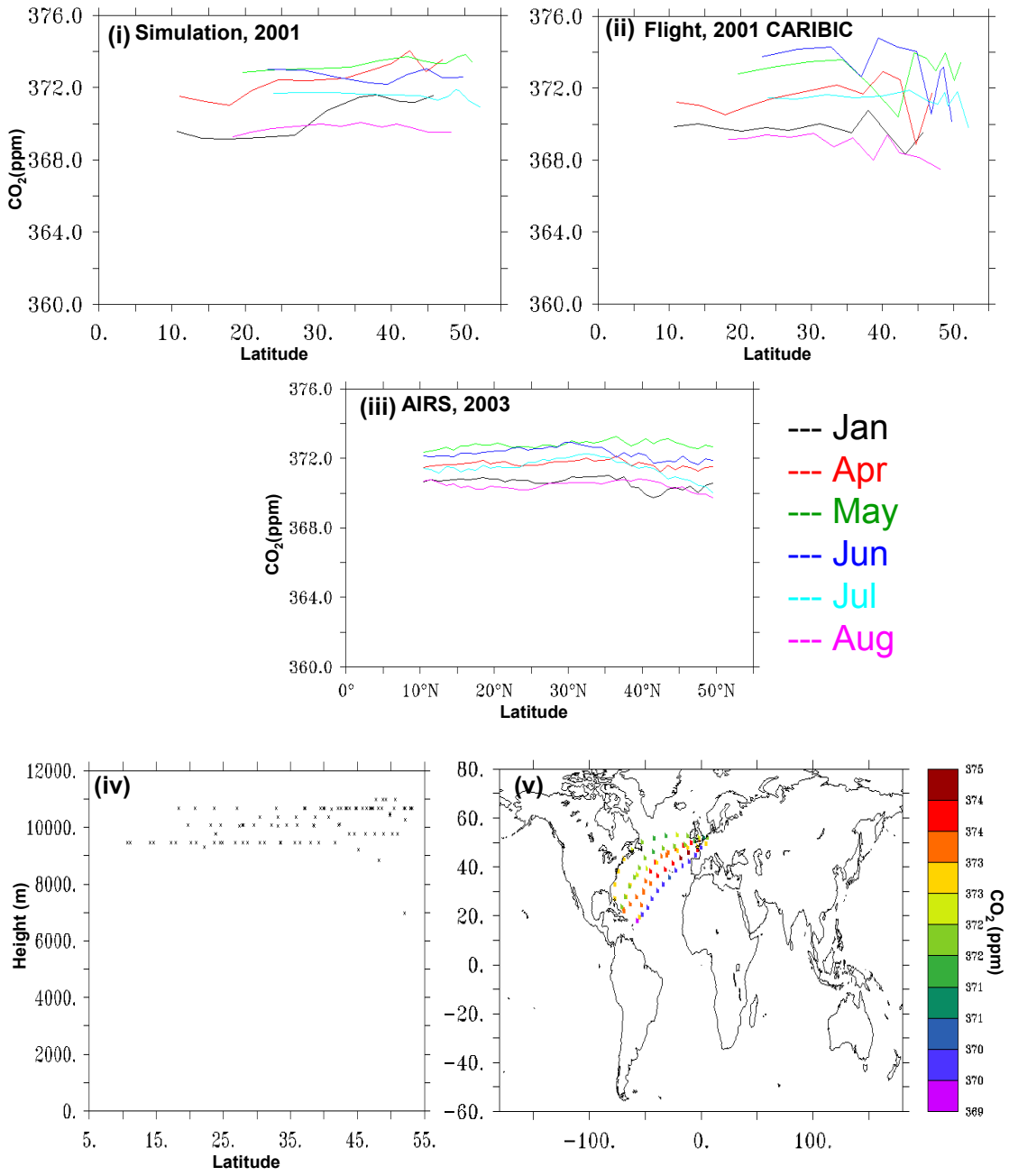

Figure 4.15d: Monthly mean latitudinal variation of CO_2(ppm): (i) as simulated by TM3 during 2001; (ii) observed by CARIBIC, 2001; and (iii) retrieved by AIRS during 2003; (iv) cruising altitude as a function of latitude; (v)CO_2 concentration along flight track

Chapter 5

Conclusions and Outlook

Atmospheric CO_2 contributes the most to radiative forcing of the earth's climate among all anthropogenic greenhouse gases and its contribution is likely to grow substantially during this century. Therefore it is important that there is a reliable capability to monitor pathways of carbon from the atmosphere to both land and oceans to capture unforeseen changes of the pathways as well as to understand underlying mechanisms to permit prognosis of system response.

A conceptually appealing method to reach this goal is inversion of atmospheric transport given atmospheric CO_2 concentration measurements. Mainly because of the limited observations in space and time this method is still more of a qualitative than quantitative nature. Recently the advent of CO_2 retrievals from space has opened a new perspective as they may fill in current observational gaps of the atmospheric CO_2 observation network. In particular *Chedin et al.* [2003] used TOVS measurements, on board NOAA-11 satellites and *Engelen and McNally* [2005] used measurements from the AIRS instrument, on board the AQUA satellite, to estimate upper troposphere CO_2. There will also be future satellite missions dedicated to CO_2. As the wavelength domain used for the upcoming missions will be different from the AIRS and TOVS instruments the retrievals will be sensitive to CO_2 throughout the entire air column in contrast to AIRS and TOVS retrievals.

As both AIRS and TOVS CO_2 retrievals are recent they should still be viewed as experimental in nature. The purpose of this study has been to analyze these retrievals in view of our current knowledge of surface sources and sinks with the goal to determine whether these retrievals indeed advance our capability to constrain carbon sources and sinks. As

these retrievals are sensitive to upper troposphere CO_2 this forces us also to study lower-to-upper troposphere transport and its representation in atmospheric transport models – an area so far largely not well covered.

Our three studies reveal first that modeled atmospheric transport is generally very good throughout the troposphere with the caveat that our validation approach based on atmospheric CO_2 flux estimates from independent inverse modeling is somewhat limited in the tropics because of the lack of surface stations there. Differences between so far unused upper troposphere CO_2 observations and forward simulations are on the order of 0.4 ppm. While both TOVS and AIRS retrievals exhibit some of the expected features like seasonal cycles and North South gradients they also exhibit many unexpected features. These include land-ocean contrasts, smaller than expected seasonality in signals and unrealistic phasing between surface flux signatures and upper troposphere signals. Given the excellent transport properties of the models this indicates that existing CO_2 retrievals are not mature enough to help constrain surface sources and sinks at this stage. This may change with results from the upcoming dedicated missions, OCO and GOSAT. Our study provides a framework for analyzing these upcoming datasets and provides a quantitative assessment of lower-to-upper troposphere transport biases to be taken into account in future inverse calculations based on these data for the purpose of constraining surface sources and sinks.

Bibliography

Andreae, M. O., J. Fishman, M. Garstang, J. G. Goldammer, C. O. Justice, J. S. Levine, R. J. Scholes, B. J. Stocks, A. M. Thompson, B. van Wilgen and the STARE/TRACE-A/SAFARI-92 Science Team (1994), Biomass burning in the global environment: First results from the IGAC/BIBEX field campaign STARE/TRACE-A/SAFARI-92, in *Global Atmospheric-Biospheric Chemistry*, R. Prinn(ed.), pp. 83-101, Plenum Press, New York.

Andres, R.J., G. Marland, I. Fung, and E. Matthews (1996), A 10^0x10^0 distribution of carbon dioxide emissions from fossil fuel consumption and cement manufacture, 1950-1990, *Global Biogeochem. Cycles, 10,* 419-429.

Aumann, H. H., D. Gregorich, S. Gaiser (2005), AIRS hyper-spectral measurements for climate research: Carbon dioxide and nitrous oxide effects, *Geophys. Res. Lett., 32,* L21802, doi: 10.1029/2005GL022564.

Aumann, H. H., et al. (2003), AIRS/AMSU/HSB on the Aqua mission: design, science, objectives, data products and processing systems, *IEEE Trans. Geosci. Remote Sensing, 41,* 253-264.

Bakwin, P.S., P.P. Tans, C. Zhao (1995), W. Ussler, and E. Quesnell, Measurements of carbon dioxide on very tall tower, *Tellus, Ser. B, 47,* 535-549.

Boering, K. A., S. C. Wofsy, B. C. Daube, H. R. Schneider, M. Loewenstein, J. R. Podolske, T. J. Conway (1996), Stratospheric mean ages and transport rates from observations of carbon dioxide and nitrous oxide, *Science, Vol 274, Issue 5291,* 1340-1343, DOI: 10.1126/science.274.5291.1340.

Bousquet, P., D.A. Hauglustaine, P. Peylin, C. Carouge, and P. Ciais (2005), Two dec-

ades of OH variability as inferredd by an inversion of atmospheric transport and chemistry of methyl chloroform, *Atmos. Chem. Phys. Discuss., 5, 1679*-1737.

Bousquet, P., P. Peylin, P. Ciais, C. Le Quere, P. Friedlingstein, and P.P. Tans (2000), Regional changes in carbon dioxide fluxes of land and oceans since 1980, *Science, 290,* 1342-1346.

Brenninkmeijer, C. A. M., et al. (2005), Analyzing atmospheric trace gases and aerosols using passenger aircraft, *EOS, Transactions, AGU, vol. 86, No. 8,* 22 February.

Brenninkmeijer, C. A. M., et al. (1999), CARIBIC – Civil aircraft for global measurement of trace gases and aerosols in the tropopause region, *J. Atmos. Oceanic Technol., 16,* 1373-1383.

Buchwitz, M., et al. (2004), Atmospheric methane and carbon dioxide from SCIAMACHY satellite data: initial comparison with chemistry and transport models, *Atmos. Chem. Phys. Discuss., 4,* 7217-7279.

Callendar, G. S. (1958), On the amount of carbon dioxide in the atmosphere, *Tellus,*10,243-248.

Chédin, A., S. Serrar, N. A. Scott, C. Pierangelo, and P. Ciais (2005), Impact of tropical biomass burning emissions on the diurnal cycle of upper tropospheric CO_2 retrieved from NOAA-10 satellite observations, *J. Geophys. Res.*, *110*, D11309, doi:10.1029/2004JD005540.

Chedin, A., S. Serrar, N.A. Scott, C. Crevoisier, and R. Armante (2003), First Global measurement of mid tropospheric CO_2 from NOAA polar satellite. Tropical zone, *J. Geophys. Res., 108,* D (18), 4591, doi: 10.1029/2003JD003439.

Chedin, A., S. Serrar, R. Armante, N.A. Scott, A. Hollingsworth (2002), Signatures of annual and seasonal variations of CO_2 and other greenhouse gases from NOAA/TOVS observations and model simulations, *J. Clim.,15,*95-116.

Chedin, A., N. A. Scott, C. Wahiche, and P. Moulinier (1985), The improved initialization inversion method: A high resolution physical method for temperature retrievals from satellites of the TIROS-N series, *J. Appl. Meteor., 24,* 128-143

Chevallier, F. M. Fisher, P. Peylin, S. Serrar, P. Bousquet, F.-M. Bréon, A. Chédin, and P. Ciais (2005), Inferring CO_2 Sources and Sinks from Satellite Observations: Method and Application to TOVS Data, *J. Geophys. Res*., in press.

Conway, T., P. P. Tans, L. S. Waterman, K.W. Thoning, D. Kitzis, K. Masarie, and N. Zhang (1994), Evidence for interannual variability of the carbon cycle from the national oceanic and atmospheric administration climate monitoring and diagnostics laboratory global air sampling network, *J. Geophys. Res., 99,* 22831-22855.

Crevoisier, C., S. Heilliette, A. Chédin, S. Serrar, R. Armante, and N. A. Scott (2004), Midtropospheric CO_2 concentration retrieval from AIRS observations in the tropics, *Geophys. Res. Lett., 31,* L17106, doi:10.1029/2004GL020141.

Crevoisier, C., A. Chedin, N.A.Scott (2003), AIRS channel selection for CO_2 and other trace gas retrievals, *Q.J.R.Meteorol.Soc., 129,* 2719-2740.

Crisp, D., et al. (2004), The Orbiting Carbon Observatory (OCO) Mission, *Advances in Space Research, 34(4),* 700-709, doi: 10.1016/j.asr.2003.08.062

Engelen, R. J., and A. P. McNally (2005), Estimating atmospheric CO_2 from advanced infrared satellite radiances within an operational 4D-Var data assimilation system: Results and validation, *J. Geophys. Res., 110, D18305,* doi:10.1029/2005JD005982.

Engelen, R. J., E. Andersson, F. Chevallier, A. Hollingsworth (2004), Estimating atmospheric CO_2 from advanced infrared satellite radiances within an operational 4D-Var data assimilation system: Methodology and first results, *J. Geophys. Res., 109,* D19309,doi:10.1029/2004JD004777.

Enting, I. G., C. M. Trudinger, and R. J. Francey (1995), A synthesis inversion of the concentration and δC^{13} of atmospheric CO_2, Tellus Series B-Chemical and Physical Me-

teorology, 47, 35–52.

Fan, S., Gloor, M., Mahlman, J., Pacala, S., Sarmiento, J., Takahashi, T., and Tans, P. (1998), A large terrestrial carbon sink in North America implied by atmospheric and oceanic CO_2 data and models, *Science*, 282, 442--446.

Fourier, J. (1824), Remarques generales sur les temperatures du globe terreste et das espaces planetaires, Annales de Chemie et de Physique, 27, 136-167, Translated in to English by James R. Fleming " The greenhouse effect, and the quest for a universal theory of terrestrial temperatures" (Endeavour, v23(2), p72-75, 1999).

Francey, R. J., M. R. Manning, C. E. Allison, S. A. Coram, D. M. Etheridge, R. L. Langenfelds, C. D. Lowe, and L. P. Steele (1999b), A history of $\delta^{13}C$ in atmospheric CH_4 from the Cape Grim Air Archive and Antarctic firn air, *J. Geophys.Res., 104,* No. D19, 23631-23643.

Francey, R. J., L. P. Steele, R. L. Langenfelds, M. P. Lacarelli, C. E. Allison, D. J. Beardsmore, S. A. Coram, N. Derek, F. de Silva, D. M. Etheridge, P. J. Fraser, R. Henry, B. Turner, E. D. Welch, D. A. Spencer, and L. N. Copper (1996), Global Atmospheric Sampling Laboratory (GASLAB): supporting and extending the Cape Grim trace gas programs in *Baseline Atmospheric Program (Australia) 1993,* edited by R. J. Francey, A. L. Dick, and N. Derek, Bureau of Meteorology and CSIRO Division of Atmospheric Research, Melbourne, Australia, 8-29.

GLOBALVIEW-CO_2: Cooperative Atmospheric Data Integration Project - Carbon Dioxide, CD-ROM, NOAA CMDL, Boulder, Colorado (2005), [Also available on Internet via anonymous FTP to ftp.cmdl.noaa.gov, Path: ccg/co2/GLOBALVIEW].

Gloor, M., N. Gruber, J. L. Sarmiento, C. Sabine, D. Feely, and. Rödenbeck (2003) , A first estimate of present and preindustrial air-sea CO_2 flux patterns based on ocean interior carbon measurements and models, *Geophys. Res. Lett., Vol.30,* doi : 10.1029/2002GL015594.

Gloor, M., S.-M. Fan, S. Pacala and J. L. Sarmiento (2000), Optimal sampling of the atmosphere for purpose of inverse modeling: A model study, *Glob. Biogeochem. Cycles, 14,* 407-428.

Gloor, M., S.-M. Fan, S. W. Pacala, J. L. Sarmiento, and M. Ramonet (1999), A model-based evaluation of inversions of atmospheric transport, using annual mean mixing ratios, as a tool to monitor fluxes of nonreactive trace substances like CO_2 on a continental scale, *J. Geophys.Res., 104,* 14245-14260.

Gruber, N., M. Gloor, S.-M. Fan, and J. L. Sarmiento (2001), Air-sea flux of oxygen estimated from bulk data: Implications for the marine and atmospheric oxygen cycles, *Global Biogeochem. Cycles*, vol.15, No.4, pp. 783-803.

Gurney, K.R., et al. (2002), Towards robust regional estimates of CO_2 sources and sinks using atmospheric transport models, *Nature,* 415,626-630.

Hansen, J. E., et al. (1988), Global climate change as forecast by Goddard Institute for Space Studies 3-dimensional model, *J. Geophys. Res., 93*: 9341-64.

Heimann, M., and S. Körner (2003), The global atmospheric tracer model TM3, Model description and user's manual release 3.8a, Max Planck Institute for Biogeochemistry, Jena, Germany.

Heimann, M. (1996), The global atmospheric transport model TM2, Tech. Rep.10, Max-Planck Institute for Meteorology, Hamburg, Germany.

Hoell, J. M., D.D. Davis, D. J. Jacob, et al. (1999), Pacific Exploratory Mission in the tropical Pacific: PEM-Tropics A, August-September 1996, *J. Geophys. Res.*, 104 (D5): 5567-5583 Mar 20.

Hoell, J. M., D. D. Davis, S. C. Liu, et al. (1997), The Pacific Exploratory Mission West phase B: February-March 1994, *J. Geophys. Res.*, 102 (D23): 28223-28239 Dec 20.

Hourdin, F., and A. Armengaud (1999), Test of a hierarchy of finite-volume schemes for

transport of trace species in an atmospheric general circulation model, *Mon. Wea. Rev., 127,* 822-837.

Houweling, S., F.-M. Breon, I. Aben, C. Rödenbeck, M. Gloor, M. Heimann, and P. Ciais (2004), Inverse Modeling of CO_2 sources and sinks using satellite data : a synthetic inter-comparison of measurement techniques and their performance as a function of space and time, *Atmos. Chem. Phys., 4,* 523-538.

Indermühle, A., B. Stauffer, T. F. Stocker (1999), Early holocene atmospheric CO_2 concentrations, *Science, vol.286,* Issue 5446, 1815.

IPCC (Intergovernmental Panel on Climate Change) (2002), Climate Change and Biodiversity, Technical Paper V, April 2002, edited by H Gitay et al., IPCC, Geneva, Switzerland, pp.85

IPCC (Intergovernmental Panel on Climate Change) (2001), Climate Change 2001: The Scientific Basis, edited by J. T.Houghton et al., Cambridge Univ. Press, New York.

Jacob, D.J., J.H. Crawford, M.M. Kleb, V.E. Connors, R.J. Bendura, J.L.Raper, G.W. Sachse, J.C. Gille, L. Emmons, and C.L. Heald (2003), The Transport and Chemical Evolution over the Pacific (TRACE-P) aircraft mission: Design, execution, and first results, *J. Geophys. Res*., 108 (D4), 9000, 10.1029/2002JD003276,

Jacob, D. J., et al. (1996), Photochemistry of the tropical troposphere, *J. Geophys. Res*., 101, October 30, 24,235-24,250.

Jaffe, B. (1942), *in new world of chemistry*, p. 358, Silver Burdett, New York.

Kalnay, E., M. Kanamitsu, R. Kistler, et al. (1996), The NCEP/NCAR 40-year reanalysis project, *Bull. Am. Met. Soc., 77,* 437-471.

Keeling, C.D., S. C. Piper, M. Heimann (1989), A three dimensional model of atmospheric CO_2 transport based on observed winds: Mean annual gradients and interannual variations, in aspects of climate variability in the Pacific and the Western Americas, *Geo-*

phys. Monogr. Ser., 55, edited by D.H.Peterson, AGU, Washington, D.C., 305-363.

Kirchhoff, V. W. J. H., J. R. Alves, F. R. da Silva, and J. Fishman (1996), Observations of ozone concentrations in the Brazilian Cerrado during the TRACE A field expedition, *J. Geophys. Res, 101(D19),* 24029-2404.

Laval, K., R. Sadourny, and Y. Serafini (1981), Land surface processes in a simplified general circulation model, *Geophys. Astrophys. Fluid Dyn., 129-150*.

Leuenberger, M., U. Siegenthaler, and C. C. Langway (1992), Carbon isotope composition of atmospheric CO_2 during the last ice age from an Antarctic ice core, *Nature, 357,* 488-490

Louis, J. F. (1979), A parametric model of vertical eddy fluxes in the atmosphere, *Boundary Layer Meteorol., 17,* 187-202.

Machida, T., K. Kita, Y. Kondo, D. Blake, S. Kawakami, G. Inoue, and T. Ogawa (2003), Vertical and meridional distributions of the atmospheric CO_2 mixing ratio between northern midlatitudes and southern subtropics, *J. Geophys. Res., 108,* D3, 8401, doi:10.1029/2001JD000910.

Mahlman, J. D. (1997), Dynamics of transport processes in the upper troposphere, *Science, 276(5315),* 1079-1083.

Manabe, S., R. F. Strickler (1964), Thermal equilibrium of the atmosphere with convective adjustment, *J. Geophys. Res.,* 21: 361-85

Marland, G., R. M. Rotty, and N. L. Treat (1985), CO_2 from fossil fuel burning: Global distributions of emissions, *Tellus B, 37,* 243-258.

Matsueda, H., H.Y. Inoue, and M. Ishii (2002), Aircraft observation of Carbon dioxide at 8-13 km altitude over the western Pacific from 1993 to 1999, *Tellus B, 54,* 1-21

Matsueda, H., H.Y. Inoue (1996), Measurement of Atmospheric CO_2 and CH_4 using a

commercial airliner from 1993 to 1994, *Atmos. Environ.,* vol.30, Nos. 10/11, pp. 1647-1655.

McNally, A. P., and P. D. Watts (2003), A cloud detection algorithm for high-spectral resolution infrared sounders, *Quart. J. Roy. Meteorol. Soc., 129,* 3411-3423, doi:10.1256/qj.02.208.

Newell, R. E., W. Hu, Z-X. Wu, Y. Zhu, H. Akimoto, B. E. Anderson, E. V. Browell, G. L. Gregory, G. W. Sachse, M. C. Shipham, A. S. Bachmeier, A. R. Bandy, D. C. Thornton, D. R. Blake, F. S. Rowland, J. D. Bradshaw, J. H. Crawford, D. D. Davis, S. T. Sandholm, W. Brockett, L. DeGreef, D. Lewis, D. McCormick, E. Monitz, J. E. Collins, Jr., B. G. Heikes, J. T. Merrill, K. K. Kelly, S. C. Liu, Y. Kondo, M. Koike, C.-M. Liu, F. Sakamaki, H. B. Singh, J. E. Dibb and R. W. Talbot (1996), Atmospheric sampling of supertyphoon Mireille with NASA DC-8 Aircraft On September 27, 1991, during PEM-West A, *J. Geophys. Res., 101*, 1853-1871.

Pak, B.C. (2000), Vertical structure of atmospheric trace gases over South east Australia,PhD Thesis, University of Melbourne, Australia, 273 pp., (Available at the Australian Digital Thesis Project via http://eprints.unimelb.edu.au/archive/00000657/).

Pearman, G. I., D. J. Beardsmore, and R. C. O'Brien (1983), The CSIRO (Australia) atmospheric carbon dioxide program: ten years of aircraft data, *CSIRO Division of Atmospheric Physics Technical Paper No. 45*, 113 p.

Peylin, P., P. Bousquet, S. Sitch, C. Lequere, P. Friedlingstein, P. Ciais, and P. Tans (2005), Multiple constraints on regional CO_2 flux variations over land and oceans, *Global Bio. Cycle*, 19, GB1011 FEB 10.

Randerson, J. T., C. B. Field, I. Y. Fung, P. P. Tans (1999), Increases in early season ecosystem uptake explain recent changes in the seasonal cycle of atmospheric CO_2 at high northern latitudes, *Geophys. Res. Let., 26*: 2765-2768.

Raper, J. L., Kleb MM, Jacob DJ, et al. (2001), Pacific Exploratory Mission in the tropical Pacific: PEM-Tropics B, March-April 1999, *J. Geophys. Res.*, 106 (D23): 32401-32425.

Rayner, P. J., and D. M. O'Brien (2001), The utility of remotely sensed CO_2 concentration data in surface source inversions, *Geophys. Res. Lett., 28,* 175-178.

Rayner, P., I. Enting, R. Francey, and R. Langenfelds (1999), Reconstructing the recent carbon cycle from atmospheric CO_2, δCO2 and O_2/N_2 observations, *Tellus B, 51,* 213-232.

Reichler, T., M. Dameris, and R. Sausen (2003), Determining the tropopause height from gridded data, *Geophys. Res. Lett., 30,* 2042, doi:10.1029/2003GL018240.

Rödenbeck, C., S. Houweling, M. Gloor, and M. Heimann (2003), CO_2 flux history 1982-2001 inferred from atmospheric data using a global inversion of atmospheric tracer transport, *Atmos. Chem. Phys., 3,* 1919-1964.

Russell, G., and J. Lerner (1981), A new finite-differencing scheme for the tracer transport equation, *J. Appl. Meteorol., 20,* 1483-1498.

Sabine, C.L., et al. (2004), The oceanic sink for anthropogenic CO_2, *Science, 305,* 367-371.

Sadourny, R. and K. Laval (1984), January and July performance of the LMD general circulation model. *In New Perspectives in Climate Modeling*, 173--198. A. Berger and C. Nicolis (Eds), Elsevier.

Smith, W. L., H. M. Woolf, C. M. Hayden, D. Q. Wark, and L. M. McMillin (1979), The TIROS-N Operational Vertical Sounder, *Bull Am. Meteorol. Soc*., 60, 1177-1187.

Stuiver, M., P. D., Quay, H. G. Ostlund (1983), *Science 219*, 849

Tans, P.P., I. Y. Fung, and T. Takahashi (1990), Observational constraints on the global atmospheric CO_2 budget, *Science, 247,* 1431-1438.

Thoning, K. W., P. P. Tans, and W. D. Komhyr (1994), Atmospheric carbon dioxide at Mauna Loa Observatory 2. Analysis of the NOAA GMCC data, 1974-1985, *J. Geophys. Res*., 94, 8549-8565.

Tiedtke, M. (1989), A comprehensive mass flux scheme for cumulus parameterization in large-scale models, *Mon. Weather Rev., 117,* 1179-1800.

Tiwari, Y.K., M. Gloor, R. J. Engelen, F. Chevallier, C. Rödenbeck, S. Körner, B.H. Braswell, M. Heimann (2005), Comparing CO_2 retrieved from AIRS on the AQUA satellite with model predictions: implications for constraining surface fluxes and lower-to-upper troposphere transport, *J. Geophys. Res.,* in press.

Tyndall, J. (1863), On radiation through the Earth's atmosphere, *Philosophical Magazine, ser.4*, 25, pp. 200-206

Van der Werf, G. R., J.T. Randerson, G. J. Collatz, L. Giglio (2003), Carbon emissions from fires in tropical and subtropical ecosystems, *Global Change Biology*, 9(4): 547-562.

Vay, S. A., B. E. Anderson, T. J. Conway, G. W. Sachse, J. E. Collins Jr., D. R. Blake, and D. J. Westberg (1999), Airborne observations of the tropospheric CO_2 distribution and its controlling factors over the South Pacific Basin, *J.Geophys. Res., 107,* D5, pp. 5663-5676, March 20.

Zahn, A., et al. (2002), Budgets of O_3 and CO in the upper troposphere: CARIBIC passenger aircraft results 1997-2001, *J.Geophys. Res., 107,* D17, 4337, doi:10.1029/2001JD001529.